

THIAZYL RADICALS AND THEIR DERIVATIVES

Master's thesis

University of Jyväskylä

Chemistry Department

Inorganic and analytical chemistry department

25.03.2017

Anni Taponen

ABSTRACT

Thiazyls are radicals built from organic moieties but they have similar physical properties conventionally considered for inorganic solids and metal oxides. Electric and magnetic properties of thiazyls have caught attention since their discovery and these odd-electron species have been used as building blocks in development of molecular magnets and conductors. Furthermore, certain thiazyls present bistability and can be seen as prospective materials for molecular switches because one radical can have two different magnetic states depending on the solid state packing. The newest branch of development has been directed to the transition metal complexes of coordinating thiazyls. By metal complex formation, the magnetism is expected to be enhanced due to magnetic communication between an unpaired electron of the radical and the paramagnetic metal center.

This master's thesis contains two parts. Part one is a literature review which presents the most recent findings about nitrogen and sulfur containing radicals. In this work, the synthesis and properties of dithiadiazolyl and dithiazolyl radicals are emphasized. In addition, coordination chemistry of thiazyl radicals has been discussed. The second part contains the experimental studies conducted during the thesis work. The main objective in the experimental part was to synthesize new radical(s) and to study their coordination chemistry. During experimental phase, two completely new radicals were synthesized and characterized. First novel radical is a member of a large family of 1,2,3,5-dithiadiazolyls and it has features similar to other members of the same class. The other new radical is modified version of dithiazolothiadiazinyl¹ with different substituent: a hydrogen atom was replaced with fluorine which induced changes in the solid-state packing when compared to hydrogen-substituted version. Coordination of dithiazolothiadiazinyl radical to various metal cations was examined but no coordination compounds were obtained.

TIIVISTELMÄ

Tiatsyyliit ovat orgaanisia radikaaleja, joilla on vastaavia fysikaalisia ominaisuuksia, joita tavallisesti esiintyy epäorgaanisilla yhdisteillä ja metallioksidoilla. Tiatsyylien sähköjohtavat ja magneettiset ominaisuudet ovat kiinnittäneet huomiota niiden löytymisestä lähtien ja niitä ollaan hyödynnetty molekulaaristen magneettien ja johteiden suunnittelussa. Tämän lisäksi tietyillä tiatsyyleillä esiintyy bistabiiliutta, joka tarkoittaa, että radikaalilla on kaksi erilaista magneettista olomuotoa riippuen kiinteän tilan pakkautumisesta. Bistabiiliutta voidaan hyödyntää esimerkiksi *molekyylilytkimissä* (molecular switches). Uusin tutkimuksen haara on tiatsyylien koordinoiminen siirtymämetallien kanssa, jonka uskotaan lisäävän magneettista vuorovaikutusta parittoman elektronin ja paramagneettisen metallin ovat välillä.

Tämä Pro gradu- tutkielma koostuu kahdesta osasta: kirjallisuustutkielmasta ja kokeellisesta osuudesta. Kirjallisuusosuudessa on kerrottu tyypeä ja rikkeä sisältävien radikaalien tuoreimmista tutkimustuloksista. Tässä tutkielmassa on tutkittu erityisesti ditiadiatsolyyli- ja ditiatsolyyliradikaalien synteesiä ja ominaisuuksia sekä tiatsyylien koordinaatiokemiaa. Toinen osio koostuu kokeellisesta tutkimuksesta, jonka pääasiallinen tavoite oli syntetisoida uusia radikaaleja. Tämän lisäksi tavoitteena oli tutkia radikaalisynteesien tuotteiden koordinoitumista metallien kanssa. Kokeellisen osuuden tuloksena saatiin kaksi uutta radikaalia karakterisoitua. Toinen näistä kuuluu laajaan 1,2,3,5- ditiadiatsolyyliin ryhmään ja on hyvin samankaltainen ominaisuuksiltaan kuin muutkin ryhmän jäsenet. Toinen syntetisoitu radikaali oli ditiatsolotiadiatsinyyli, joka on muokattu versio aikaisemmin raportoidusta ditiatsolotiadiatsinyylistä: vety on korvattu fluorilla ja tämä johti muutoksiin molekyylin kidepakkautumisessa. Ditiatsolotiadiatsinyyliin koordinoitumista kokeiltiin useamman metallin kanssa, mutta koordinaatiokomplekseja ei saatu aikaiseksi tämän tutkimuksen aikana.

PREFACE

Experimental part of the thesis was carried out between 6th of June and 5th of October 2016 in the University of Jyväskylä and the thesis was written between October 2016 and February of 2017. The articles were mostly sought by using Reaxys, Scifinder and Google Scholar and the main terms used were: thiazyl radical, 1,2,3,5-dithiadiazolyl, 1,3,2-dithiazolyl, molecule-based magnet, thiazyl conductors, metal complexes of thiazyls.

I would like to express my greatest gratitude to my supervisor Professor Heikki Tuononen for giving an opportunity to work among this research topic and his support during the whole project. I was tempted into world of radicals and their metallic features by my friend Petra Vasko. She asked what were my plans regarding to my thesis and explained the research area of Prof. Heikki Tuononen's group. After that conversation, I knew what I hoped to do in my thesis. I also want to thank Aaron Mailman being my instructor during the experimental part. His enthusiasm towards chemistry, after all these years he has been practising it, is a true inspiration. Also I want to thank everyone else who has been part of my thesis and my chemistry studies. Financial support from the Academy of Finland and from EU H2020-MSCA-IF project number 659123 is gratefully acknowledged.

Jyväskylä, February 20th 2017

Anni Taponen

TABLE OF CONTENTS

LITERATURE PART

1	INTRODUCTION	1
2	BACKGROUND	4
2.1	STABILITY OF RADICALS	4
2.2	CONDUCTIVITY	8
2.3	MAGNETIC MATERIALS.....	12
3	DITHIADIAZOLYL RADICALS.....	15
3.1	1,2,3,5-DITHIADIAZOLYL.....	17
3.2	1,3,2,4-DITHIADIAZOLYL.....	22
4	DITHIAZOLYL RADICALS	24
4.1	1,3,2- DITHIAZOLYL	24
4.2	1,2,3-DITHIAZOLYL	27
5	COORDINATION COMPOUNDS OF THIAZYLS	37
5.1	COORDINATION COMPLEXES OF 1,2,3,5-DITHIADIAZOLYLS	38
5.2	COORDINATION COMPLEXES OF 1,3,2-DITHIAZOLYLS	48
6	CONCLUSIONS.....	50

EXPERIMENTAL PART

7	AIM OF THE WORK.....	51
8	EXPERIMENTAL METHODS	52
8.1	GENERAL METHODS AND PROCEDURES	52
8.2	SYNTHESES	54
8.3	REDUCTIONS.....	65
8.4	COMPLEXATION.....	69
9	RESULTS AND DISCUSSION	71
9.1	STARTING MATERIALS	71
9.2	PREPARATION OF CATIONS	72

9.3	REDUCTION OF CATIONS	77
10	CONCLUSIONS.....	83
11	REFERENCES	85
12	APPENDICES	91

ABBREVIATIONS

Cp	Cyclopentadiene
DCM	Dichloromethane
DMFc	Dimethyl ferrocene
DTA	Dithiazolyl
DTDA	Dithiadiazolyl
EPR	Electron paramagnetic resonance
Hfac	Hexafluoroacetylacetonate
MeCN	Acetonitrile
MO	Molecular orbital
OMFc	Octamethyl ferrocene
OTf	Triflate, trifluoromethanesulfonate
PCN	Propionitrile
RT	Room temperature
SCE	Saturated calomel electrode
SOMO	A singly occupied molecular orbital
TBAF	Tetrabutylammonium fluoride
Th	Thiophene
THF	Tetrahydrofuran

VIII

TMPDA	N,N,N,N-Tetramethyl-p-phenylenediamine
TTTA	1,3,5-trithia-2,4,6-triapentalenyl
U	Coulombic repulsion
W	Electronic bandwidth
χ_T	Molar magnetic susceptibility

THE LITERATURE PART

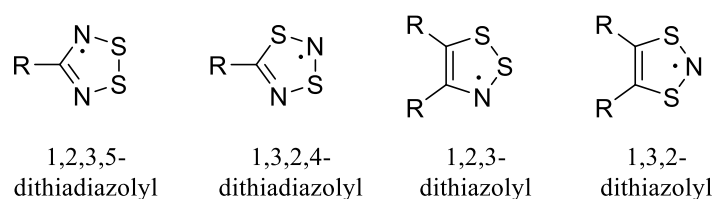
1 INTRODUCTION

Metals, their oxides and alloys are commonly utilized in modern electronic devices due to their magnetic and conductive properties. However, metals are not the only materials possessing magnetic and conductive features as these metal-resembling qualities have been also observed for radicals^{2,3,4} – chemical species containing an unpaired electron. Illustrative example of these radicals are *thiazyls* which potentially can be utilized in spintronics such as molecular switches, spin valves, data storage and quantum computers.^{5,6,7,8,9,10} Exploiting organic radicals in this type of applications can provide formability of electronic properties and cost-effective processes compared to traditional inorganic materials.¹¹ The great advantage of thiazyls as molecular building blocks in functional materials is the capability of fine tune their physical properties by utilizing adjustable organic synthetic routes.^{11,12}

Radicals containing -NS fragment are called *thiazyls*.⁵ The chemistry of thiazyls is highly interesting because of their outstanding stability along with qualities derived from unpaired electron like conductivity and magnetism.⁹ Obtaining these attributes is not a straightforward task, but the potential rewards render the research very appealing.

The beginning of thiazyl chemistry dates back to 1835 when extremely sensitive binary tetrasulfur tetranitride (S_4N_4) was discovered.^{13,14} For a long time, sulfur-nitrogen chemistry was very limited because of challenging synthetic procedures¹⁴ resulting from thermodynamically driven formation of N_2 and S_8 which makes sulfur-nitrogen compounds to be shock sensitivity and thermally unstable.⁵ Furthermore, determination of the reaction mechanisms in this branch of chemistry was highly challenging because skeletal rearrangement reactions are typical for -NS compounds.⁵ Although, the first thiazyl-based radical $S_3N_2^+$ was reported already in 1880 by Demarçay,⁹ it took almost another hundred years before thiazyl chemistry started to bloom.⁵ In 1970s when polythiazyl (polymeric structure of -NS units) was observed to have both metallic and superconducting properties the interest towards thiazyls was considerably increased.⁵

After the discovery of polythiazyls, the development of the thiazyl chemistry has continued, to dithiadiazolyls (Scheme 1). In the early stage, researchers concentrated on simple dithiadiazolyls and for a long time the core research objective was to understand the crystal packing and its effects on the qualities of these radicals.⁹ The main difficulty with dithiadiazolyls was their high tendency to dimerize: dimerization leads to the closed shell structure and the formed dimer becomes diamagnetic and loses its paramagnetic properties.⁹ Hence, the studies of dithiadiazolyls focused on suppressing the dimerization to enhance their paramagnetic and ferromagnetic properties.



Scheme 1. Dithiadiazolyls and dithiazolyls covered in this work.

The dithiadiazolyls have higher tendency to dimerize compared to slightly simpler dithiazolyls radicals (Scheme 1). For example, the dimerization enthalpy for 1,2,3,5-dithiadiazolyls is approximately 35 kJ mol^{-1} whereas for 1,3,2-dithiazolyls the enthalpy is generally around 0 kJ mol^{-1} . The stability of dithiazolyls originates from the bulky substituents residing in close proximity to the $-\text{NS}$ fragment. However, large substituents can commonly lead to insulating states diminishing the conducting properties.⁹

Development of the field proceeded toward more complex thiazyl molecules. These are for example hybrids of dithiazolyl and dithiazinyl by Oakley and the co-workers¹, but also other arrangements with functional groups such as pyridines, thiophenes, nitriles or plain aromatics.⁵ In addition, metal coordination of thiazyls is continuously growing research field.⁹ The coordination complexes of organic radicals and inorganic metals are expected to deliver more information about exchange coupling pathways between an unpaired electron and paramagnetic metals. This information is particularly important in development of novel molecular materials such as molecular magnets.¹³

This thesis focuses on thiazyl radicals and is divided into two main sections: the literature part and the experimental part. The literature part introduces to reader the preparation,

properties and applications of organic thiazyl radicals. The background of the stability of radicals in general is presented in the Section 2.1. As the thiazyls are expected to be exploited as functional conductive and magnetic materials, the basic concepts of conductivity (section 2.2) and magnetism (section 2.3) has been also discussed. After presenting the theoretical background, different classes of thiazyls are comprehensively introduced. Dithiadiazolylys are discussed in the section 3 and dithiazolylys in the section 4. The effects of crystal packing and variation of substituents to the conductivity and magnetism of thiazyl-based molecules are emphasized. Also other factors, such as light (4.2.3), pressure (4.2.2) and heat (4.2.3) can be utilized in improving physical properties of thiazyl radicals are discussed. Finally, the novel research field of thiazyl radical metal complexes is presented in section 5.

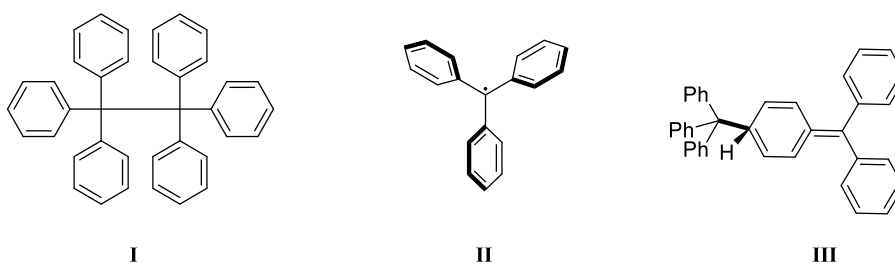
The latter part introduces the reader to the goals of experimental the work (section 7). The experimental methods and equipments are presented in the section **Error! Reference source not found.** The syntheses are presented in section 8.2, reductions of cations in 8.3 and the metal complexation syntheses in the section **Error! Reference source not found.** The results have been discussed in the section 9 and the results concluded in the paragraph 10.

2 BACKGROUND

2.1 STABILITY OF RADICALS

2.1.1 THE HISTORY

Due to the unpaired electron, radicals are usually very reactive molecules that dimerize, reorganize to form new compounds or abstract hydrogen.⁴ However, also isolable and stable radicals exist. The first persistent organic radical was found by Gomberg in 1900. Gomberg attempted to synthesize hexaphenylethane **I** but accidentally synthesized triphenylmethyl **II** (Scheme 2).¹⁵ Under an inert atmosphere, a molecule **II** is persistent, but in dilute degassed solution it is in equilibrium with a dimer form **III** (Scheme 2). The spin density is mostly concentrated on central carbon atom but because of sterically protecting substituents the radical **II** is relatively stable. However, small amount of spin is distributed on phenyl groups and tension between big bulky groups enables formation of **III**.¹⁶



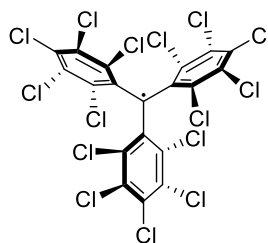
Scheme 2. Hexaphenylethane **I**, triphenylmethyl **II** and dimeric species **III** of triphenylmethyl.

Gomberg's discovery opened the field of organic free radical chemistry. Because his work among radicals was widely and highly praised, he was nominated many times for Nobel Prize, but was never awarded. However, in 1971 Gerhard Herzberg won the Nobel based on his studies of structure and spectroscopy of free radicals.^{5,17}

2.1.2 DEFINITIONS OF STABILITY

Radicals are named differently based on their lifetime. Griller and Ingold proposed in 1975 that radicals should be defined in relation to the methyl radical and they suggested that a *persistent radical* is an odd-electron compound which has a significantly longer lifetime than the methyl radical in the same conditions. *Stable* radicals, on the other hand, can be handled and stored in the aerobic conditions and do not undergo any reactions common for *transient* radicals which can be defined as short-living compounds.¹⁸ In chemistry, a transient radical means a radical which reacts rapidly after its formation.⁵

The difference between two radicals and their stability can be easily demonstrated. If triphenylmethyl **II** and tris(pentachlorophenyl)methyl **IV** (called also polychlorotriphenylmethyl, PTM) are compared, it can be seen that even small changes alter the stability. Triphenylmethyl **II** is a highly *persistent* radical but it dimerizes in solution and thus is not *stable*. On the contrary radical **IV** tris(pentachlorophenyl)methyl, which is chlorinated analogue for **II**, is stable both in solution and solid state and do not react with oxygen due to additional steric protection gained from chlorine atoms (Scheme 3).^{4,19}



IV

Scheme 3. Tris(pentachlorophenyl)methyl IV.

2.1.3 GENERAL FEATURES OF STABILITY

There are two main features that have an influence on the stability of radicals: steric bulk and spin delocalization. Steric protection provides kinetic and thermodynamic stability⁵ and is widely utilized in preparation of stable radicals. However, this method has certain pitfalls. The remarkable features of odd electron species, such as magnetic and conducting

properties, arise from the interplay of spins with other molecules. If the radical site is too isolated because of steric bulk, all the communication between different spins is suppressed and the system of interest may lose intriguing qualities.¹⁶

Other aspect of stability arises from the spin delocalization over the whole molecule. Delocalization reduces reactivity by fading the spin localization on certain atom(s) and spreading the spin density between several atoms. Thus, the unpaired electron does not react so readily as it is “hidden” for example into large π -system.¹⁶ This effect is based on thermodynamic stabilization which originates from decreasing the energy of the ground state.²⁰

In addition, there are other approaches which have not drawn as much attention as aforementioned two main methods. One example is *captodative effect* which results from different type of substituents bound into the molecule. One group is an electron withdrawing while other is an electron donating group.²¹ Together these groups will have a net effect on the singly occupied molecular orbital (SOMO). The energy of singly occupied molecular orbital rises when it interacts with the highest occupied molecular orbital (HOMO) of donor group. As a result, SOMO is closer in the energy to the acceptor's lowest unoccupied molecular orbital (LUMO) and can interact with it. In consequence of this interaction, the energy of SOMO is lowered leading to overall stabilization of the compound (Figure 1).

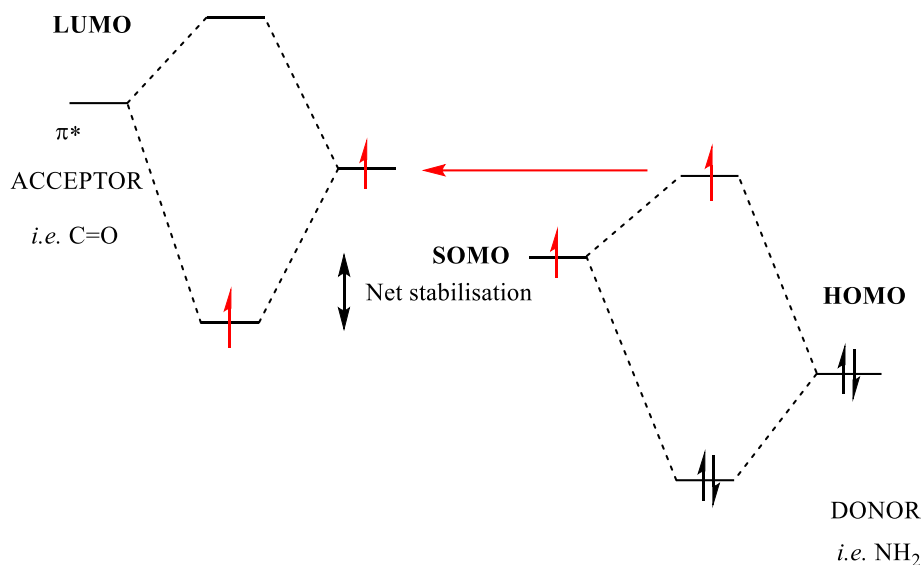
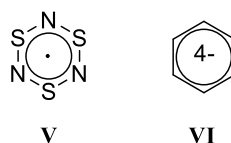


Figure 1. The captodative effect stabilizes radical by lowering the energy of singly occupied molecular orbital. On the right hand side is a molecular orbital of electron donating group *e.g.* NH₂ and on the left hand side is electron withdrawing group *e.g.* R₂C=O. SOMO interacts with empty antibonding MO of the carbonyl group.²⁰

2.1.4 STABILITY OF THIAZYLS

Many stable or persistent radicals include first row p-block elements such as oxygen and nitrogen because they have an ability to form π -bonds and contain free electron pairs. Both of these qualities stabilize radicals by allowing the spin to distribute over the π -framework. In general, after first row, producing odd electron species with p-block elements becomes much more difficult.²² However, sulfur makes a major exception, especially when it is connected to nitrogen. Sulfur is a peculiar p-block element in many ways because it is in the same group with oxygen but has the same electronegativity than carbon. Therefore sulfur is often compared to these elements.⁵ If the stability of carbon-only and sulfur/nitrogen containing radicals is compared, significant difference can be seen: cyclic six-membered S₃N₃ ring **V** is stable whereas isovalent and isoelectronic benzene tetra-anion **VI** is highly reactive. Sulfur is a soft base and has more diffuse orbitals. When sulfur is combined with nitrogen in radical species, the molecules show high persistence and stability. In addition to sulfurs effects – the SN fragment stabilizes radical by being an

electronegative moiety. Otherwise electropositive molecule achieves stabilization because of gained electronegativity from the $-\text{SN}$ fragment.⁵



Scheme 4. S_3N_3 **V** and benzene tetra-anion **VI** are isoelectronic structures. Their reactivity is remarkably different.

2.2 CONDUCTIVITY

Conductivity is inversely proportional to resistivity and describes how easily electrons flow in certain material. The high interest towards sulfur-nitrogen radicals and their conductivity arose from the discovery of the polythiazyl (Figure 2).⁵ Polythiazyl has unusual solid state properties and it is highly conductive material which has conductivity approximately 1000 S/cm in room temperature.^{5,23} Resistance can be reduced in lower temperatures and polythiazyl reaches superconductivityⁱ at 0.26 K.²⁴ The development of radical-based neutral thiazyl conductors started in the 1970s.

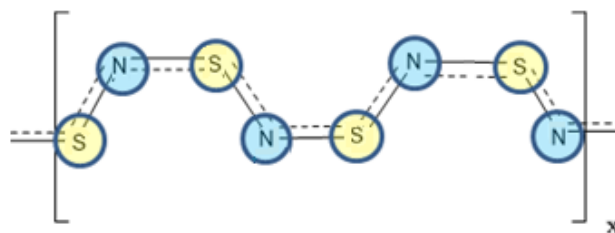


Figure 2. Discovery of superconductive polythiazyl was a starting point of research of thiazyls as conductive materials.

Conductivity has been described mainly with two different models: *an electron sea model* and *the band theory*. An electron sea model describes conductivity of metals. Metals have

ⁱ Superconductivity was found in 1911 by Dutch physicist K. Onnes. Superconductive material loses resistance completely at very low temperatures due to quantum mechanical effects.³⁰

low ionization energies hence they lose electrons relatively easily. When metals form a solid structure all atoms donate at least one electron to the electron sea. In crystal lattice electrons are not localized to certain atoms but are free to move. The band theory in turn is a more advanced version of the electron sea model and it relies on the molecular orbital (MO) theory. In the MO theory, the atomic orbitals of individual atoms are combined and constructed into a picture of the whole orbital organization and the crystal is described with molecular orbitals instead of individual atomic orbitals.²⁵

Conductivity of radicals is commonly described using band theory. Instead of freely moving electrons of metal, radicals have unpaired electrons, which can act as charge carriers.⁵ In a simplest case, if we have N amount of radicals, then there is N amount of unpaired electrons. When the amount of unpaired electrons is substantial, the energy difference between them is infinitesimally small and energy levels can be seen inseparable. This inseparable construction of energy levels is called a *band*. The other half of the amount of N molecular orbitals is bonding orbitals and the other half is antibonding orbitals.²⁵ In 0 K temperature, all electrons have occupied the bonding orbitals and antibonding orbitals have no electrons. At higher temperatures, electrons can excite from the highest occupied molecular orbital (HOMO) to higher in energy lying unoccupied orbitals.

The occupied molecular orbitals are called a *valence band* and the empty orbitals *conduction band*. The energy difference between these two energy levels defines whether molecule is a *conductor*, a *semi-conductor* or an *insulator* (Figure 3). With small energy difference, electrons can easily advance over the energy gap aka *band gap* and therefore the material can conduct electricity. Semi-conductor materials show limited conductivity compared to conductors. On the other hand, if the energy gap is very large, the material do not conduct electricity and is called an insulator.²⁵

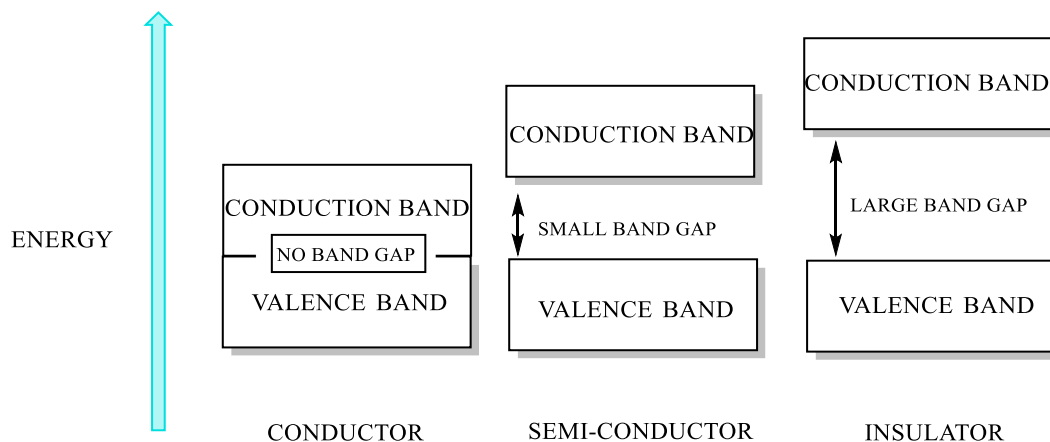


Figure 3. Correlation between a band gap and conductivity.

Neutral conductor material could be constructed from π -stacked radicals where each molecule has an unpaired electron.²⁶ However, the method is not this straightforward. The band theory does not take electron-electron repulsions into account. For example, many transition-metal oxides with a partially filled d -electron band were expected to be conductors but nevertheless were poorly conducting materials or insulators.²⁷ The repulsion between electrons is electrostatic force called *coulombic repulsion* (U) and it was predicted to be the reason for phase called *Mott's insulation state*. This means that unpaired electron of radical cannot act like charge transporter but it is localized to the host molecule.^{26,28} Some classes of thiazyl radicals have high tendency to dimerize and can be called *Peierls instable*. The dimerization problem can be often prevented by adding steric bulk (see above). However, this can lead to decrease in *electronic bandwidth* (W) and may result the Mott's insulating state (Figure 4). Hence, the balance between electronic bandwidth and coulombic repulsion is crucial in development of thiazyl-based metal like materials. Situation in Figure 4b is ideal for π - radical stacks when W is bigger than coulombic repulsion.²⁶

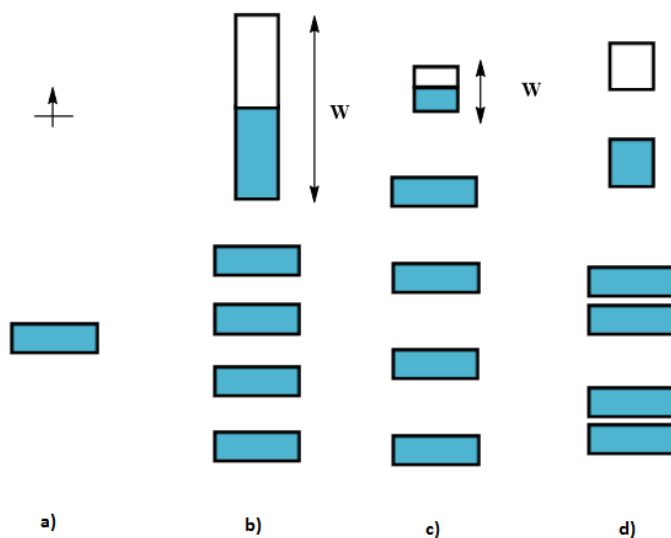
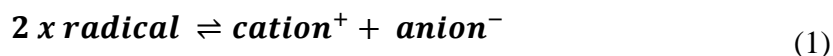


Figure 4. Schematic description of energy levels and related conduction bands: a) π -radical b) intensely interacting π - stack ($W > U$) c) weakly interacting π -stack ($W < U$) d) Peierl's distortion.²⁶

In chemical terms, weak Coulombic repulsion is expressed as small disproportionation energy ΔH_{disp} . The free energy of disproportionation reaction (1) should be as small as possible.²⁹



Cell potential (Equation 3) can be used as an indirect measure of disproportionation energy for reaction (1)

$$E_{\text{cell}} = - \{ E^{\text{ox}} - E^{\text{red}} \} \quad (3)$$

where E^{ox} is a half-cell potential for oxidation of radical to cation and E^{red} is a half-cell potential for reduction of radical to anion. Low disproportionation energy and cell potential value are required to facilitate good conductivity.²⁹

2.3 MAGNETIC MATERIALS

2.3.1 GENERAL CONSIDERATIONS OF MAGNETISM

Magnetic properties of matter arise from atomic-level events. A classical model of an atom pictures a negative electron orbiting positive nucleus thus creating a current loop. A microscopic current loop creates a microscopic magnetic dipole. However, orbital magnetic moments do not explain magnetism of material as several orbiting electrons cancel the net magnetic moment to close to zero. Material magnetism principally originates from the electron spin and alignment of (unpaired) electron spins. The magnetic flux is created by spin interactions.³⁰

Magnetic materials can be divided into classes based on the *magnetic flux* Φ . Magnetic flux describes the amount of magnetic field passing through certain area.³⁰ A *Diamagnetic* compound has less magnetic flux Φ inside the material than outside. In general, all materials have diamagnetic character but in some materials other magnetic phenomena are stronger than diamagnetism. Diamagnetic matter repulses externally applied magnetic field and aligns antiparallel to it (Figure 5). If material is *paramagnetic* or *antiferromagnetic*, magnetic flux inside the matter is marginally larger than outside. Antiferromagnets have dipole moments antiparallel to each other when paramagnets have arbitrarily oriented dipole moments. If Φ is notably larger inside the matter than outside, the material is called *ferromagnetic* or *ferrimagnetic*. Both ferromagnets and ferrimagnets have net magnetic dipole moment. Ferromagnets tend to align all the spins parallel to external applied magnetic field whereas in ferrimagnets the spins are aligned antiparallel to each other. However, in ferrimagnets the spins parallel to external magnetic field have larger magnetic moment and thus net magnetization does not cancel out (Figure 5).³¹

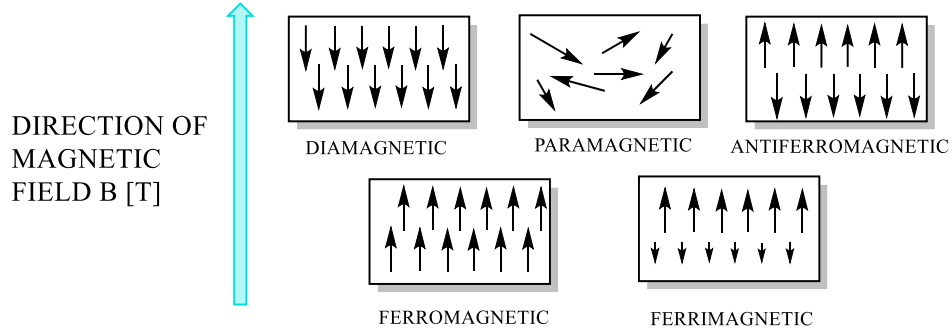


Figure 5. Alignment of spins in different materials in an external magnetic field.³¹

Susceptibility indicates how magnets act in an external applied magnetic field whether they are attracted or repelled. Susceptibility is defined as ratio in equation (4)

$$\chi = \frac{M}{H}, \quad (4)$$

where M is magnetization (emu) and H is magnetic field ($\text{cm}^3 \text{Oe}$). *Permeability* μ indicates how the material directs magnetic flux Φ and is defined by equation (5):

$$\mu = \frac{B}{H}, \quad (5)$$

where B is *magnetic induction* (in tesla, T). If magnetization is presented as a graph of M or B versus H , for paramagnetic, antiferromagnetic and diamagnetic materials magnetization plots are linear lines (Figure 6). Magnetization plots of ferromagnets and ferrimagnets behaves nonlinearly. The magnetization values can be 10^3 -times larger for ferro- and ferrimagnets than for para-, anti- and diamagnets. These three latter classes do not retain magnetization when magnetic field is removed. On the contrary, ferro- and ferrimagnets do retain magnetization.³¹

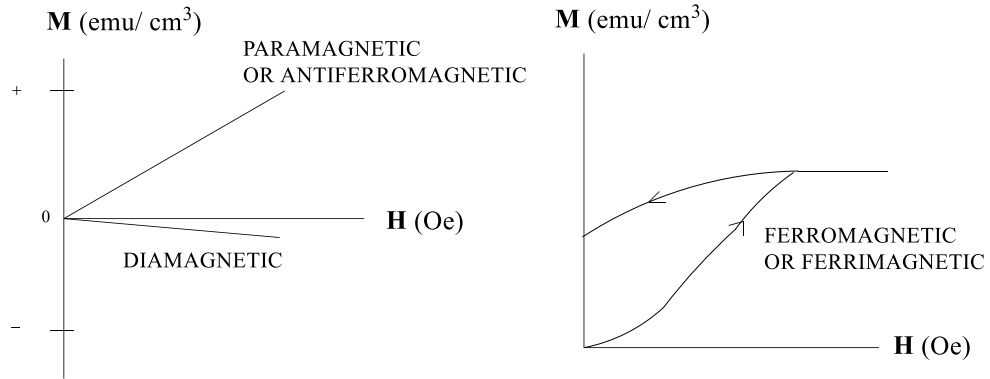


Figure 6. Magnetization is presented as a function of applied magnetic field. Magnetization behaves linearly for paramagnetic, antiferromagnetic and diamagnetic materials whereas for ferromagnetic and ferrimagnetic adopt magnetization curves.³¹

The quality of retaining magnetization is divided into two classes: soft and hard magnets. This concept is defined by Oliver Kahn as follows: “A magnetic material may present a magnetic hysteresis loop. When a sufficiently large magnetic field is applied, the magnetization becomes saturated. When the magnetic field is switched off, the magnetization does not vanish but takes a so-called remnant magnetization value. To suppress the magnetization, it is necessary to apply a certain field, called a *coercive field*, to the opposite direction. It is the coercivity which confers a memory effect on a magnet. A magnet is said to be soft or hard according to whether the coercive field is weak or large.”³² Schematic presentation of the hysteresis phenomenon is presented in Figure 7. Coercive field used for soft magnets is approximately less than 10 Oe and for hard magnets more than 100 Oe.³³

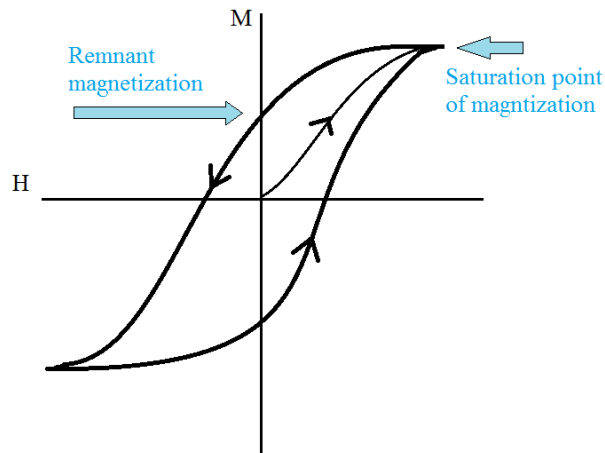


Figure 7. Hysteresis occur when external field is applied and magnet achieves a remnant magnetization. Coercive field is required to reverse magnetization.³³

2.3.2 MAGNETIC COUPLING

Magnetic coupling describes the ability of two distinct spins communicate magnetically via exchange pathways.⁹ Magnetic interaction is described by coupling term J and it acquires positive or negative values for the ferromagnetic or antiferromagnetic interaction, respectively.^{9,34} Ferromagnetic or antiferromagnetic coupling can increase or decrease the susceptibility.³³ Curie-Weiss law describes susceptibility and it is derived from Curie law which is an idealization and describes interactions between unpaired electrons well in low temperatures. However, hardly any system is ideal hence the *Weiss constant* Θ is used to improve validity of the susceptibility equation (7),

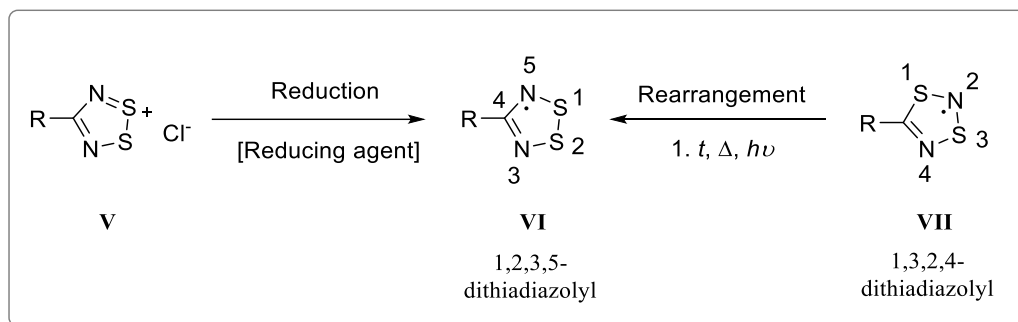
$$\chi = \frac{C}{(T - \Theta)}, \quad (7)$$

where C is a Curie constant and T is a temperature.³⁴ When coupling is ferromagnetic the susceptibility increases and Weiss constant, which express short-range interactions, is positive ($\Theta > 0$). With antiferromagnetic coupling the susceptibility decreases and Weiss constant gains negative values ($\Theta < 0$). Both of these magnetic interactions occur below a *critical temperature* T_c . The critical temperature is often called the Curie temperature (ferromagnets) or the Néel temperature (antiferromagnets). It is very important to notice that being a ferromagnet or showing ferromagnetic coupling are two distinct phenomena. A substance might have a ferromagnetic ordering but still display either antiferromagnetic or ferromagnetic coupling.³³

3 DITHIADIAZOLYL RADICALS

Dithiadiazolyls are important class of thiazyl radicals because of their high stability and relatively easy synthetic routes. Furthermore, their general structural features are well-known. When searching for a new class of conducting thiazyl based molecules, 1,2,3,5-

dithiadiazolyl (DTDA) were discovered in the 1970s and have been intensively studied since. Another group of dithiadiazolyls are 1,2,3,4-dithiadiazolyls. These compounds are not as well-studied as DTDA and are mostly known only from their rearrangement reactions.



Scheme 5. The two different synthetic routes to 1,2,3,5- DTDA. Reductions are done by using reducing agents *e.g.* octamethylferrocene, dimethylferrocene. **VII**'s rearrangement to **VI** can be induced thermally or photochemically but occurs also spontaneously at slow rate.⁵

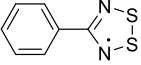
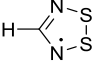
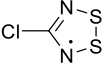
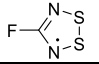
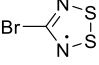
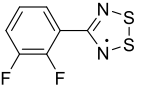
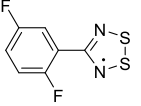
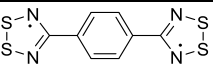
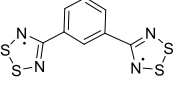
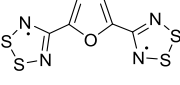
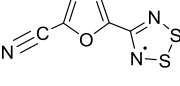
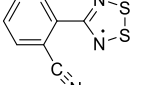
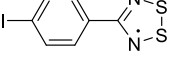
Synthetic routes to DTDA progress normally via cation **V** but can also proceed via rearrangement of 1,3,2,4- dithiadiazolyl **VII** (Scheme 5). There are few different approaches to prepare cationic **V**. The first ones utilized $\text{S}_3\text{N}_3\text{Cl}_3$ and its reactions with nitriles and diazenes but nowadays a common route is using sulfur monochloride with amidines or *N,N,N'*-tris(trimethylsilyl) derivatives. In the latter case the cycle formation is called the Herz condensation.⁵

The most common synthetic route to form 1,3,2,4-dithiadiazolyls is reduction from corresponding cations. The rearrangement of 1,3,2,4-dithiadiazolyls **VII** to 1,2,3,5-dithiadiazolyls **V** is promoted thermally or photochemically and R group was discovered to have a central effect on the speed of rearrangement. Electron withdrawing groups increase the speed of the rearrangement. On the other hand, electron rich R groups produced radicals that persisted days or weeks in solution.⁵

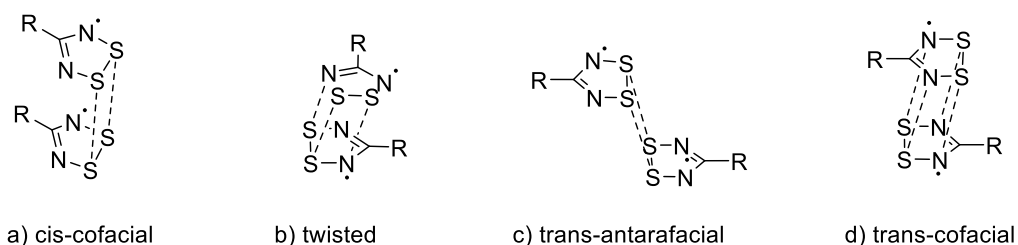
3.1 1,2,3,5-DITHIADIAZOLYL

The first studied DTDA consistently formed dimeric closed-shell species in the solid state whereas in solution state they were in equilibrium between radical and dimeric state.¹⁶ An early example of DTDA dimers is the 4-phenyl-1,2,3,5-dithiadiazolyl synthesized by Bannister *et al.*^{35,36} There are many other dimeric structures (Table 1) representing aromatic, heteroaromatic derivatives or having small R-groups (hydrogen, halogens).⁵ The tendency of DTDAs to dimerize can be suppressed by modifying the substituent in the 4-position of DTDA ring.; in general, the bulkier substituents the less prone DTDA is for dimerization.³⁷

Table 1. Selected DTDAs and their packing structures.

<i>Molecule</i>		<i>Dimers</i>	<i>Bond distances</i>	<i>Reference</i>
	VIII	<i>Cis</i> -cofacial	S–S: 3.402 Å	35
	IX	<i>Cis</i> -cofacial	S–S: 3.76 Å	38
	X	α : <i>Cis</i> -cofacial dimers, two molecules in asymmetric unit.	S–S: 3.004(1)Å and 3.138(1)Å Cl–Cl: 3.583 Å (vdw 3.56Å)	39
		β : Twisted dimer, four molecules in asymmetric unit.	S–S 3.145Å, 3.012Å No Cl–Cl contacts	39
		γ : <i>Cis</i> -cofacial dimer, eight molecules in asymmetric unit.	geometry similar to α S–S: 2.925-3.156 Å Cl–Cl contacts 3.500-3.566Å	39
	XI	<i>Cis</i> -cofacial	F–F: 3.265 Å (vdW 2.76Å)	40
	XII	Twisted dimer	S–S: 2.800 Å	40
	XIII	Twisted dimers	S–S: 3.020 (4)Å Mean plane separation: ca. 3.1 Å	41
	XIV	Uniformly spaced monomers	S–S: 3.544(3)Å Longer than “normal” distances in DTDAs but still shorter than vdw 3.6 Å	41
	XV	<i>Cis</i> -cofacial	S–S: 3.121 Å	42
	XVI	<i>Cis</i> -cofacial	S–S: 3.140 Å	42
	XVII	<i>Cis</i> -cofacial	S–S: 3.137 Å Furan-Furan: longer than S–S, bent formation	42
	XVIII	<i>Cis</i> -Cofacial packing	S–S: 3.126 Å. Head-to-tail CN–S contacts 3.048Å	42
	XIX	<i>Trans</i> -antarafacial	S–S: 3.121 (1) Å	43
	XX	<i>Trans</i> -cofacial	S–S: 3.696 Å	44

1,2,3,5-dithiadiazolyl radicals have four different known dimeric structures in solid-state: *cis*-cofacial, twisted, *trans*-antarafacial and *trans*-cofacial (Scheme 6). Sulfur-sulfur contacts between rings vary slightly depending on the packing. A *cis*-cofacial has S–S distances of *ca.* 3.0–3.1 Å when a twisted structure has one S–S interaction approximately 2.8–3.1 Å (Scheme 6).⁵ The most abundant arrangement is a *cis*-cofacial (Scheme 6). For example, compounds **VII**, **IX**, **X α** , **X γ** , **XI**, **XVI**, **XVII**, **XVIII** form *cis*-cofacial dimers (Table 1).^{5,35,38,39,40,42} The twisted structure is adopted when substituents are sterically demanding groups or halogens (**X β** , **XII**, **XIII**)(Table 1).^{5, 39, 40, 42} Only few radicals adopting *trans*-antarafacial or *trans*-cofacial are known. **XIX** is an example of *trans*-antarafacial and **XX** of *trans*-cofacial arrangement.^{5,43, 44}



Scheme 6. Four different packing structures which DTDAs adopt in solid-state. *Cis*-cofacial a) is the most abundant of these crystal structures of 1,2,3,5-dithiadiazolylys. Twisted structure b) is adopted by DTDAs with bulky or halogen substituents. *Trans*-antarafacial c) and *trans*-cofacial d) are not as common as the aforementioned structures.

The majority of 1,2,3,5- DTDAs form dimers like presented in Table 1 and are therefore closed shell species. There are some exceptions and one of the best known is radical **XXI**. **XXI** (Figure 8) displayed decreased tendency to dimerize because of rigorously chosen substituents and showed weak ferromagnetic behaviour at 36 K. The majority of known odd-electron species undergo ferromagnetic ordering below 1 K and **XXI** was the first main-group radical, which ordered above 1 K.⁴⁵ There were two main characters achieved from well-chosen substituents: the competing interactions and the repulsions between molecules. Cyano-sulfur interactions suppressed dimerization by competing with dimer formation between NSSN fragments whereas fluorine-fluorine repulsions prevent dimerization through phenyl rings.⁴⁵

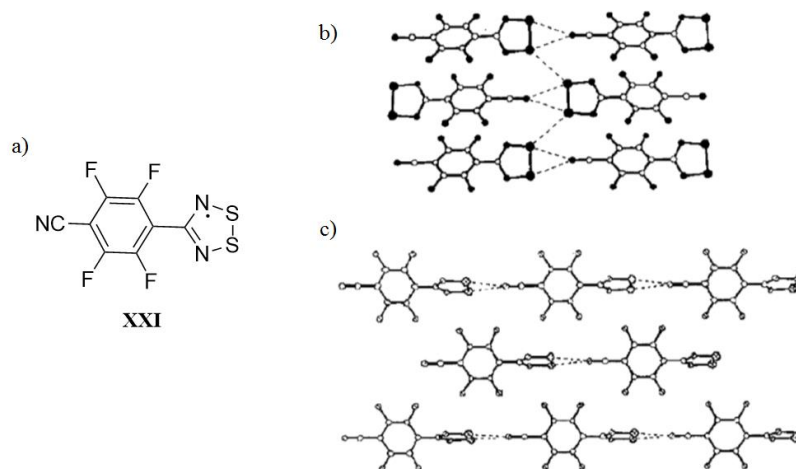


Figure 8. a) 4-(4-cyano-2,3,5,6-tetrafluorophenyl)-1,2,3,5-dithiadiazolyl radical **XXI** shows ferromagnetic like behaviour at 36 K. b) Packing structure of alpha-phase **XXI** and c) beta-phase **XXI** in crystal lattice.⁴⁶

Molecule **XXI** has two polymorphs: α - and β -phase and by varying sublimation conditions the phase formation was controlled. α - and β -phases have different twist-angles between heterocycle and the plane of fluorinated aryl ring. α - phase has a twist-angle of 32° and intermolecular CN–S interaction between 3.068 \AA and 3.105 \AA . For β -phase the same values were 58° and distance between CN group and sulfur was 2.986 \AA . α -phase is not as symmetrical as β -phase. In beta-structure all the chains were aligned in the same direction but the alpha had antiparallel organization in solid state (Figure 8).⁴⁵

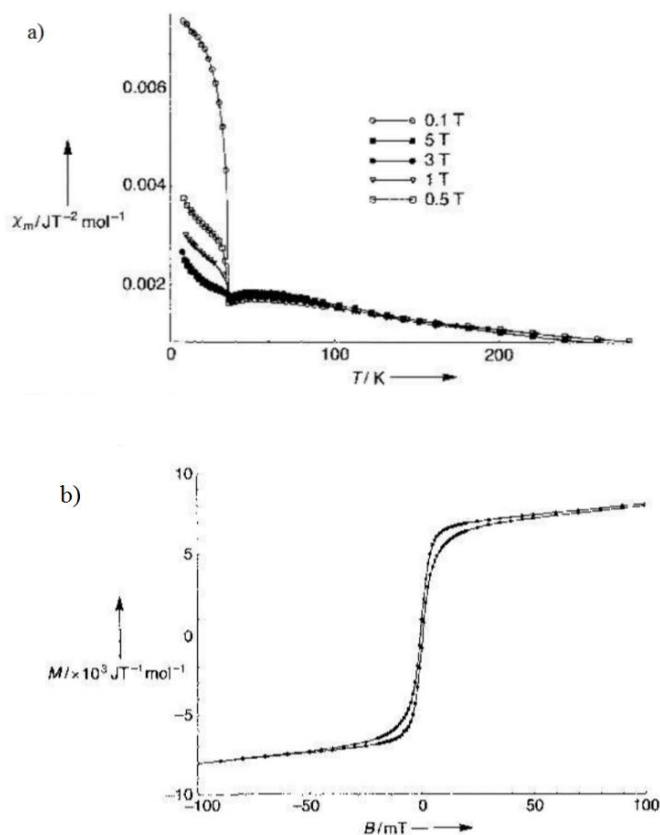


Figure 9. a) Beta-phase shows saturated magnetization towards 0 K in the plot. Molar magnetic susceptibility is presented as a function of employed magnetic field and temperature. b) Beta- phase retains slight amount of magnetization.⁴⁵

The solid state structure of **XXI** α -phase is a head-to-tail packed (Figure 8) and showed paramagnetic behaviour at room temperature with a magnetic moment $1.60 \mu_B$ following Curie-Weiss framework. β -phase was measured to have an effective magnetic moment of $1.55 \mu_B$ which is slightly less than expected spin-only moment of $1.73 \mu_B$ and Weiss constant of 102 K was derived from susceptibility versus temperature plot by extrapolation above 120 K (Figure 9). β -phase showed increasing magnetization below 36 K and saturated towards 0 K (Figure 9) and was also discussed to demonstrate spin-canting^{ii, 45}

ⁱⁱ Compound's ground state is antiferromagnetic yet spins are not completely aligned but are slightly perturbed. Due to spin canting, material shows weak residual magnetic moment.³²

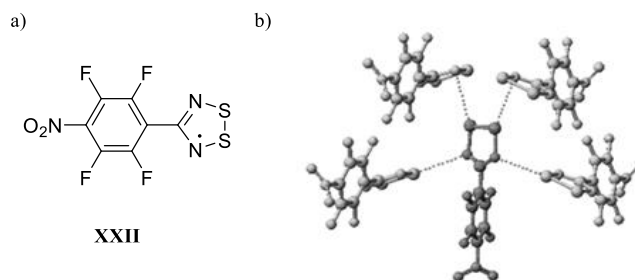
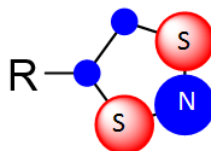


Figure 10. a) The 4-(4-nitrophenyl-2,3,5,6-tetrafluoro)-1,2,3,5-dithiadiazolyl radical **XXII**.
 b) the crystal structure of **XXII**. Contacts between nitrogens and sulfurs mediated ferromagnetic interaction observed. Reprinted from “A Thiazyl-Based Organic Ferromagnet” by Antonio Alberola, Robert J. Less, Christopher M. Pask, Jeremy M. Rawson, Fernando Palacio, Patricia Oliete, Carley Paulsen, Akira Yamaguchi, Robert D. Farley, D. M. Murphy, 2003, *Angewandte Chemie International Edition*, Copyright © 2003 WILEY-VCH Verlag GmbH & Co. KGaA, Weinheim

Another magnetically interesting example of DTDA- radicals is closely related to molecule **XXI** where only alteration is that nitrile group is changed to nitro group ($-\text{NO}_2$). This radical has also ordering temperature above 1 K. Due to nearly orthogonal S–N interactions (3.681 \AA) between heterocycles (Figure 10) led to ferromagnetic interaction between the radicals.⁴⁷

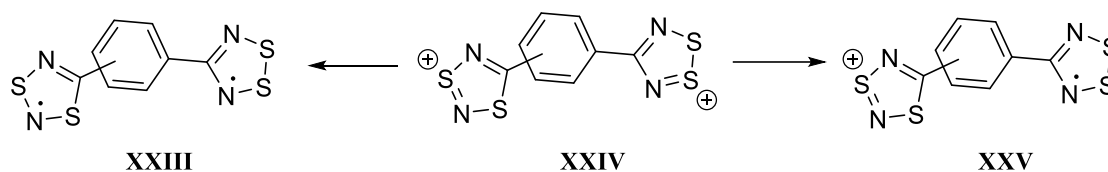
3.2 1,3,2,4-DITHIADIAZOLYL

EPR spectra of 1,3,2,4-DTDAs have hyperfine coupling values approximately 11 G for the triplet resulting from nitrogen squeezed between two sulfurs. Antibonding π orbital is significantly localised on SNS moiety (Scheme 7) and therefore coupling to nitrogen next to carbon is smaller ($0.5\text{-}0.6\text{G}$).⁵



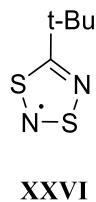
Scheme 7. Antibonding π -orbital of 1,3,2,4-DTDA.

Several *polyradical* 1,3,2,4-dithiadiazolyls have been reported and generally they consist a phenyl bridge. Also the polyradicals rearrange slowly and form 1,2,3,5-DTDAs. Hybrid dications have been synthesized by Banister *et al.* (compound **XXIV** in Scheme 8) from 1,3,2,4-dithiadiazolyls and 1,2,3,5-dithiadiazolyls and have been reduced further to form the diradicals.⁴⁸ Interestingly, 1,3,2,4-DTDA and 1,2,3,5-DTDA have distinct reduction potentials and 1,3,2,4-DTDAs can be reduced in much lower potentials than comparable 1,2,3,5-DTDAs. This property enables partial reduction producing radical cation **XXV** (Scheme 8).



Scheme 8. Formation of hybrid diradical **XXIII** from analogous dication **XXIV**. Compound **XXIV** can be partially reduced to afford radical cation **XXV**.

Conductive and magnetic liquids have been vastly studied for inorganic systems but only very few organic paramagnetic ionic liquids exist. 1,3,2,4-DTDAs are present in this class and compound **XXVI** has showed paramagnetic liquid behaviour at room temperature.²⁸



Scheme 9. Compound **XXVI** is paramagnetic liquid at room temperature.²⁸

4 DITHIAZOLYL RADICALS

1,3,2-dithiazolyls (DTA) were spectroscopically observed in the 1970s as by-products from the reactions of S_4N_4 and S_4N_2 with alkynes. The synthetic procedures of DTAs have developed since and the modern routes are much more practical.

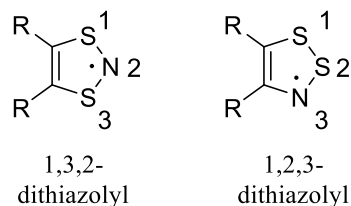
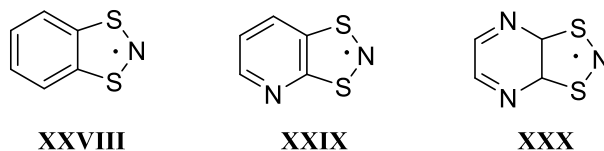


Figure 11. General structures and numbering of 1,3,2-dithiazolyl and 1,2,3-dithiazolyl.

Commonly 1,3,2-dithiazolyl radical and 1,2,3-dithiazolyl proceeds via reduction of a corresponding cation (Scheme 10). Development of 1,2,3-dithiazolyls further has relied heavily on the research of Oakley and co-workers.

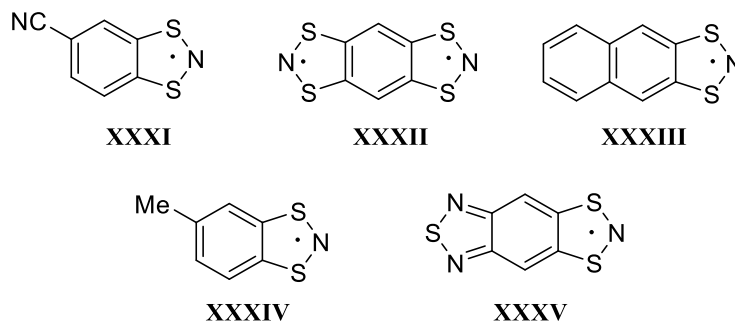
4.1 1,3,2- DITHIAZOLYL

The electrochemical studies (cyclic voltammetry) of radicals are important due to investigation of conductivity. From the electrochemical analysis of 1,3,2-dithiazolyls it has been observed that oxidation and reduction potentials depend on whether radical includes electron withdrawing or electron donating atoms or groups. If radical contains electron rich groups, oxidation potentials tend to be low and if electron withdrawing groups are present, the potentials tend to reverse. For example the oxidation potential of **XXVIII**, **XXIX**, **XXX** are +0.15 V, +0.30 V, and +0.53V, respectively.



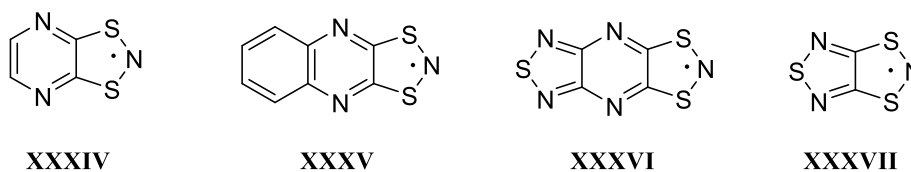
Scheme 10. 1,3,2-dithiazolyl radicals **XXVIII**, **XXIX** and **XXX** have a difference in oxidation values due to different electronic structures.

Like DTDAs also 1,3,2-DTAs have a tendency to dimerize. Generally 1,3,2-DTAs adopt cofacial arrangements but also rare centrosymmetric arrangement has been observed for radical **XXVIII**. However, there exists certain 1,3,2-DTAs that remain monomers in solid-state at the room temperature. Illustrative examples such a monomeric radicals are **XXXI**, **XXXII**, **XXXIII**, **XXXIV** and **XXXV**.⁵ In fact, **XXXV** consisted of undimerized and dimerized antiparallel chains in the asymmetric unit.⁴⁹



Scheme 11. Benzo-fused odd-electron monomers.⁴⁹

1,3,2-DTA **XXXII** has a herringbone arrangement in the solid-state and it shows paramagnetic behaviour at room temperature. Adjoining rings of **XXXII** display edge-to-face alignment but this feature disappears when structure is modified by changing two benzene rings to nitrogen containing pyrazine **XXXIV** or quinoxaline **XXXV** derivatives.⁴⁹



Scheme 12. Examples of 1,3,2-DTAs fused with heterocycles.

Interestingly, molecules **XXXIV** and **XXXVII** have shown magnetic bistability. These radicals have two different temperature dependent conformations and thus two different magnetic states.⁴⁹ Monomers were paramagnetic while the dimer stacks were diamagnetic. Compound **XXXVII**, referred as 1,3,5-trithia-2,4,6-triapentalenyl (*TTTA*) in the literature, showed paramagnetic behaviour at room temperature but when temperature was lowered the susceptibility started to decrease. At temperature between 300 K and 230 K the drop

was only minor but after 230 K the susceptibility started to reduce considerably quickly (Figure 12).⁸

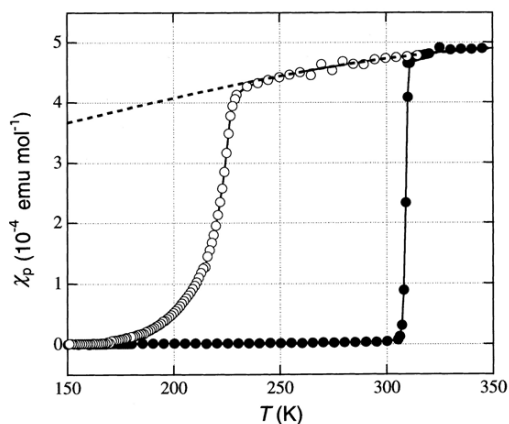


Figure 12. Hysteresis loop of **XXXVII**. Open circles describe cooling process behaviour and filled circles describe behaviour upon heating. Reprinted from “Room-Temperature Magnetic Bistability in Organic Radical Crystals” by Wataru Fujita and Kunio Awaga, 1999, Science, Copyright © 1999, The American Association for the Advancement of Science.

At 170 K, the susceptibility became zero and below this temperature, **XXXVII** was diamagnetic. Furthermore, **XXXVII** has a wide hysteresis loop since susceptibility remains at zero up to 300 K during the heating and experienced a rapid increase at 305 K. The structural investigations revealed two divergent structures. High-temperature polymorph arranges uniformly divided stack of single radicals, whereas low-temperature polymorph forms S–S' interactions between two radicals that leads to dimeric stacking structure.⁸

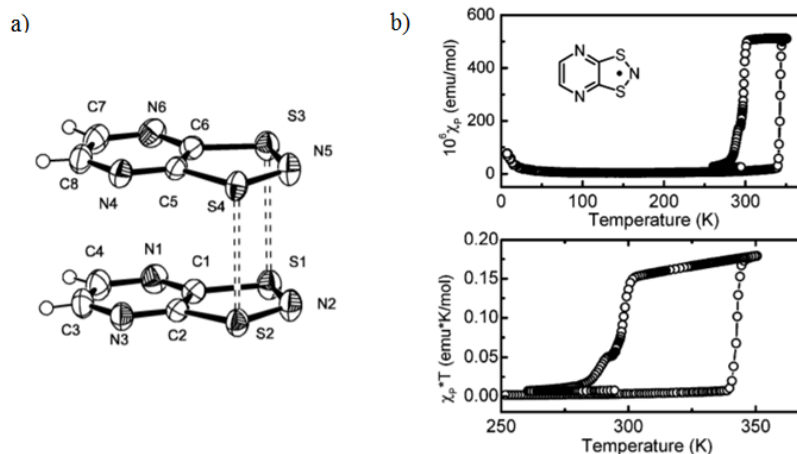


Figure 13. a) Dimeric structure of **XXXIV** exists at low temperatures. Crystal structure is presented with 50 % probability ellipsoids. b) Hysteresis loop for **XXXIV**. Reprinted from “Bistabilities in 1,3,2-Dithiazolyl Radicals” by Jaclyn L. Brusso, Owen P. Clements, Robert C. Haddon *et al.*, 2004, American Chemical Society, Copyright © 2004, American Chemical Society.⁴⁹

In addition, **XXXIV** showed also bistability. From Hysteresis loop of radical **XXXIV** (Figure 13) was seen that the compound was diamagnetic below room temperature. Until 340 K there was no increase in the susceptibility, but after 340 K the incline was rather steep. When the compound was heated to 350 K paramagnetism reached its saturation point. As the sample was cooled down it retained magnetization, but from 300 K to lower temperatures the susceptibility declined sharply and became diamagnetic. This differing behaviour of two dissimilar magnetic states is due to transformation between diamagnetic dimers at low temperatures and dissociated radical monomers at higher temperatures.⁴⁹

4.2 1,2,3-DITHIAZOLYL

The variation of different substituent is essential in the research of all the thiazyls as the groups have an effect on the features of the radicals. The 1,2,3-dithiazolyls can be monocycles or attached to another groups such as phenyl groups or pyridines. EPR spectra of 1,2,3-dithiazolyls show large variation in hyperfine coupling constants depending strongly on substituents and values can vary from 4.5 G to 8.0 G. SOMO of 1,2,3-

dithiazolyl radical is antibonding and nodal plane of SOMO goes through carbon-4 atom adjacent to nitrogen atom and has no significant spin density (Figure 14). Nevertheless, carbon-5 has a large spin contribution which allows spin delocalization to R₁ substituent or attached group. Reactivity and electronic structure are highly influenced by this feature and spin can delocalize over the constructed framework *i.e.* π - framework. Carbon-5 spin contribution makes 1,2,3- dithiazolyls so reactive that they are hard to isolate.⁵

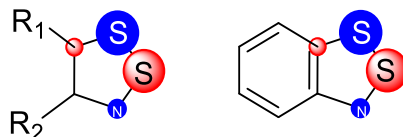
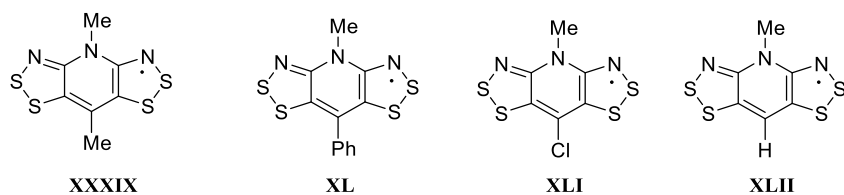


Figure 14. The π -symmetric SOMO of 1,2,3-dithiazolyl. Spin density on C5 increases the reactivity of DTA.⁵

1,2,3- dithiazolyl radicals adopt four different kind of dimeric structures. *Cis*-cofacial dimer structure, cofacial centrocymmetric, twisted gauche and slipped π -stack structures have been reported. Intriguing fact is that dimerized derivatives have longer S–S interactions between rings than S–S distances in other thiazyl dimers.⁵

4.2.1 DITHIAZOLODITHIAZOLYL

A category of different fused compounds such as dithiazolodithiazolyls (also referred as bis-DTAs) and dithiazolothiadiazinyls are considered under a hypernym of 1,2,3-dithiazolyls. Dithiazolodithiazolyls were developed by Oakley and co-workers from the 1990s to this moment in an effort to improve molecular conductive materials. Their aim was to develop material which has π -stacks composed of radicals to achieve high *W/U* ratio and thus mimic the electron transfer features of metals.²⁶ One approach was to combine two dithiazolyls together with pyridine ring that lead to the synthesis of dithiazolodithiazolyls.⁵⁰



Scheme 13. Four bis-DTAs with various R_2 (=Me, Ph, Cl and H) substituents were studied.

Bis(dithiazolodithiazolyl) (bis-DTA, Scheme 13) radicals were investigated when Oakley and co-workers constructed a radical with four different R_2 substituents (**XXXIX**, **XL**, **XLI** and **XLII**) and examined their effects on crystal packing. These radicals had anticipated low disproportionation enthalpy values (ΔH_{dis}) and crystal structure showed S-S interaction network which affected positively to W/U ratio. Even though sulfur interactions increased the bandwidth (W), Mott's insulation features dominated and the conductivity was $\approx 10^{-5}$ S cm^{-1} at room temperature for both compounds **XXXIX** and **XL**. Substituents R_1 and R_2 were suspected not to have much effect on U but they could affect bandwidth via changes in crystal packing. In solid-state, bis-DTA **XXXIX** was stacked to layers. Between adjacent radicals S1–S1' interactions were formed and distances (3.368(2) Å) were within van der Waals interaction (3.6 Å). Between the chains there is no S–S contacts *i.e.* these interactions are observed only within the chains (Figure 15 a). Methyl groups were also found to prevent these interactions. When R_2 substituent was changed to Cl or H, solid-state structure **XLI** and **XLII** adopted zig-zag orientation (Figure 15 b). **XL** also had the same zig-zag structure as presented in Figure 15 b) parallel to xy plane.⁵⁰

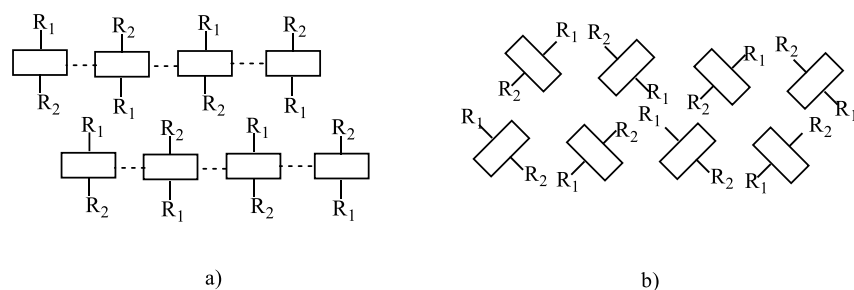


Figure 15. Slipped π -stacks of **XXXIX** have been oriented in chains in x -axis. S1–S1' interactions have been indicated with dashed lines a). When R_2 substituent is changed to H or Cl and implements zig-zag formation b).⁵⁰

Large phenyl groups cause **XL** to adopt unusual “wheel” arrangement (Figure 16) and methyl and phenyl groups are oriented towards the centre of the wheel. There is a node where three different wheels join together and this node forms a triangle through S–S’ interactions. S1–S2’ interaction within the node, between two adjacent radicals, have distances d_2 (3.507(1) Å) and d_3 (3.467(1) Å). At the time of publication, S1–S1’ (d_1) exhibited the shortest known sulfur–sulfur distance (3.287(1) Å) for undimerized thiazyl structure.⁵⁰

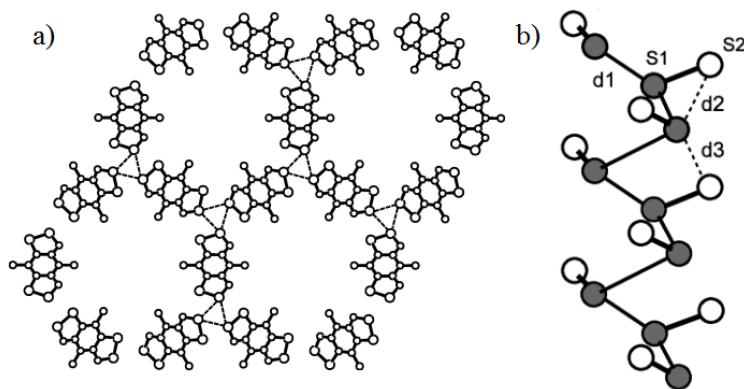


Figure 16. a) The “wheel” structure of **XL**. The radical is pictured in xy plane and phenyl groups are omitted for clarity. b) Distances d_1 , d_2 and d_3 presented. Reprinted from “Dithiazolodithiazolyl Radicals: Substituent Effects on Solid State Structures and Properties” by Leanne Beer, James F. Britten, Owen P. Clements *et al.*, 2004, American Chemical Society, Copyright © 2004, American Chemical Society.⁵⁰

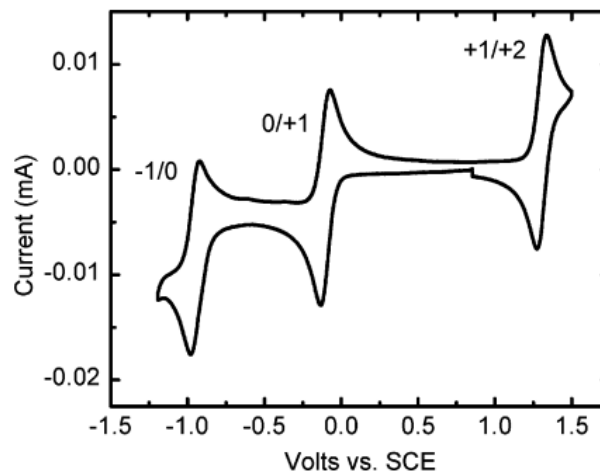


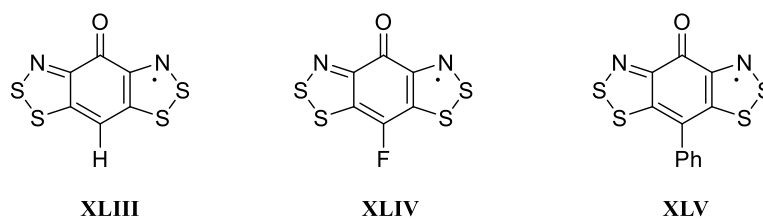
Figure 17. Cyclic voltammetry of **XL** in CH_3CN with $[n\text{-Bu}_4\text{N}]\text{-[PF}_6\text{]}$ as a supporting electrolyte. Reprinted from “Dithiazolodithiazolyl Radicals: Substituent Effects on Solid State Structures and Properties” by Leanne Beer, James F. Britten, Owen P. Clements *et al.*, 2004, American Chemical Society, Copyright © 2004, American Chemical Society.⁵⁰

Electrochemistry of bis-DTAs was also examined. In cyclic voltammetry measurements three reversible waves $^{-1}/_0$, $^0/_{+1}$ and $^{+1}/_{+2}$ were observed for radicals **XL** and **XLI** (Figure 17). **XXXIX** and **XLII** also showed similar wave pattern but the cycle was irreversible. This feature was suspected to occur due to **XL** (Ph) and **XLI** (Cl) having more electronegative substituents compared to **XXXIX** (Me) and **XLII** (H). Also the S-S bond gets cleaved more readily on the two latter compounds. Even though the electronic bandwidth increased, still W/U ratio was too small to overcome Mott’s insulating state.⁵⁰

4.2.2 EFFECTS OF PRESSURE ON BIS(DITHIAZOLYL) RADICALS

The main approach to enrich the properties of thiazyls have been the modification of crystal packing by altering building blocks of radicals and varying the substituents. Oakley and co-workers published results in 2015 from a study of pressure affecting to the crystal packing of radicals and their conductivity. Radicals with three different substituents were examined: hydrogen (**XLIII**), fluorine (**XLIV**) and phenyl group (**XLV**) (Scheme 14). One main objective was to investigate the change in packing by changing the amino group to carbonyl

group and see how the structural packing of bis- DTAs (**XXXIX-XLII**) alters. Also the effect of pressure on solid-state packing was studied.⁵¹



Scheme 14. The structures of oxobenzenebridged bisdithiazolyl radicals **XLIII**, **XLIV**, **XLV**.

It was noticed that when the pressure was increased, the solid-state structures of all three species were compressed. **XLIII** underwent two structural phase changes from its initial 1D slipped π -architecture. **XLIV** and **XLV** retained their solid-state conformations having quasi- 2D brick-wall and 1D π -stacked structures, respectively (Scheme 13). The pressure was varied from 0 GPa to 15 GPa and the pressure change increased the conductivity at room temperature (Figure 19). The pressure reliance of conductivity was observed for all bis-DTAs **XLIII**, **XLIV** and **XLV** and conductivity was from 10^{-4} to 10^{-2} S cm^{-1} .⁵¹

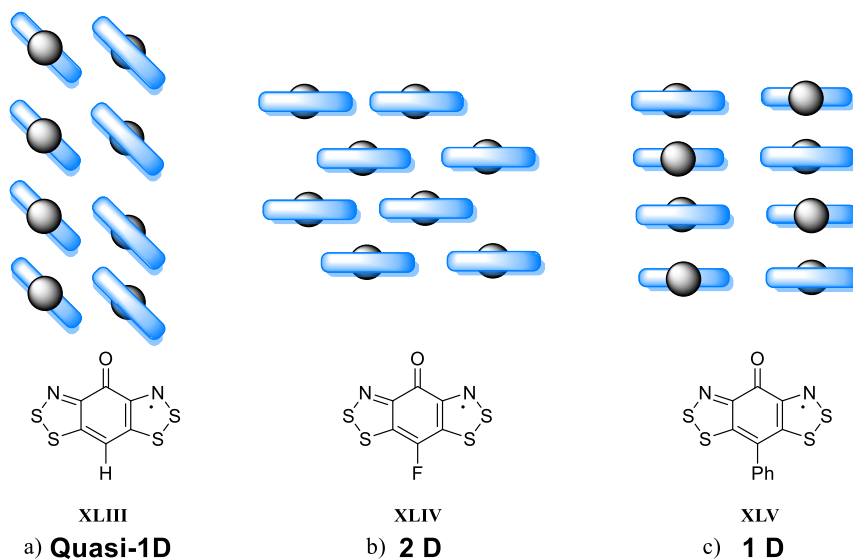


Figure 18. The crystal packing of **XLIII**, **XLIV** and **XLV**. The grey ball indicates oxygen. Packing structures are a) quasi-1D slipped ribbon π -stacks (**XLIII**) and b) quasi- 2D brick-wall π -stacks (**XLIV**) c) 1D π -stacks (**XLV**).⁵¹

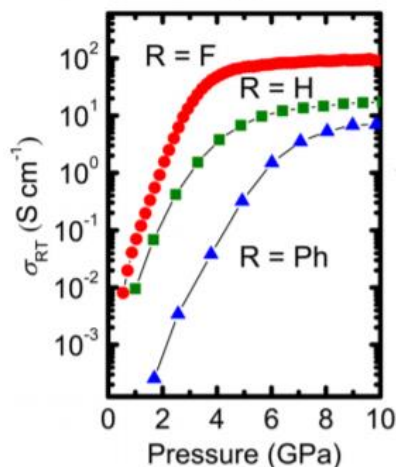


Figure 19. Conductivity at room temperature as a function of pressure for **XLIII**, **XLIV** and **XLV**. Reprinted from “The Metallic State in Neutral Radical Conductors: Dimensionality, Pressure and Multiple Orbital Effects” by Di Tian, Stephen M. Winter, Aaron Mailman, et al, 2013, American Chemical Society, Copyright © 2015, American Chemical Society.

It was assumed that radicals **XLII**, **XLIV** and **XLV** containing amino groups have quite similar electronic properties as radicals **XXXIX**, **XL**, **XLI** and **XLII** having carbonyl groups. Naturally, the packing was changed since amino group was changed to carbonyl group. However, the coulombic repulsion (U) values were expected to be close to ones observed for **XXXIX**, **XL**, **XLI** and **XLII**. It should be noted that changing the amino group to carbonyl group was expected to be isolobal. *Isolobal principle* means a method in which inorganic and organic fragments can be related to estimate for example bonding properties (e.g. MnH_5^{5-} and methyl radical). Isolobal fragments are not isostructural or isoelectronic but they have resembling frontier orbitals which can be utilized to predict the behavior and bonding.⁵² Nevertheless, the observed U values were not equal as expected from DFT calculations. The observed cell potential for example for **XLII** was 0.78 V⁵⁰ while for analogous carbonyl substituted compound **XLIII** had cell potential of only 0.56 V.⁵¹ Difference between calculated and observed values revealed an essential change in electronic structures of **XLII** and **XLIII**. EPR studies revealed that the SOMO of both compounds was alike. The difference became from antibonding π -orbital of the carbonyl group that causes π -type LUMO drop in energy. Low-lying empty π -LUMO of carbonyl effects on magnetic and charge transport properties of **XLII**, **XLVI** and **XLV**. Charge

transport is influenced by two distinct effects. Firstly, the electrons can avoid each other more easily because of the second orbital influence (low-lying LUMO). Secondly, the conductivity is enhanced because of an extra option for electron to advance.⁵¹

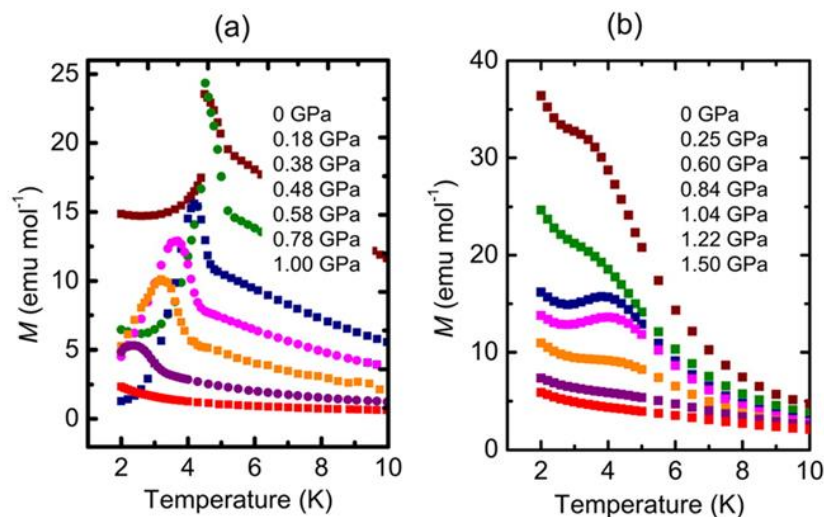


Figure 20. Zero-field-cooled (ZFC) magnetization measurement for a) **XLV** and b) **XLIV**

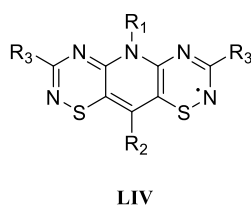
Magnetization (emu mol⁻¹) is plotted against temperature as a function of pressure.

Reprinted from “The Metallic State in Neutral Radical Conductors: Dimensionality, Pressure and Multiple Orbital Effects” by Di Tian, Stephen M. Winter, Aaron Mailman, et al, 2013, American Chemical Society, Copyright © 2015, American Chemical Society.⁵¹

Magnetic measurements were performed for radicals ranging the pressure from 0.0 to 1.5 GPa. It was observed that all three compounds ordered as spin-canted antiferromagnets. The ordering temperatures decreased as a function of a pressure and the susceptibility had the same trend. **XLV** obtained almost identical results with **XLIV**. The magnetization decreased when pressure was increased and at the same time ordering temperature fled closer to 0 K (**Figure 20**). The ordering temperatures were 13 K for **XLIV** and 4.5 K for **XLV**. For **XLIII** the magnetization was also diminished but the ordering temperature did not vary as much as for **XLV** (**Figure 20**). For **XLII** the ordering temperature was 4 K.⁵¹

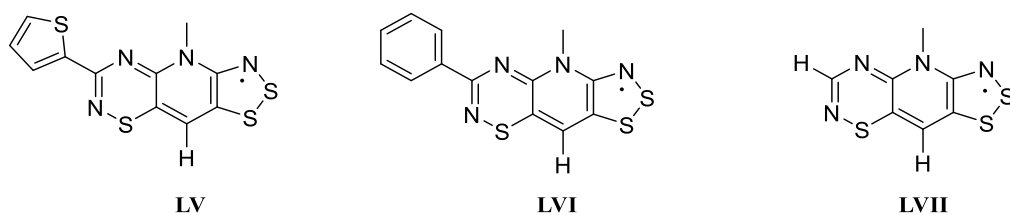
4.2.3 EFFECT OF LIGHT, HEAT OR PRESSURE ON RADICAL AND DIMER STATES

Promising results were gained from magnetic and conductive measurements of bis-DTAs **XXXIX-XLII** (Scheme 13).⁵⁰ Another thiazyl group investigated was bisdithiazinyls (bis-TDAs, **Scheme 15**). The R₃-substituents of bis-TDA was found to decrease the bandwidth because of partly blocked intermolecular overlap and they did not conduct electricity especially well (σ (300K) < 10⁻⁷ S cm⁻¹).⁵³ Nevertheless, R₃ substituents could assist the solid-state packing and therefore have a beneficial effect on U.¹



Scheme 15. General structure of bisdithiazinyl.

A new subgroup of thiazyls was created when dithiazolyl and thiadiazinyl were combined in the same radical forming dithiazolothiadiazinyls (Scheme 16). The hope was to enhance the conductivity and obtain the best features from these two radicals in one molecule.



Scheme 16. Three dithiazolothiadiazinyls with different R₃ substituents:

LV=Thiophene(Th), **LVI**=phenyl and **LVII**=hydrogen.

Reversible cell potentials were not achieved for molecules **LV**, **LVI**, **LVII** but the values were evaluated from the difference between E_{pc} peaks (E_{pc} peaks are cathodic peaks in cyclic voltammetry). Radical **LV** adopted π – stacked structure where distance between planes was $d = 3.452(2)$ Å. Radical **LVI** on the other hand had a herringbone organization with π -stacked interactions ($d = 3.434(6)$ Å) and close S1- S2' interactions ($d = 3.487(3)$ Å). The DTA radicals are linked to adjacent radical motifs via close S1- S2' interactions.

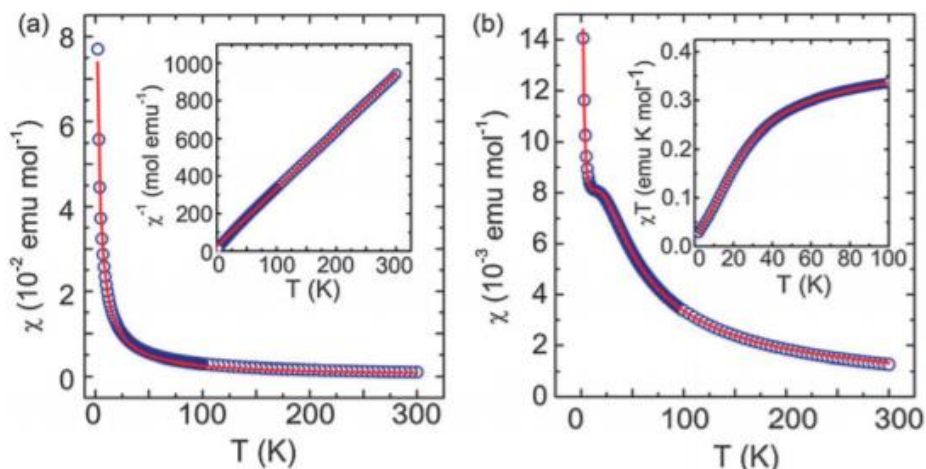


Figure 21. Susceptibility of a) **LV** and b) **LVII** presented as a function of temperature. Reprinted from “Hybrid dithiazolothiadiazinyl radicals; versatile building blocks for magnetic and conductive materials” by Stephen M. Winter, Aidin R. Balo, Ryan J. Roberts, Kristina Legin, Abdeljalil Assoud, Paul A. Dube, Richard T. Oakley, 2013, Royal Society of Chemistry, Copyright © 2013 Royal Society of Chemistry.

The magnetic susceptibility χ was examined and neither **LV** nor **LVI** were Peierls distortedⁱⁱⁱ (Figure 21). Radicals (**LV**) magnetic exchanges were studied by using calculations of different methods (broken symmetry DFT and quantum Monte Carlo simulation). Interactions between S1–S3' ties three neighbor ribbons and interactions have ferromagnetic character. Radical **LVI** showed anti-ferromagnetic coupling and therefore could act as an antiferromagnetically coupled Curie-Weiss paramagnet ($\theta = -8.4$ K).¹

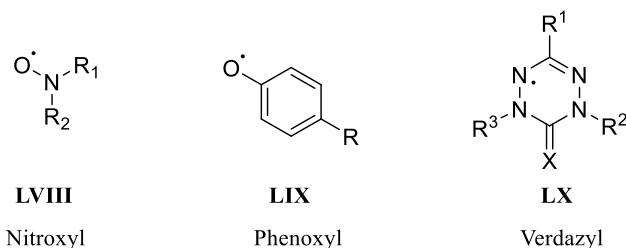
ⁱⁱⁱ “Distortion of a regular one-dimensional structure with a partially occupied band to give bond alternation, eventually leading to dimerization or oligomerization... The Peierls distortion for chain compounds is analogous to the Jahn–Teller effect for molecules.”⁷⁶

5 COORDINATION COMPOUNDS OF THIAZYL

Magnetic properties of radicals can be enhanced for example by developing new frameworks, changing substituents or producing new hybrid materials. Another approach is magnetically coupled systems. The spin on the odd-electron ligand can be a bridge between two or more paramagnetic metal centres and, thus, act as an exchange coupler. Another aspect of using radical ligands in coordination complexes is to increase total spin of the system.

Radical-metal complexes can be used as model systems for magnetic coupling. This fundamental knowledge can help developing new materials such as molecular magnets. Another interesting application is bioinorganic processes that can be modelled using coordination compounds of radicals as many metalloproteins contain radical ligands. Third appealing angle of radical-metal complexes is their viable use as redox active molecules. This is because many organic odd-electron compounds can be one-electron oxidized or reduced affording more than one stable oxidation states often as a reversible process.¹³ Redox active ligands are also called as non-innocent.⁵⁴

Typical radicals that have been used in metal-radical complexes are nitroxyls, phenoxy and verdazyls (Scheme 17). Nitroxyls **LVIII** form stable complexes with most transition metals. Phenoxy **LIX** form coordination compounds for example with vanadium, chromium, manganese and iron.⁵ In addition, coordination compounds containing verdazyl radicals **LX** have been extensively studied.^{5,55} The research amongst thiazyl radical metal complexes is somewhat new research area even though the other radical-metal complexes are relatively broadly known.¹³



Scheme 17. The generic structures of nitroxyl, phenoxy and verdazyl groups. Their coordination compounds are relatively well known. There are two main approaches to the

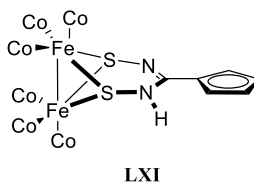
coordination of thiazyls. Either the neutral thiazyls are coordinated with neutral metal-containing moiety or metal anion is interacting with thiazyl cation. Coordination of thiazyls has focused mainly on 1,2,3,5-dithiadiazolyls and 1,3,2-dithiazolyls.¹³

5.1 COORDINATION COMPLEXES OF 1,2,3,5-DITHIADIAZOLYLS

The peculiar property of 1,2,3,5-dithiadiazolyls is that they consist two different heteroatoms (N and S) and the spin density is distributed over both of these atoms. Because N and S can act as donors to metal there are two main categories 1,2,3,5-dithiadiazolyl **V** complexes. The others are coordinated via sulfur and the others via nitrogen to the metal.

5.1.1 COORDINATION OF 1,2,3,5-DITHIADIAZOLYLS VIA SULFUR ATOMS

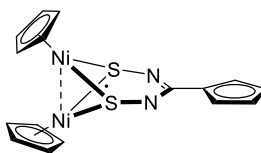
The first metal coordination compound of thiazyls was **LXI** which was synthesized by reaction of **V** (R=Ph) and $\text{Fe}_2(\text{CO})_9$ or $\text{Fe}_3(\text{CO})_{12}$.⁵⁶ Interesting phenomenon was observed with the coordination. Molecule **LXI** had remarkably longer S–S distances (2.930(2) Å) than thiazyl **V** (R=Ph) had in its dimeric structure (~ 2.1 Å). It was suspected that S–S bond breaks due to complex formation. Subsequently it was found out that one of the two nitrogens had abstracted hydrogen as shown by ^1H NMR and IR-spectroscopy. Hence, eventually **LXI** was not a radical species anymore but a closed shell molecule related to imines.



Scheme 18. The complex formed of 1,2,3,5-DTDA and iron.

Resembling structure **LXII** was obtained when the metal was changed to nickel; the S-S (2.905(2) Å) bond distance was again elongated compared to **V** (~ 2.1 Å). However, contrast to **LXI**, **LXII** did not abstract hydrogen and retained its open shell structures. Spin density was mainly delocalized over the nickel, sulfur and carbon atoms and marginal

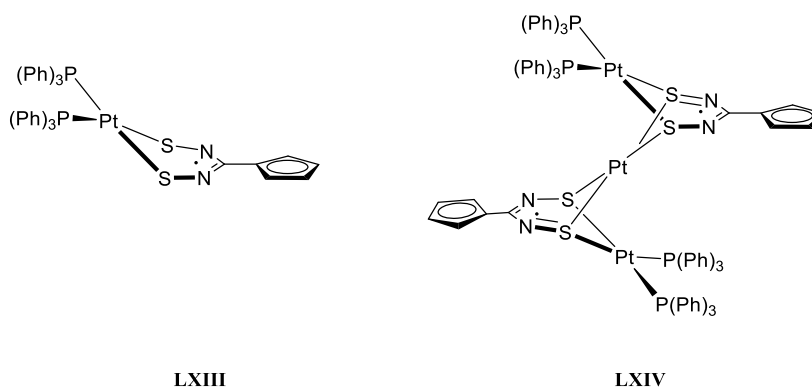
contribution remained on nitrogen. This finding was determined by EPR-spectroscopy and extended Hückel molecular orbital calculations. The electron count of thiazyl was justified to be $6 e^-$. Thiazyl acted as an electron donor ligand. Consequently, thiazyl seemed to be better described as an odd-electron donor and spin density was more localized on the metal part of the molecule.¹³



LXII

Scheme 19. Complex formed from 1,2,3,5-DTDA and nickel.

Another kind of coordination geometry was observed for **LXIII** from the reaction of **V** ($R=Ph$) with $Pt(PPh_3)_3$. During the reaction S-S bond breaks and platinum forms two bonds with sulfurs and two triphenylphosphines stay intact. Platinum centre had pseudo-square planar coordination geometry but the whole molecule was not planar (Scheme 20). To optimize N-S-Pt bond angle, the platinum atom is oriented out of the plane. The complex was defined to be paramagnetic and found to have strong contribution of spin on nitrogen, platinum and phosphorus nuclei regarding to EPR-spectroscopy.¹³ In solution **LXIII** slowly decayed and formed trinuclear platinum complex **LXIV** that was diamagnetic.^{13,57}

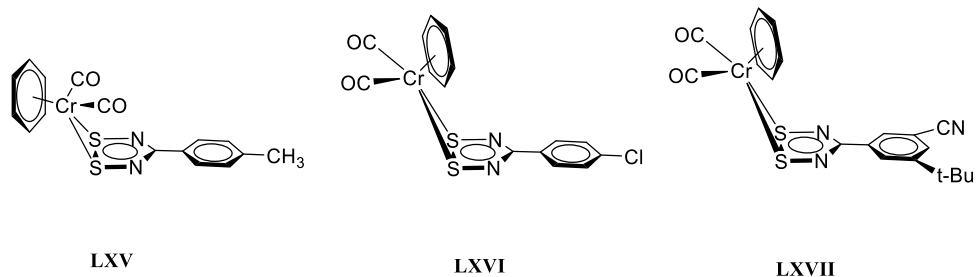


LXIII

LXIV

Scheme 20. Mono (**LXIII**) and trinuclear (**LXIV**) platinum complex of 1,2,3,5-DTDA
Platinum had pseudo-square planar coordination geometry.¹³

Analogous structures of **LXIV** for palladium were observed with phenyl, 3-pyridyl and 4-pyridyl substituents. No mononuclear palladium complex was identified from these reactions. A reaction of **V** with $\text{Pd}(\text{dppe})_2$ produced paramagnetic Pd-analogue for **LXIII**.



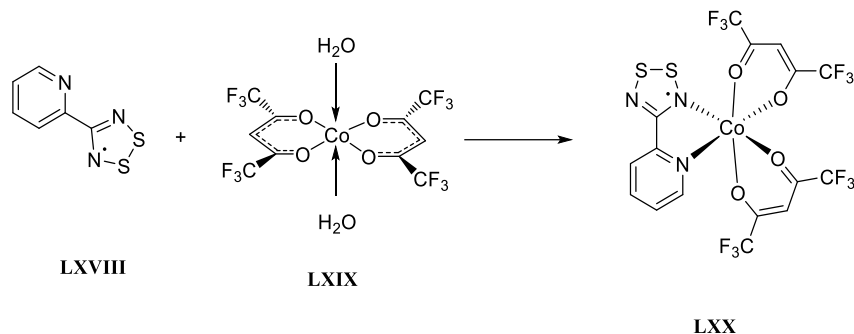
Scheme 21. Three cyclopentadienylchromium complexes with 1,2,3,5-dithiadiazolyl. **LXV** has *exo* conformation and two others (**LXVI** and **LXVII**) have *endo*.⁵⁸

All above mentioned 1,2,3,5-dithiadiazolyl coordination complexes undergone S–S bond dissociation during the complexation process. However, when 1,2,3,5-DTDA was coordinated with $[\text{CpCr}(\text{CO})_3]_2$, the S–S bond stayed intact. Substituents of **V** were varied (R=4'-CH₃-, 4'-Cl-, 3'-CN- and 5'-t-Bu-) and bond distances for compounds were 2.114(1), 2.132(2) and 2.146(3) Å, respectively. Chromium complexes had two possible conformations: *exo* (**LXV**) and *endo* (**LXVI** and **LXVII**) as shown in Scheme 21.^{13,58} DFT calculations suggested that energy difference between *endo* and *exo* conformations is only 2.5 kJ mol⁻¹. Thus in lower temperatures (below -20 ° C) in solution phase, all the three complexes display both conformers.⁵⁸

5.1.2 COORDINATION OF 1,2,3,5-DITHIADIAZOLYLS VIA NITROGEN ATOMS

Metal coordination via nitrogen atoms in 1,2,3,5-DTDA molecules have been also observed. Electron-withdrawing groups aid metal coordination since nitrogen is comparatively hard and electronegative atom in contrast to sulfur. . Metal has planar coordination orientation with respect to nitrogen in all compounds. Due to lone pair of nitrogen, which acts as σ -donor, nitrogen forms strong σ -bonds with metals. Therefore, nitrogens stay intact and no bond dissociation occurs.¹³

Preuss and co-workers published 2004 results from coordinating 1,2,3,5-DTDA (R=[4-(2'-pyridyl)] with cobalt. The ligand 4-(2'-pyridyl)-1,2,3,5-DTDA **LXVIII** was defined to have coupling of an unpaired electron on two equal nitrogens ($a_N = 5.02$ G, $g = 2.010(6)$) by EPR-spectroscopy. Voltammetry measurements were done for radical **LXVIII** and was found to have a reversible oxidation wave $E_{1/2(ox)} = 0.62$ V (vs. saturated calomel electrode, SCE) and $E_{1/2(red)} = -0.81$ V (vs. SCE).⁵⁹



Scheme 22. Starting materials of cobalt complex **LXX**. 4-(2'-pyridyl)-1,2,3,5-DTDA **LXVIII** is bidentate radical ligand.⁵⁹

During the complexation the bond distances and angles did not change considerably in DTDA ring. Susceptibility measurement was done by using SQUID magnetometer. Chelate **LXX** reached its maximum susceptibility $3.66 \text{ emu K mol}^{-1}$ at 70 K (Figure 22) when temperature was varied from 2 K to 300 K and the used field was 4000 G. Ferromagnetic coupling between the Co(II) centre and the unpaired electron on the ligand was indicated by the drop of temperature and simultaneous raise in the susceptibility χ_T .⁵⁹

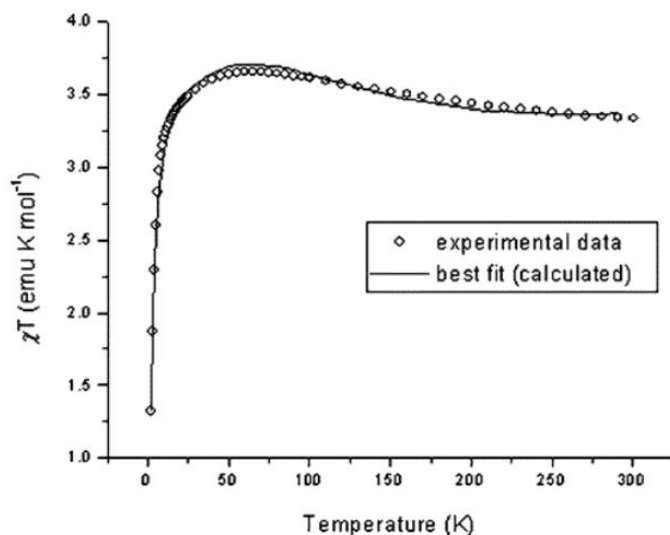
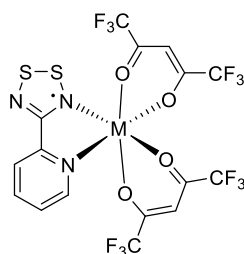


Figure 22. Susceptibility of **LXX** measured at varied temperatures (2 K- 300K). The complex reaches its maximum susceptibility $3.66 \text{ emu K mol}^{-1}$ at temperature 70 K.

Reprinted from “Design and Synthesis of a 4-(2′Pyridyl)-1,2,3,5-Dithiadiazolyl Cobalt Complex” by Nigel G. R. Hearn, Kathryn E.

Preuss, John F. Richardson, et al, 2004, Journal of the American Chemical Society, Copyright © 2004, American Chemical Society.⁵⁹

After cobalt complex **LXX**, other transition metals were tried to complexate using the same synthetic approach. Two analogous complexes with copper **LXXI** and with manganese **LXXII** were managed to synthesize (Scheme 23).⁶⁰

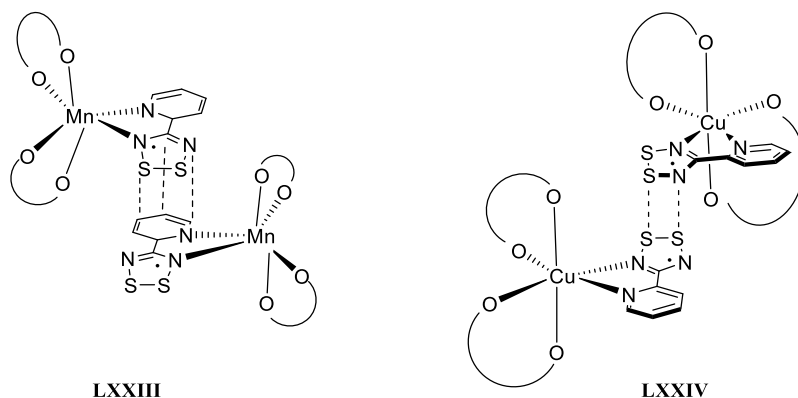


LXXI: M=Cu
LXXII: M= Mn

Scheme 23. Coordination complex of 4-(2′-pyridyl)-1,2,3,5-dithiadiazolyl and copper **LXXI** and manganese **LXXII**.⁶⁰

The chelate of radical ligand and metal adopted similar chelation pattern in **LXXI** and **LXXII** as in the cobalt complex **LXX**. However, the angle between N–C–C–N in **LXXI** and **LXXII** was smaller than in cobalt complex **LXX** or for the free ligand **LXVIII**. The significant difference between **LXX** and copper/manganese counterparts is that **LXX** showed no notable interactions between DTDA rings. Conversely **LXXI** and **LXXII** had diminutive interactions in solid state indicating dimerization.⁶⁰

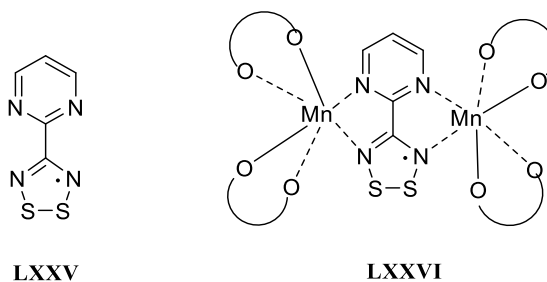
The magnetism of all three complexes (**LXX**, **LXXI**, **LXXII**) were similar in both solvent and in the solid state. For **LXXI** the susceptibility value $4.2 \text{ emu K mol}^{-1}$ was close to the expected room temperature value of $4.377 \text{ emu K mol}^{-1}$. For **LXXI** and **LXXII** the χT followed same pattern as susceptibility remained unchanged until the temperature reached 50 K where χT values started to decline. Both complexes had negative Weiss constants which denoted a weak antiferromagnetic intermolecular interaction. Because **LXXI** and **LXXII** formed dimers **LXXIII** and **LXXIV**, respectively, (Scheme 24) it was proposed that the short interaction between monomers would have been conveyed an antiferromagnetic coupling between metal cations. J value of -0.29 cm^{-1} was calculated for **LXXIII** and -3.5 cm^{-1} for **LXXIV**.⁶⁰



Scheme 24. Dimerization patterns of bis(hexafluoroacetylacetonate)manganese **LXXIII** and bis(hexafluoroacetylacetonate)copper **LXXIV**. Hexafluoroacetylacetonate (hfac) ligands are indicated using coordinating oxygens and curves.⁶⁰

The next step was coordination of two metals to one radical to utilize the radical as bridging ligand (**LXXVI**). The selected radical was bis(bidentate) 1,2,3,5-dithiadiazolyl with two bidentate coordination pockets arising from pyrimidine substituent (compound **LXXV** in

Scheme 25). The ligand itself had fairly similar properties as other resembling DTDA radicals.⁶¹ The EPR-spectrum of **LXXV** showed pentet with relative intensities of 1:2:3:2:1 demonstrating spin distribution on two equivalent nitrogens. The reversible oxidation wave $E_{1/2}(\text{ox})=+1.22$ V (vs. SCE) and reversible reduction wave $E_{1/2}(\text{red})= -0.79$ V (vs. SCE) were observed in cyclic voltammetry measurements.



Scheme 25. 4-(2'-pyrimidyl)-1,2,3,5-dithiadiazolyl ligand **LXXV** and dimanganese complex **LXXVI**.

In complex **LXXVI** S–S and N–S bond distances remained approximately same as in free radical **LXXV**. No dimer formation was observed for the dimanganese complex **LXXVI**. The magnetic properties were measured at temperature range from 2 K and 300 K. Experimental g value was 2.03 and susceptibility $9.4 \text{ cm}^3 \text{ K mol}^{-1}$ in field strength of 1000 G. Corresponding calculated values for dimanganese complex were $9.1 \text{ cm}^3 \text{ K mol}^{-1}$ and $g= 2$. The values were derived from the sum of contribution from isolated odd-electron ligand and two isolated manganese(II) ions and corresponded well to observed ones. The susceptibility showed antiferromagnetic coupling as was anticipated from the irregular spin state structure^{iv,61} The irregular spin state prediction resulted ferromagnetic coupling with $S= 9/2$ for the coupling between the central site and outer Mn(II) sites. Susceptibility showed minor fall when temperature decreased from 300 K to $\sim 150\text{K}$ (Figure 23). After passing temperature 150 K, the susceptibility started to incline distinctly. The drop of susceptibility between 300- 150 K originates from depopulation of highest spin state ($S= 11/2$). An increase of χT in temperature below 150 K results from depopulation of excited states with lower spin than the ground state.⁶¹

^{iv} *Regular spin state* is a state of dinuclear system AB composed of local spins S_A and S_B of magnetic ions A and B. In regular spin state the spin multiplicity of the low-lying states varies monotonically. When the molecule is trinuclear (or contains three isolated paramagnetic centers) ABA instead of binuclear, the situation is slightly different. Trinuclear system has regular spin state but because the spin multiplicity does not vary monotonically versus the energy, this state is called *irregular state*.⁷⁷

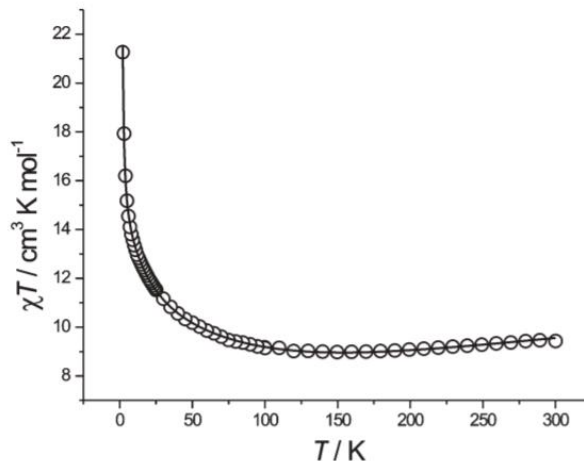
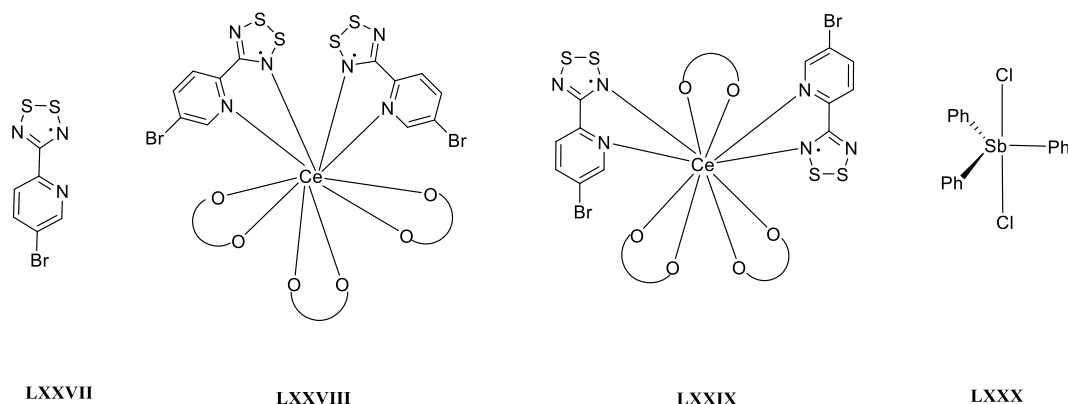


Figure 23. The molar magnetic susceptibility data of dimanganese complex **LXXVI** presented as a function of temperature between 2 and 300 K. Magnetic field applied was 1000 Oe. Reproduced from Jennings, M. *et al.* Synthesis and magnetic properties of a 4-(2'-pyrimidyl)-1,2,3,5-dithiadiazolyl dimanganese complex. *Chem. Commun.* **22**, 341–343 (2006) with permission of The Royal society of Chemistry.

Using 4-(5'-bromopyrid-2'-yl)-1,2,3,5-dithiadiazolyl) as ligand **LXXVII** Preuss *et al.* synthesized a supramolecular entity where two radicals bind to cerium (Scheme 26). The molecule was able to bind SbPh_3Cl_2 **LXXX** inside the cavity via “pancake-bonding”. During the formation of supramolecular complex the ligand undergoes a rearrangement from state **LXXVIII** to **LXXIX**. Molecule **LXXIX** acts as a host molecule for guest **LXXX** and complex is formed (Figure 24).⁶²



Scheme 26. Ligand **LXXVII** forms complex **LXXVIII** which undergoes rearrangement to complex **LXXIX** when guest molecule **LXXX** binds between two of these **LXXIX** molecules.

The host-guest complex was prepared by gentle heating under reduced pressure and was purified by sublimation. The Cl–S contacts between host and guest and Br–Br contacts between host-host can be observed in the complex. Br–Br contacts 3.646(2) Å were shorter than van der Waals radii 3.74 Å.^{62,63} These interactions will notably stabilize complex. The interesting coordination sphere rearrangement could be utilized in development of new lanthanide-based materials as the metal coordination sphere has a remarkable effect on the physical properties of the material.⁶²

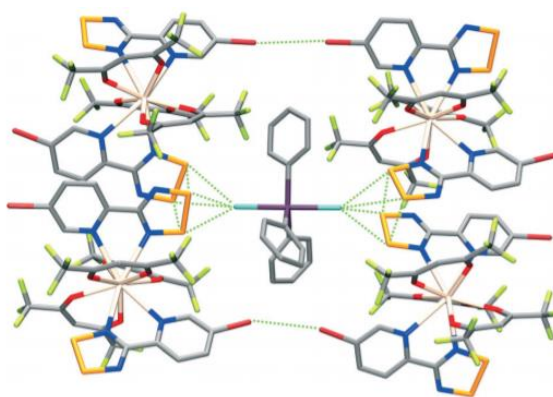
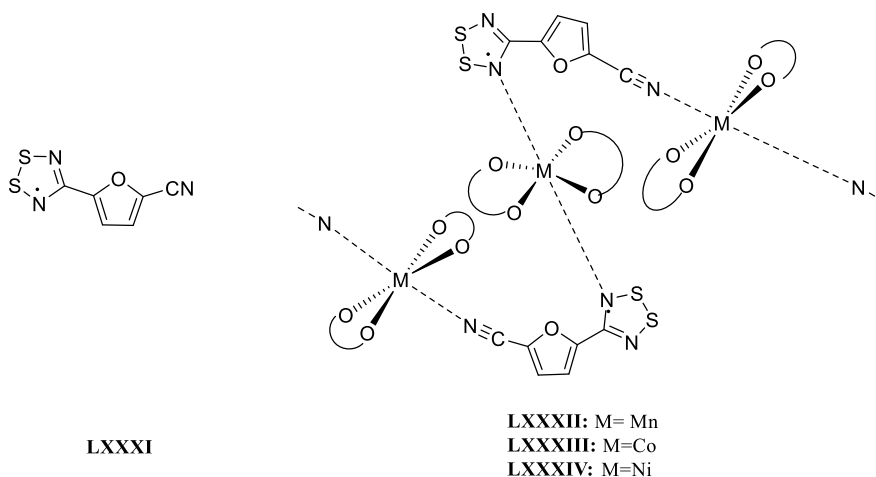


Figure 24. Pancake complex where **LXXX** is the guest molecule and two **LXXIXs** act as host. Reprinted from “Isomerization of a lanthanide complex using a humming top guest template: a solid-to-solid reaction” by Michelle B. Mills, Andrew G. Hollingshead, Adam C.

Maahs, Dmitriy V. Soldatov, Kathryn E. Preuss, 2015,

CrystEngComm, Copyright © 2015 Royal Society of Chemistry.

By changing the stoichiometry of reaction and altering the radical ligand Preuss *et al.* obtained another coordination mode: 4-(2'-cyanofuryl-5')-1,2,3,5-DTDA ligand **LXXXI** generated unexpected chain like structure with various metal(II) cations (Mn^{2+} , Co^{2+} , Ni^{2+}) (**Scheme 27**). Interestingly, the ligand coordinated to metal only in a monodentate fashion and the furan oxygen did not interact with the metal cation in any of the complexes.



Scheme 27. Hexafluoroacetylacetonate ligands are indicated by using coordinating oxygens. Hfac ligands are in equatorial plane in respect of metal and nitrogen atoms are in axial position.⁶⁴

Interactions between DTDA rings lead to co-facial dimerization (Figure 25). Structures of **LXXXII**, **LXXXIII** and **LXXXIV** are relatively similar, only the M–N distances varied between 2.309(5) and 2.459(5) Å. It should be noted that metal-nitrogen bond distances were longer in monodentate coordinated complexes **LXXXII**, **LXXXIII** and **LXXXIV** than in bidentate coordination complexes **LXX**, **LXXI** and **LXXII** (2.288(6)-2.082(15)Å).⁶⁴

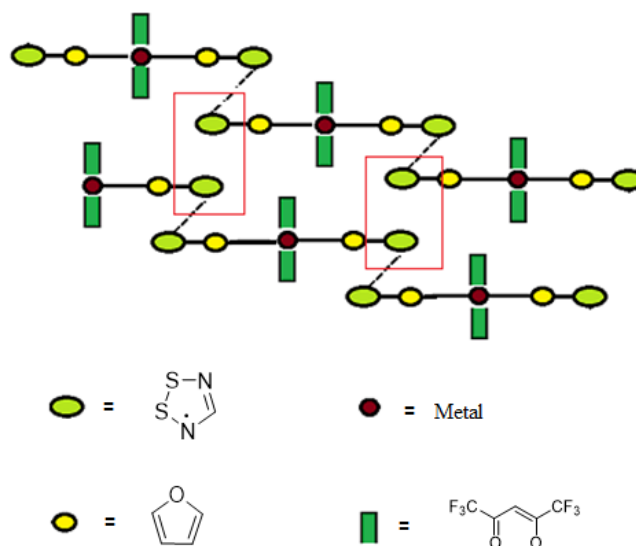


Figure 25. Schematic presentation of dimerization pattern of metal complexes **LXXXII**, **LXXXIII** and **LXXXIV**. Structure is presented from the side and red boxes indicate π -stacking of dimers in complex.

5.2 COORDINATION COMPLEXES OF 1,3,2-DITHIAZOLYLS

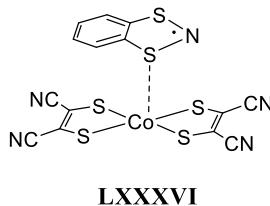
Cofigure ordination complexes of thiazyl radicals and metals are still relatively novel research field. Several complexes have been observed for 1,2,3,5- dithiadiazolylys and metals but other classes of thiazyls are unrepresented. However, two complex of 1,3,2-dithiadizolylys have been observed: one with complex with cobalt and another with copper.

5.2.1 COORDINATION OF 1,3,2-DITHIAZOLYLS VIA SULFURS

The coordination via sulfur had been observed also for **XXVIII** (referred in literature as BDTA=1,3,2-benzodithiazolyl) with cobalt maleonitriledithiolate $[\text{Co}(\text{mnt})_2]$ (Scheme 28) and complex **LXXXVI** was formed. When temperature was decreased from 253K to 100 K, compound **LXXXVI** showed ability to transfer electron. The electron transfer, which is not as complete when compared with other similar transition metal complexes, is explained by back-donation^v. The electron is transferred from $[\text{Co}(\text{mnt})_2]^{2-}$ to **XXVIII**⁺ to from an

^v “A description of the bonding of π -conjugated ligands to a transition metal which involves a synergic process with donation of electrons from the filled π -orbital or lone electron pair orbital of the ligand into an

cation-anion pair. However, π -donation from the metal fragment reduces the positive charge on ligand thus increasing the capability of **XXVIII** ligand to form a coordination bond and return the gained electron partially back.⁶⁵

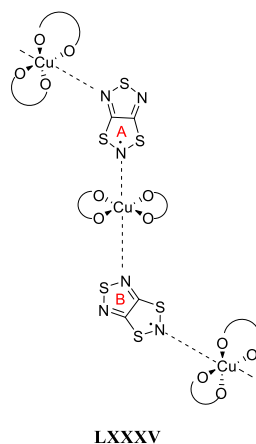


Scheme 28. Coordination compound LXXXVI formed of radical **XXXVIII** with $[\text{Co}(\text{mnt})_2]$.

5.2.2 COORDINATION OF 1,3,2-DITHIAZOLYLS VIA NITROGENS

Already earlier discussed radical **XXXVII** (1,3,5-trithia-2,4,6-triapentalenyl, *TTTA*) forms a coordination polymer **LXXXV** with $\text{Cu}(\text{hfac})_2$ (Scheme 29). In solid state, the *TTTA* molecules bridge between two $\text{Cu}(\text{II})$ ions and coordinate to axial positions of the copper cations. The distances between copper and nitrogen differ depending on whether the bond is between part A of *TTTA* (2.342 Å) or with part B copper (2.478 Å) (Scheme 29). Complex **LXXXV** showed ferromagnetic coupling as χ_{pT} values increased while temperature decreased.⁶⁶

empty orbital of the metal (donor–acceptor bond), together with release (back donation) of electrons from an *nd* orbital of the metal (which is of π -symmetry with respect to the metal–ligand axis) into the empty π^* -antibonding orbital of the ligand.⁷⁶



Scheme 29. Two different coordination modes of TTTA ligand in **LXXXV**.

6 CONCLUSIONS

The last 40 years have been a vivid era of thiazyl research. The synthesis has developed greatly and there are dozens of known 1,2,3,5-dithiadiazolyls. The packing structure of the molecules is the key to intriguing features. Thiazyl radicals have interactions between the π -stacks and between nitrogens and sulfurs. Moreover, their bond distances indicate whether the radicals are monomers or dimers. 1,2,3,5-dithiadiazolyls have high tendency to dimerize. 1,3,2-dithiazolyls have also propensity form dimers whereas 1,2,3-dithiazolyls are more stable and remain monomers. The researchers have found ways to suppress dimerization: adding steric bulk, enhancing the spin delocalization by expansion of radical framework or by utilizing competing interactions *e.g.* cyano–sulfur interactions and repulsions between adjacent monomers such as fluorine–fluorine repulsions. Thiazyls have intriguing conductive and magnetic properties such as bistability and these properties can potentially be utilized in thiazyl-based molecular conductors and magnetic materials. In addition, thiazyls have nowadays limited amount of known metal complexes and these demonstrate magnetic exchange coupling which can strengthen the magnetism compared to plain organic radical moiety. Hence, 40 years of research have resulted considerable amount of packing structures and information about metal like qualities. However, there are still more to learn about these more complex systems as hybrid materials and metal–radical complexes.

EXPERIMENTAL PART

7 AIM OF THE WORK

Thiazyls are sulfur–nitrogen radicals with surprisingly high stability that arises from the combination of electronegative elements and delocalization of spin density over the π -framework. General interest towards thiazyl radicals began to develop after the discovery of the superconducting polythiazyl in the 1970s.^{5,23} Since that time, many different classes of thiazyls have been synthesized and structurally characterized. Of particular importance have been the structural properties of thiazyl radicals, *i.e.*, their solid-state packing and weak radical–radical interactions, as these are fundamental for the development of bulk materials with novel conductive and magnetic properties.⁵ The highest magnetic ordering temperature obtained for thiazyl radical is 36 K.⁴⁵ Also, more than one thiazyl radical have showed magnetic bistability which could be utilized in spintronics such as magnetic data storing.^{7,49,67}

The experimental part of this work was motivated by the results of Oakley and co-workers who recently described the synthesis of new dithiazolothiadiazinyl radicals and characterized the first members of these species.¹ Thus, the synthetic work began by repeating the reported experimental results to obtain important benchmark data and to become familiar with handling of air and moisture sensitive compounds and Schlenk techniques in particular. Once these syntheses were completed and the required skill level was achieved, the synthetic work was targeted towards the preparation of new dithiazolothiadiazinyl radicals and the study of their physical properties. The primary objective of the work was to realize new derivatives of dithiazolothiadiazinyl radicals by substitution. Two different approaches were followed: i) replacement of the basal hydrogen atom with fluorine and ii) replacement of the thiophene substituent with either pyridine or pyrimidine. An additional objective of the work was to examine the possibility to use the synthesized dithiazolothiadiazinyl radicals as coordinating ligands to realize metal–radical coordination complexes.

8 EXPERIMENTAL METHODS

8.1 GENERAL METHODS AND PROCEDURES

All syntheses were performed under an argon atmosphere using Schlenk techniques and/or an inert atmosphere glove box. The majority of the end products were stable in air, if not stated differently. All solvents were dried by distillation and using common solvent-specific drying agents such as Na, P₂O₅ and/or CaH₂. Solvents used for reductions were thoroughly degassed (three cycles) to ensure that they contain no air. A single degassing cycle was performed by dipping the solvent flask into liquid nitrogen and keeping it there until the solvent was almost completely frozen, after which the flask was evacuated under vacuum (five to ten minutes, depending on the volume) and allowed to warm to room-temperature.

8.1.1 LARGE-SCALE EQUIPMENT

All spectroscopic measurements were performed at room-temperature. ¹H NMR spectra were recorded on a *Bruker Avance II 300* spectrometer using deuterated solvents (CD₃CN and CDCl₃) and referenced internally to the residual solvent peak (1.94 and 7.26 ppm, respectively). IR spectroscopy was performed using *Bruker Alpha Platinum* single reflection diamond ATR module in an argon filled glove box. EPR data were collected on a *Magnettech GmbH MiniScope 200* X-band spectrometer using CH₂Cl₂ as the solvent. Cyclic voltammetry was performed with *Gamry Instruments Reference 600* potentiostat using a single compartment cell under an argon atmosphere. Single-crystal X-ray measurements were performed by using either *Agilent SuperNova* dual wavelength diffractometer equipped with an Atlas CCD area detector (Cu-K α radiation) or with *Agilent Supernova* single wave source diffractomereee equipped with an Eos CCD detector (Mo-K α radiation). The structures were solved using *ShelXS* and refined on F^2 by full-matrix least-squares techniques with *ShelXL*.⁶⁸ Solid-state packing figures were drawn with the *Mercury CSD 3.8* program.⁶⁹

8.1.2 SMALL-SCALE EQUIPMENT

Sublimation is the transition of a substance from the solid state to the gas phase without going via liquid phase. Consequently, this technique can be used in purification of solids. In a typical setup, the sublimation apparatus is kept under dynamic vacuum and the system is heated to volatilize the solid that then condenses on a cool surface, a cold finger, inside the apparatus (Figure 26a).

An H-cell is a glass cell that can be used to perform controlled (electro)reductions (Figure 26b). It consists of two compartments separated by a small frit. In a typical setup, the compartments are filled with solutions, one containing the reducing agent and the other one containing the species to be reduced. The two solutions gradually mix by diffusion, allowing the reagents to slowly react on the interface, thereby promoting crystal growth.

a)



b)

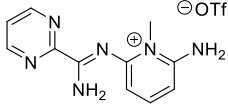
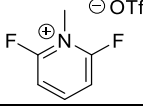
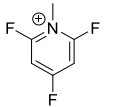
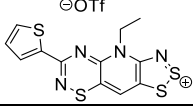


Figure 26. Examples of a) sublimation with a sublimation apparatus and b) combined degassing and reduction with an H-cell.

8.2 SYNTHESSES

Table 2 lists all the reagents used in the synthetic work.

Table 2. Used reagents, their suppliers and purity.

Compound	Supplier	Purity
2-Amino-6-((amino(pyrimidin-2-yl)methylene)amino)-1-methylpyridin-1-ium trifluoromethanesulfonate 	Aaron Mailman	-
2,6-Difluoro-1-methylpyridin-1-ium trifluoromethanesulfonate 	Aaron mailman	-
2,4,6-Trifluoro-N-methylpyridinium trifluoromethanesulfonate 	Aaron Mailman	-
4-Ethyl-6-(thiophen-2-yl)-4H-[1,2,3]dithiazolo[5',4':5,6]pyrido[2,3-e][1,2,4]thiadiazin-2-ium trifluoromethanesulfonate 	Aaron Mailman	-
Bis(silyl)amide etherate	Aaron Mailman	-
Lithium bis(silyl)amide etherate	Aaron Mailman	-
N,N,N'-Tris(trimethylsilyl)pyridine-2-carboximidamide	Aaron Mailman	-
2-Amino-1-ethyl-6-fluoropyridin-1-ium	Aaron Mailman	-
Co(hfac) ₂ · 2 THF	Aaron Mailman	-
Ni(hfac) ₂ · 2 THF	Aaron Mailman	-
Benzyltriethylammonium chloride	Aldrich-Chemie	99 %
Trimethylsilyl trifluoromethanesulfonate	Apollo Science	98 %
Triphenyl animony	Fluka	98 %
Trimethylsilyl chloride (TMSCl)	Fluka	≥98 %
Acetonitrile (MeCN)	J.T. Baker	≥99.9 %
Copper nitrate trihydrate	Merck	99.5 %
Sodium	Riedel de Häen	99 %
Disulfur dichloride (S ₂ Cl ₂)	Riedel de Häen	98 %
Hexafluoroacetylacetone	Sigma- Aldrich	98 %
Calcium hydride (CaH ₂)	Sigma-Aldrich	95 %

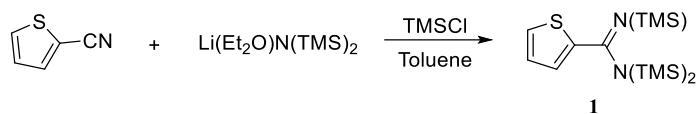
Tetrabutylammonium fluoride (TBAF)	Sigma-Aldrich	1 M in THF
1,2-Dichloroethane (DCE)	Sigma-Aldrich	99 %
Methanol (MeOH)	Sigma-Aldrich	≥99.8 %
2-Thiophenecarbonitrile	Sigma-Aldrich	99 %
Toluene	Sigma-Aldrich	≥99.7 %
Tetrahydrofuran (THF)	Sigma-Aldrich	≥99.9 %
N,N,N,N-Tetramethyl-p-phenylenediamine (TMPDA)	Sigma-Aldrich	≥99 %
Octamethyl ferrocene (OMFc)	Sigma-Aldrich	≥94 %
Tris(trimethylsilyl)amine	Strem	98 %
Dimethyl ferrocene (DMFc)	Strem	98 %
Tris(2,2,6,6-tetramethyl-3,5-heptadionato dysprosium (III))	Strem	≥98 %
Phosphorus pentoxide (P ₂ O ₅)	VWR Intl.	97 %
Dichloromethane (DCM)	VWR Intl.	≥99.5 %
Carbon disulfide (CS ₂)	VWR Intl.	99 %
Sodium acetate	VWR Intl.	≥99 %

8.2.1 N,N,N'-Tris(trimethylsilyl)thiophene-2-carboxamide 1

2-Thiophenecarbonitrile (5.0 g, 46 mmol, 1 eq.) was dissolved into dry toluene (20 ml) and combined with lithium bis(silyl)amide etherate (13 g, 54 mmol, 1.2 eq.) in dry toluene (80 ml) via addition funnel (Scheme 30). The round-bottom flask was kept in ice-water bath during the addition of 2-thiophenecarbonitrile and let to warm up gradually to room temperature. Mixture was stirred for 2 h. After that, trimethylsilyl chloride (TMSCl, 6.0 g, 7.0 ml, 55 mmol, 1.2 eq.) was added via syringe and the mixture was refluxed overnight. The cooled mixture was filtered with glass frit and celite. After filtration, it was flash distilled and then vacuum distilled. First drops of product were received in 50 °C and the whole product was distilled between 50-66 °C to give a yellow liquid. Yield: 3.5 g (10 mmol, 22 %).

¹H NMR (CDCl₃, 300 MHz): δ (ppm) 7.24 (m, 1H), 7.11 (m, 1H), 6.94 (m, 1H), 0.12 (s, 27H) (

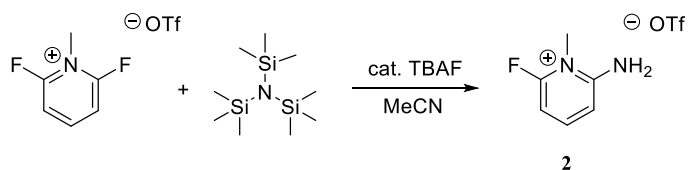
Appendix 1).



Scheme 30. Synthesis of N,N,N'-tris(trimethylsilyl)thiophene-2-carboxamide **1**.

8.2.2 2-Amino-6-fluoro-1-methylpyridin-1-ium trifluoromethanesulfonate 2

2-Amino-6-fluoro-1-methylpyridin-1-ium trifluoromethanesulfonate was synthesized by the method of Oakley *et al.* (Scheme 31) by adding tris(trimethylsilyl)amine (4.3 g, 19 mmol, 1 eq.) to 2,6-difluoro-1-methylpyridin-1-ium trifluoromethanesulfonate (5.1 g, 18 mmol, 1 eq.) in 60 ml of dry acetonitrile (MeCN).¹ To this mixture, catalytic amount (0.3 ml, 0.3 mmol) of tetrabutylammonium fluoride (TBAF, 1 M solution in tetrahydrofuran) was added. The solution was stirred overnight and 5 ml of methanol (MeOH) was added. All volatiles were removed using rotary evaporator. Obtained white solid was washed with dichloroethane (DCE) and recrystallized from 6:1 DCE/MeCN mixture producing white needles. Yield: 3.99 g (14 mmol, 79 %).

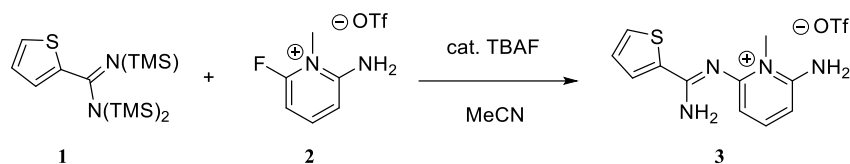


Scheme 31. Synthesis of 2-amino-6-fluoro-1-methylpyridin-1-ium trifluoromethanesulfonate **2**.

8.2.3 2-Amino-6-((amino(thiophen-2-yl)methylene)amino)-1-methylpyridin-1-ium trifluoromethanesulfonate 3

Compound **3** (Scheme 32) was synthesized by dissolving **1** (2.0 g, 5.8 mmol, 1 eq.) and **2** (1.6 g, 5.8 mmol, 1 eq.) into 30 ml of MeCN. TBAF (0.5 ml, 0.5 mmol, 0.086 eq., 1 M in THF) was added via syringe and solution turned to yellow. The reaction mixture was left stirring overnight. MeOH (2.5 ml) was added in the morning and the product was flash distilled and filtered to obtain a yellow solid. Yield: 1.1 g (2.9 mmol, 50 %).

^1H NMR (CD_3CN , 300 MHz): δ (ppm) 7.81 (m, 1H), 7.67 (m, 2H), 7.16 (m, 1H), 6.58 (d, 1H, $J = 8.6$ Hz), 6.46 (d, 1H, $J = 7.81$ Hz), 3.59 (s, 3H) (Appendix 2).

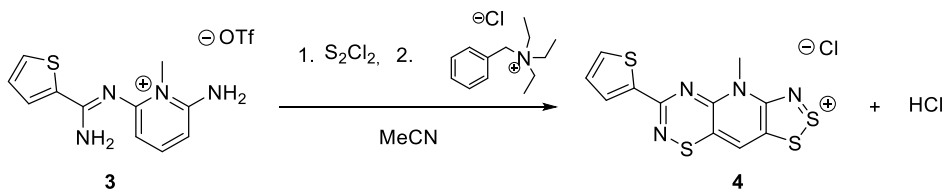


Scheme 32. Synthesis of 2-amino-6-((amino(thiophen-2-yl)methylene)amino)-1-methylpyridin-1-ium trifluoromethanesulfonate **3**.

8.2.4 4-Methyl-6-(thiophen-2-yl)-4H-[1,2,3]dithiazolo[5',4':5,6]pyrido[2,3-e][1,2,4]thiadiazin-2-ium chloride **4**

Disulfur dichloride (2.0 g, 1.2 ml, 15 mmol, 5 eq.) was added to mixture of the **3** (1.1 g, 3.0 mmol, 1 eq.) in 70 ml MeCN (Scheme 33). After addition of disulfur dichloride, the solution first turned into clear green and then ultimately to dark green. The solution was heated and refluxed for 2 h and then cooled down to room temperature. To the filtrate was added benzyltriethylammonium chloride (1.5 g, 6.6 mmol, 2.2 eq.) in MeCN (20 ml) to ensure anion exchange. The solution was stirred for 20 minutes and then collected on a frit. The solid was washed with MeCN (40 ml), suspended in 30 ml of DCE and then refluxed, hot filtered and washed with 60 ml of dichloromethane (DCM). Yield 1.1 g (3.1 mmol, 106 %). The crude product contained sulfur-based impurities and moisture, and was used as such in subsequent reactions.

IR ν_{max} (cm^{-1}): 1423 (s), 1385 (s), 1354 (s), 1320 (s), 1091 (m), 1006 (s), 944 (m), 841 (m), 810 (m), 727 (s), 643 (m), 634 (m), 606 (m), 499 (m), 475 (m) (Appendix 3).

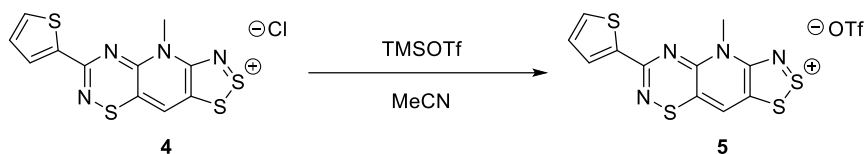


Scheme 33. Synthesis of 4-methyl-6-(thiophen-2-yl)-4H-[1,2,3]dithiazolo[5',4':5,6]pyrido[2,3-e][1,2,4]thiadiazin-2-ium chloride **4**.

8.2.5 4-Methyl-6-(thiophen-2-yl)-4H-[1,2,3]dithiazolo[5',4':5,6]pyrido[2,3-e][1,2,4]thiadiazin-2-ium trifluoromethanesulfonate **5**

Metathesis was done by suspending **4** (1.1 g, 3.1 mmol, 1 eq.) in 70 ml MeCN (Scheme **34**). To the slurry was added excess of trimethylsilyl trifluoromethanesulfonate (1.0 g, 0.8 ml, 4.0 mmol, 1.3 eq.) via syringe. The solution was refluxed for 1 h and hot filtered on a fine glass frit. The solution was flash distilled and dark purple product was dried under vacuum. Crude product had impurities and moisture, and was purified by recrystallization. Product was recrystallized by adding MeCN and bringing to boil on the hot plate. Then solution was hot filtered by using a warm Buchner funnel. After filtering the solution was concentrated slightly and then let to cool down to room temperature. The Erlenmeyer was put into freezer overnight where big purple crystals were received. Yield: 0.027 g (0.057 mmol, 18 %).

IR ν_{\max} (cm⁻¹): 1488 (s), 1427 (m), 1366 (m), 1326 (m), 1263 (m), 1221 (s), 1148 (m), 1009 (s), 941 (w), 885 (w), 716 (s), 633 (s), 570 (w), 514 (w), 475 (w) (Appendix 4).



Scheme 34. Synthesis of 4-methyl-6-(thiophen-2-yl)-4H-[1,2,3]dithiazolo[5',4':5,6]pyrido[2,3-e][1,2,4]thiadiazin-2-ium trifluoromethanesulfonate **5**.

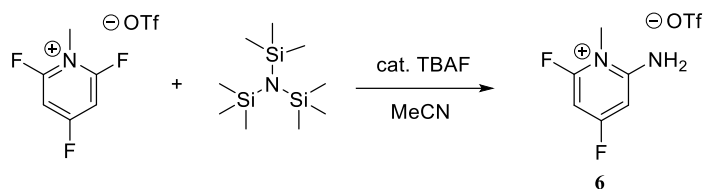
8.2.6 2-Amino-4,6-difluoro-1-methylpyridin-1-ium trifluoromethanesulfonate **6**

2,4,6-Trifluoro-N-methylpyridinium trifluoromethanesulfonate (1.5 g, 5.1 mmol, 1 eq.) and tris(trimethylsilyl)amine (1.2 g, 5.1 mmol, 1 eq.) were dissolved in 35 ml dry MeCN (Scheme 35). Catalytic amount of TBAF (0.3 ml, 0.3 mmol, 1 M solution in THF) was added via syringe and the mixture was stirred at ambient temperature for 16 h. MeOH (1.0 ml) was added and the mixture was left stirring for further 1.5 h. Solvent was then flash distilled away to yield an off-white precipitate. Solid product was washed and triturated

with DCM and filtered using Buchner funnel. The crude product was recrystallized from 40 ml of 8:1 DCE/MeCN, hot filtered and placed into freezer overnight. Colorless crystals were collected next day by filtering using Buchner funnel. Yield 1.0 g (3.5 mmol, 69 %).

^1H NMR (CD_3CN , 300 MHz): δ (ppm) 7.22 (s, 2H), 6.69 (m, 2H), 3.59 (s, 3H), 2.14 (s, 2H) (

Appendix 5).

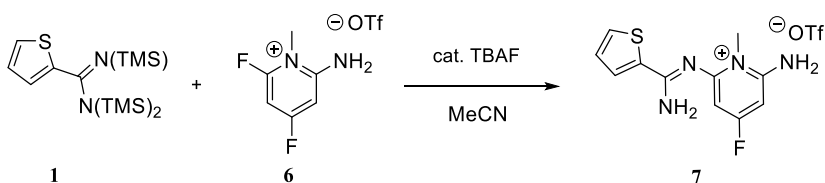


Scheme 35. Synthesis of 2-amino-4,6-difluoro-1-methylpyridin-1-ium trifluoromethanesulfonate **6**.

8.2.7 2-Amino-6-((amino(thiophen-2-yl)methylene)amino)-4-fluoro-1-methylpyridin-1-ium trifluoromethanesulfonate **7**

Compound **1** (2.1 g, 6 mmol, 1eq.) was dissolved in 60 ml of MeCN in a round bottom flask, after which compound **6** (1.7 g, 5.8 mmol, 1 eq.) and TBAF (1.0 ml, 1 mmol, 0.17 eq.) were added (Scheme 36). The resulting solution turned yellow and stirred overnight. MeOH (3 ml) was added in the morning and the product was flash distilled, filtrated and washed with DCM (5 ml) after stirring for 2 h. Yield 0.88 g (2.2 mmol, 37 %).

¹H NMR (CD₃CN, 300 MHz): δ (ppm) 7.72 (m, 2 H), 7.19 (m, 1H), 6.61 (s, 4H), 6.38 (d, 2H, *J* = 9.1 Hz), 3.58 (s, 3 H) (Appendix 6).

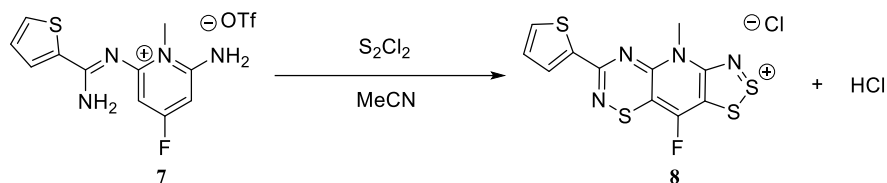


Scheme 36. Synthesis of 2-amino-6-((amino(thiophen-2-yl)methylene)amino)-4-fluoro-1-methylpyridin-1-ium trifluoromethanesulfonate **7**.

8.2.8 9-Fluoro-4-methyl-6-(thiophen-2-yl)-4H-[1,2,3]dithiazolo[5',4':5,6]pyrido[2,3-e][1,2,4]thiadiazin -2-ium chloride **8**

Disulfur dichloride (2.0 g, 1.2 ml, 15 mmol, 5.3 eq.) was added to a solution of **7** (1.1 g, 2.8 mmol, 1 eq.) in 70 ml MeCN (Scheme 37). The solution received a greenish dark colour.

The solution was refluxed for 2 h and hot filtered through a glass frit. Solution was flash distilled and 40 ml of DCE was added into flask. Mixture was refluxed for further 30 minutes, hot filtered and washed with a mixture of DCM (50 ml) and carbon disulfide (CS₂, 10 ml). Yield 1.1 g (2.9 mmol, 80 %).

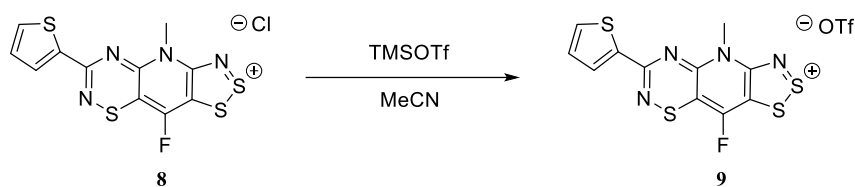


Scheme 37. Synthesis of 2-amino-6-((amino(thiophen-2-yl)methylene)amino)-4-fluoro-1-methylpyridin-1-ium trifluoromethanesulfonate **8**.

8.2.9 9-Fluoro-4-methyl-6-(thiophen-2-yl)-4H-[1,2,3]dithiazolo[5',4':5,6]pyrido[2,3-e][1,2,4]thiadiazin-2-ium trifluoromethanesulfonate **9**

Metathesis was done by suspending **8** (0.82 g, 2.2 mmol, 1 eq.) in MeCN (100 ml). To the slurry was added excess of trimethylsilyl trifluoromethanesulfonate (0.52 ml, 2.9 mmol, 1.3 eq.) via syringe (Scheme 38). The solution was refluxed for 35 minutes, hot filtered and flash distilled. The oily product was meticulously dried under vacuum. Product was recrystallized by adding MeCN and bringing to boil on a hot plate. Then solution was hot filtered by using a warm Buchner funnel. After filtering the solution was concentrated slightly and then let to cool down to room temperature before putting into freezer for overnight. Yield: 0.120 g (0.25 mmol, 11 %).

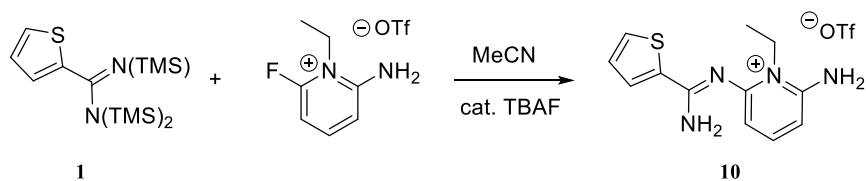
IR ν_{\max} (cm⁻¹): 1504 (s), 1475 (s), 1416 (m), 1361 (m), 1328 (m), 1272 (m), 1239 (s), 1221 (s), 1150 (m), 1120 (m), 1091 (w), 1046 (w), 1026 (s), 939 (w), 877 (w), 851 (w), 814 (w), 767 (m), 733 (m), 685 (w), 649 (m), 572 (w), 516 (w), 486 (w), 455 (w) (Appendix 7).



Scheme 38. Synthesis of 9-fluoro-4-methyl-6-(thiophen-2-yl)-4H-[1,2,3]dithiazolo[5',4':5,6]pyrido[2,3-e][1,2,4]thiadiazin-2-ium trifluoromethanesulfonate **9**.

8.2.10 2-Amino-6-((amino(thiophen-2-yl)methylene)amino)-1-ethylpyridin-1-ium trifluoromethanesulfonate **10**

2-Amino-1-ethyl-6-fluoropyridin-1-ium (0.90 g, 3.1 mmol, 1 eq.) and **1** (1.3 g, 3.7 mmol, 1.2 eq.) were added in a flask with 21 ml dry MeCN (Scheme 39). The mixture was stirred and TBAF (0.3 ml, 0.3 mmol, 0.097 eq., 1 M solution in THF) was added. The colour was yellow brownish. The solution was stirred 22 h. Methanol was added and the mixture was let to stir for further 2 h. Solvent was flash distilled and the product was washed with 7 ml of DCM and kept in freezer for a few days. Yield: 0.55 g (1.4 mmol, 45 %).



Scheme 39. Synthesis of 2-amino-6-((amino(thiophen-2-yl)methylene)amino)-1-ethylpyridin-1-ium trifluoromethanesulfonate **10**.

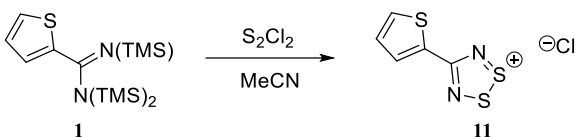
8.2.11 4-(Thiophen-2-yl)-1,2,3,5-dithiadiazol-1-ium chloride **11**

Intermediate **1** (0.86 g, 2.5 mmol) was dissolved in 25 ml of dry MeCN in a Schlenk flask and disulfur dichloride (1.4 g, 0.8 ml, 10 mmol, 4 eq.) was added to the mixture (Scheme 40). The solution changed colour from dark yellow to orange. The reaction mixture was refluxed for 30 minutes and filtered with filter stick. The crude product was washed with

dry MeCN (20 ml) and then with DCM (40 ml) to give an orange product. Yield: 0.26 g (1.2 mmol, 47 %).

IR ν_{\max} (cm⁻¹): 3082 (w), 2962 (w), 1659 (w), 1529 (s), 1425 (s), 1390 (s), 1335 (s), 1259 (s), 1067 (s), 1044 (s), 1020 (s), 890 (m), 874 (m), 848 (m), 829 (s), 796 (s), 760 (s), 664 (m), 639 (m), 543 (w), 522 (m) (

Appendix 8).

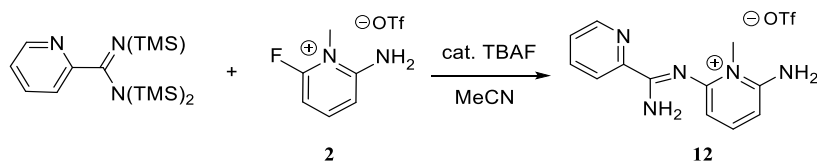


Scheme 40. Synthesis of 4-(thiophen-2-yl)-1,2,3,5-dithiadiazol-1-ium chloride **11**.

8.2.12 (Z)-2-Amino-6-((amino(pyridin-2-yl)methylene)amino)-1-methylpyridin-1-ium trifluoromethanesulfonate **12**

N,N,N'-Tris(trimethylsilyl)pyridine-2-carboximidamide (1.8 g, 5.2 mmol, 1 eq.) was added to a Schlenk flask together with dry MeCN (25 ml) and compound **2** (1.4 g, 5.2 mmol, 1 eq.) (Scheme 41). TBAF (0.2 ml, 1 M solution in THF, 0.2 mmol, 0.04 eq.) was added and colour changed from slight to bright yellow and to darker yellow. The solution was stirred overnight at room temperature. MeOH (2 ml) was added and the solution was let to stir for 2 h before flash distillation. Crude product was vacuum dried and then triturated with DCM (5 ml). Product was filtered by using a Buchner funnel. Yield 1.3 g (3.7 mmol, 69 %).

¹H NMR (CD₃CN, 300 MHz): δ (ppm) 8.67 (d, 1H *J* = 4.8 Hz), 8.35 (d, 1H, *J* = 7.9 Hz), 7.97 (t, 1H, *J* = 1.7 Hz), 7.73 (t, 1H, *J* = 8.0 Hz), 7.61-7.58 (m, 1H, *J* = 3.7 Hz), 6.66 (d, 1H, *J* = 8.6 Hz), 6.59 (d, 1H, *J* = 8.31 Hz), 3.64 (s, 3H) (Appendix 9).

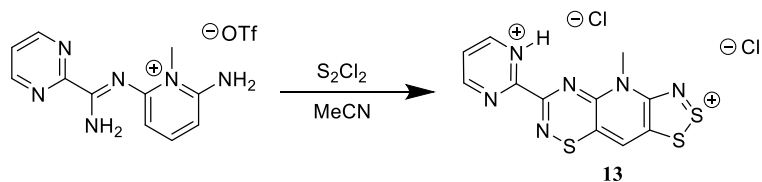


Scheme 41. Synthesis of 2-amino-6-((amino(pyridin-2-yl)methylene)amino)-1-methylpyridin-1-ium trifluoromethanesulfonate **12**.

8.2.13 4-Methyl-6-(pyrimidin-1-ium-2-yl)-4H-[1,2,3]dithiazolo[5',4':5,6]pyrido[2,3-e][1,2,4]thiadiazin-2-ium chloride **13**

Compound **13** was prepared in a similar way as **5** using 2-amino-6-((amino(pyrimidin-2-yl)methylene)amino)-1-methylpyridin-1-ium trifluoromethanesulfonate (0.76 g, 2.0 mmol,

1 eq.) and disulfur dichloride (1.7 g, 1 ml, 13 mmol, 6.2 eq.) in 40 ml of MeCN (Scheme 42). An immediate colour change from yellow to blue was observed. Benzyltriethylammonium chloride (0.68 g, 3.0 mmol, 1.5 eq.) was added to the solution after refluxing it for 2 h. The solution was then stirred for 1 h and hot filtered. Yield 1.1 g (2.9 mmol, 144 %). The crude product contained sulfur-based impurities and moisture, and was used as such in subsequent reactions.

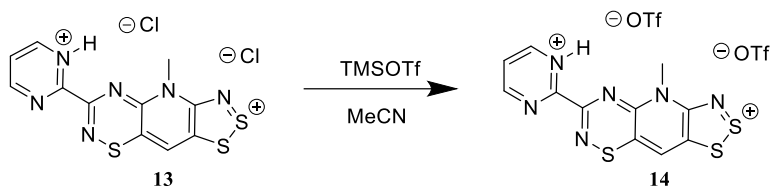


Scheme 42. Synthesis of 4-methyl-6-(pyrimidin-1-ium-2-yl)-4H-[1,2,3]dithiazolo[5',4':5,6]pyrido[2,3-e][1,2,4] thiadiazin-2-ium chloride **13**.

8.2.14 4-Methyl-6-(pyrimidin-1-ium-2-yl)-4H-[1,2,3]dithiazolo[5',4':5,6]pyrido[2,3-e][1,2,4] thiadiazin-2-ium bis(trifluoromethanesulfonate) **14**

To intermediate **13** (1.1 g, 2.9 mmol, 1 eq.) in MeCN (100 ml) trimethylsilyl trifluoromethanesulfonate (1.5 ml, 8.3 mmol, 2.9 eq.) was added via syringe (Scheme 43). The solution was hot filtered and then flash distilled twice. The resulting green product was dried in vacuo and recrystallized from 60 ml of MeCN. Yield 0.7 g (1.1 mmol, 39 %).

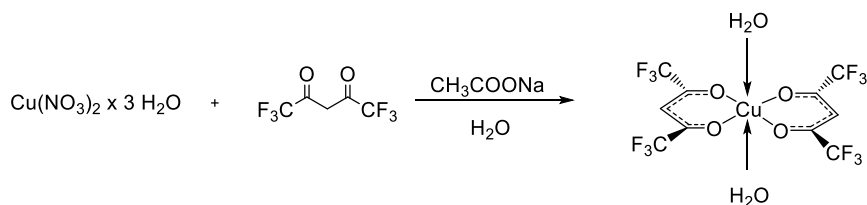
IR ν_{\max} (cm⁻¹): 3092 (w), 1614 (w), 1585 (m), 1543 (w), 1510 (m), 1493 (s), 1438 (w), 1402 (w), 1374 (m), 1283 (s), 1239 (s), 1220 (s), 1158 (s), 1099 (m), 1064 (m), 1021 (s), 1000 (s), 954 (m), 885 (m), 806 (m), 773 (m), 760 (m), 741 (s), 704 (m), 659 (m), 632 (s), 573 (m), 516 (m), 494 (m), 477 (m), 458 (m) (Appendix 10).



Scheme 43. Synthesis of 4-methyl-6-(pyrimidin-1-ium-2-yl)-4H-[1,2,3]dithiazolo[5',4':5,6]pyrido[2,3-e][1,2,4]thiadiazin-2-ium bis(trifluoromethanesulfonate) **14**.

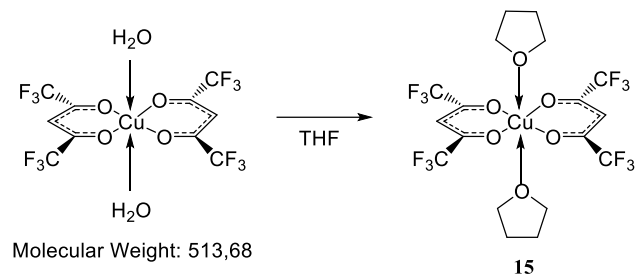
8.2.15 Bis(hexafluoroacetylacetonate)copper(II) ditetrahydrofuran **15**

Copper hexafluoroacetylacetonate dihydrate $[\text{Cu}(\text{hfac})_2 \cdot 2\text{H}_2\text{O}]$ was made according to procedure of Bertrand and Kaplan.⁷⁰ Copper nitrate trihydrate (2.9 g, 12 mmol) was dissolved in deionized water (150 ml). To solution was added hexafluoroacetylacetone (5 g, 24 mmol, 2 eq.) (Scheme 44) and sodium acetate (2.0 g, 24 mmol) dissolved in water (20 ml). The combined solution was stirred for 30 minutes and the formed precipitate was filtered to yield a light green solid. Yield: 4.7 g (9.1 mmol, 76 %).



Scheme 44. Synthesis of bis(hexafluoroacetylacetonate)copper(II) dihydrate.

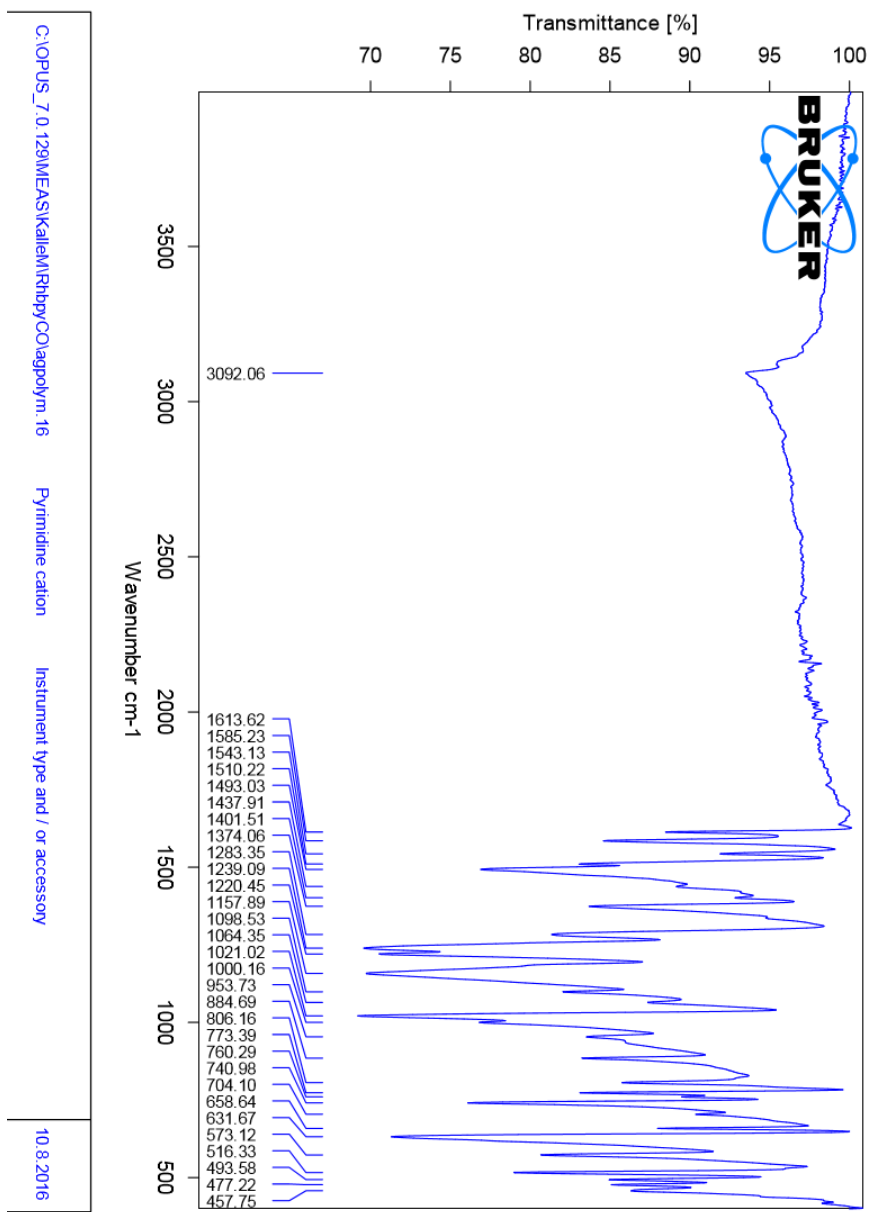
In 10 ml of dry tetrahydrofuran (THF) was added $\text{Cu}(\text{hfac})_2 \cdot 2\text{H}_2\text{O}$ (Scheme 45) to give a saturated solution which was heated, hot filtered and heated again to induce crystallization. The solution was put into freezer and crystals were collected on a fine glass frit and dried in vacuo. Yield: 0.39 g (0.6 mmol, 6.9 %).



Scheme 45. Synthesis of bis(hexafluoroacetylacetonate)copper(II) ditetrahydrofuran **15**.

IR ν_{\max} (cm^{-1}): 3148 (w), 2892 (w), 1637 (m), 1471 (m), 1249 (m), 1140 (s), 1141 (s), 1105 (s), 1041 (m), 801 (m), 679 (m), 594 (m) (

Appendix 10. IR- spectrum of compound 14.

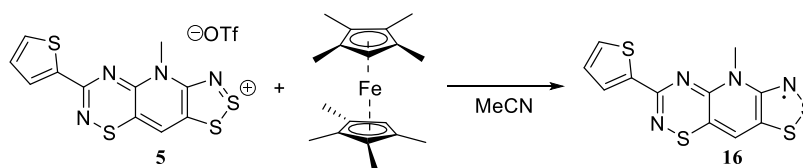


Appendix 11).

8.3 REDUCTIONS

8.3.1 Reduction of 4-methyl-6-(thiophen-2-yl)-4H-[1,2,3]dithiazolo[5',4':5,6]pyrido[2,3-e][1,2,4]thiadiazin-2-ium trifluoromethanesulfonate to radical **16**

Product **5** (0.32 g, 0.70 mmol, 1 eq.) was dissolved in 125 ml of MeCN (Scheme 46) in a 200 ml Schlenk flask and the solution was degassed three times. The reducing agent octamethyl ferrocene (OMFc, 304 mg, 1.0 mmol, 1.5 eq.) was added into another flask and a suitable filter stick was placed between the two flasks. The reduction was performed by pouring the solution of **5** slowly into the other flask while the resulting mixture was stirred. Yield: 0.15 g (0.45 mmol, 67 %).



Scheme 46. Reduction of 4-methyl-6-(thiophen-2-yl)-4H-[1,2,3]dithiazolo[5',4':5,6]pyrido[2,3-e][1,2,4]thiadiazin-2-ium trifluoromethanesulfonate to radical **16**.

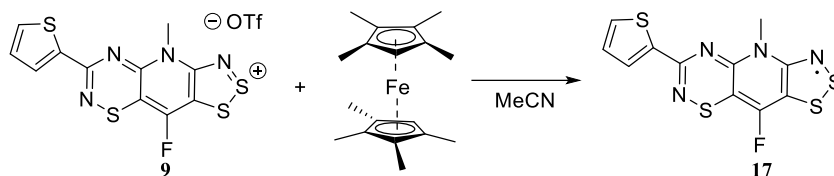
8.3.2 Reduction of 9-fluoro-4-methyl-6-(thiophen-2-yl)-4H-[1,2,3]dithiazolo[5',4':5,6]pyrido[2,3-e][1,2,4]thiadiazin-2-ium in acetonitrile to radical **17**

Reduction of **9** (Scheme 47) was done by using an H-cell. Into one bulb was added intermediate **9** (0.055 g, 0.12 mmol, 1 eq.) with dry MeCN (20 ml) and into the other OMFc (0.051 g, 0.17 mmol) with MeCN (10 ml). Both solutions were degassed three times while keeping them separated from each other. After degassing, the solutions were allowed

to mix and let to react through the fine frit under static vacuum. Dark green needles were formed overnight and washed with MeCN and dried under an argon flow.

IR ν_{\max} (cm^{-1}): 1514 (m), 1470 (m), 1352 (m), 1107 (m), 1036 (m), 823 (m), 752 (m), 713 (s), 611 (m), 462 (m) (

Appendix 12).



Scheme 47. Reduction of 9-fluoro-4-methyl-6-(thiophen-2-yl)-4H-[1,2,3]dithiazolo[5',4':5,6]pyrido[2,3-e][1,2,4]thiadiazin-2-ium to radical **17**.

8.3.3 Reduction of 9-fluoro-4-methyl-6-(thiophen-2-yl)-4H-[1,2,3]dithiazolo[5',4':5,6]pyrido[2,3-e][1,2,4]thiadiazin-2-ium in propionitrile to radical **17**

Reduction of **9** was repeated exactly as described before but using propionitrile (PCN) as the solvent. Compound **9** (0.055 g, 0.11 mmol, 1 eq.) and OMFc (0.051 g, 0.17 mmol, 1.5 eq.) were completely dissolved in dry PCN (20 and 10 ml, respectively) in separate bulbs. Degassing was done three times after which the solutions were slowly combined. Dark green needles were formed overnight and washed with PCN and dried under an argon flow.

8.3.4 Large scale reduction of 9-fluoro-4-methyl-6-(thiophen-2-yl)-4H-[1,2,3]dithiazolo[5',4':5,6]pyrido[2,3-e][1,2,4]thiadiazin-2-ium to radical **17**

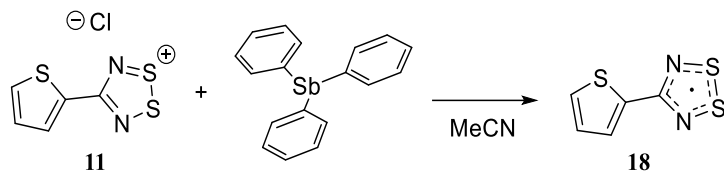
Intermediate **9** (0.140 g, 0.29 mmol, 1 eq.) and the reducing agent OMFc (0.130 g, 0.44 mmol, 1.5 eq.) were dissolved in MeCN (35 and 25 ml, respectively). Both solutions were degassed three times using an evacuation time of 10 minutes. After degassing, the solutions were combined and the resulting mixture was stirred while crystallization took place. The crystals were collected on a frit and washed repeatedly with small amounts of dry MeCN.

8.3.5 Reduction of 4-(thiophen-2-yl)-1,2,3,5-dithiadiazol-1-ium chloride with stoichiometric amount of reducing agent to radical **18**

Product **11** (0.26 g, 1.2 mmol, 1 eq.) was added to a Schlenk flask in the glove box, while triphenyl antimony (0.42 g, 1.2 mmol, 1 eq.) was dissolved in dry MeCN (25 ml) in another flask (Scheme 48). The flasks were connected with a filter stick and the chloride salt was backwashed with the solution containing the reducing agent. The resulting mixture was stirred for 30 minutes after which the solution was filtered to give a solution that was flash distilled to yield a medium purple colored solid. The solid was purified by sublimation at 80 °C. Yield: 0.15 g (0.78 mmol, 67 %).

IR ν_{max} (cm⁻¹): 3061 (w), 3039 (w), 2071 (w), 1527 (w), 1428 (s), 1370 (s), 1331 (s), 1261 (m), 1105 (m), 1063 (m) (

Appendix 13).



Scheme 48. Reduction of 4-(thiophen-2-yl)-1,2,3,5-dithiadiazol-1-ium chloride to radical **18**.

8.3.6 Reduction of 4-(thiophen-2-yl)-1,2,3,5-dithiadiazol-1-ium chloride with sub-stoichiometric amount of reducing agent to radical **18**

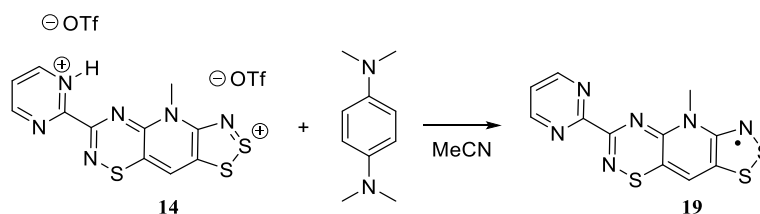
The reduction of **11** (0.36 g, 1.6 mmol, 1 eq.) was repeated exactly as described before but using a sub-stoichiometric amount (0.40 g, 1.1 mmol, 0.7 eq.) of triphenyl antimony. The product was purified by sublimation at 50 °C. Yield: 0.17 g (0.88 mmol, 77 %).

IR ν_{max} (cm⁻¹): 3061 (w), 3039 (w), 2071 (w), 1527 (w), 1428 (s), 1370 (s), 1331 (s), 1261 (m), 1105 (m), 1063 (m) (

Appendix 13)

8.3.7 Reduction of 4-methyl-6-(pyrimidin-2-yl)-4H-[1,2,3]dithiazolo[5',4':5,6]pyrido[2,3-e][1,2,4]thiadiazin-2-ium) with N,N,N,N-tetramethyl-p-phenylenediamine to radical **19**

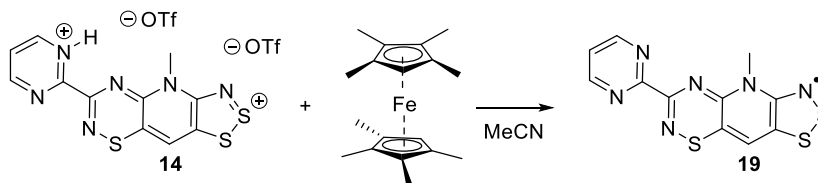
Reduction of **14** (Scheme 49) was done by using an H-cell and similarly as described for **17**. Compound **14** (0.064 g, 0.10 mmol, 1 eq.) and N,N,N,N-tetramethyl-p-phenylenediamine (TMPDA, 0.040 g, 0.24 mmol, 2.4 eq.) were dissolved in MeCN (19 and 12 ml) and the solutions were degassed three times after which they were slowly combined. A non-crystalline product was obtained.



Scheme 49. Reduction of 4-methyl-6-(pyrimidin-2-yl)-4H-[1,2,3]dithiazolo[5',4':5,6]pyrido[2,3-e][1,2,4]thiadiazin-2-ium) to radical **19**.

8.3.8 Reduction of 4-methyl-6-(pyrimidin-2-yl)-4H-[1,2,3]dithiazolo[5',4':5,6]pyrido[2,3-e][1,2,4]thiadiazin-2-ium with octamethyl ferrocene to radical **19**

Reduction of **14** (0.051 g, 0.082 mmol, 1 eq.) was done with OMFc (0.060 g, 0.20 mmol, 2.4 eq.) as described above (Scheme 50). A non-crystalline product was obtained.

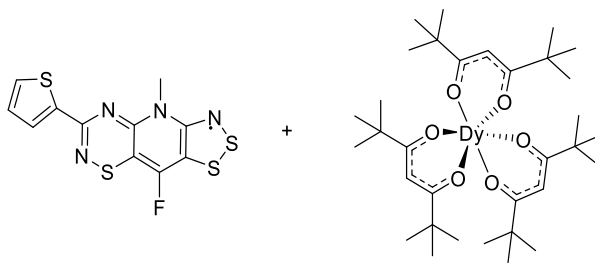


Scheme 50. Reduction of 4-methyl-6-(pyrimidin-2-yl)-4H-[1,2,3]dithiazolo[5',4':5,6]pyrido[2,3-e][1,2,4]thiadiazin-2-ium to radical **19**.

8.4 COMPLEXATION

8.4.1 Radical 17 and Dy(^tBu-acac)₃

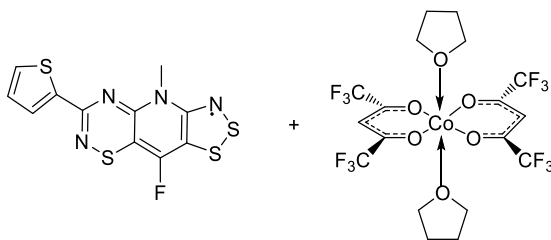
Radical **17** (0.035 g, 0.10 mmol, 1 eq.) and tris(2,2,6,6-tetramethyl-3,5-heptadionato dysprosium (III))(0.083 g, 0.12 mmol, 1.1 eq.), also known as Dy(^tBu-acac)₃, were combined to a single Schlenk flask inside a glove box (Scheme 51). The solvent (DCM, 30 ml) was added and the resulting solution was brought out of the box and degassed twice. The mixture was stirred overnight (17 h), filtered with a cannula and then distilled under reduced pressure using cryogenic distillation. No crystals suitable for X-ray diffraction were obtained.



Scheme 51. Complexation of radical **17** with Dy(^tBu-acac)₃

8.4.2 Radical 17 and Co(hfac)₂ · 2 THF

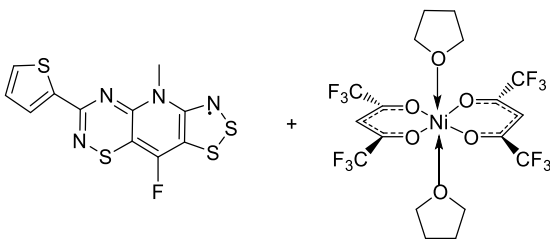
Radical **17** (0.025 g, 0.073 mmol, 1 eq.) and Co(hfac)₂ · 2 THF (0.051 g, 0.081 mmol, 1.1 eq.) were combined to a single Schlenk flask inside a glove box (Scheme 52). The solvent (15 ml of DCM) was added and the resulting solution was brought out of the box and degassed twice. The mixture was stirred overnight (17 h), filtered with a cannula and then distilled under reduced pressure using cryogenic distillation. No crystals suitable for X-ray diffraction were obtained.



Scheme 52. Complexation of radical **17** and $\text{Co}(\text{hfac})_2 \cdot 2 \text{ THF}$.

8.4.3 Radical **17** and $\text{Ni}(\text{hfac})_2 \cdot 2 \text{ THF}$

Radical **17** (0.025 g, 0.073 mmol, 1 eq.) and $\text{Ni}(\text{hfac})_2 \cdot 2 \text{ THF}$ (0.054 g, 0.088 mmol, 1.2 eq.) were combined to a single Schlenk flask inside a glove box (Scheme 53). The solvent (15 ml of DCM) was added and the resulting solution was brought out of the box and degassed twice. and then mixture was stirred overnight. The mixture was stirred overnight (17 h), filtered with a cannula and then distilled under reduced pressure using cryogenic distillation. No crystals suitable for X-ray diffraction were obtained.



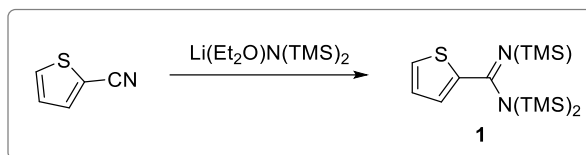
Scheme 53. Complexation of radical **17** and $\text{Ni}(\text{hfac})_2 \cdot 2 \text{ THF}$.

9 RESULTS AND DISCUSSION

9.1 STARTING MATERIALS

9.1.1 (E)-N,N,N'-tris(trimethylsilyl)thiophene-2-carboximidamide **1**

As most of the target compounds were thiophene-substituted derivatives, the synthesis of the starting material (E)-N,N,N'-tris(trimethylsilyl)thiophene-2-carboximidamide (**1**) was essential for the work performed (Scheme 54). The synthesis of **1** was not particularly high-yielding (*ca.* 20 %), which meant that it needed to be performed repeatedly throughout the work. The reaction was done under an argon atmosphere and in dry conditions. The reaction mixture was refluxed overnight and then let to cool down. The cooled mixture was filtered either with glass frit or cannula, and distilled to obtain **1** as a yellow liquid.



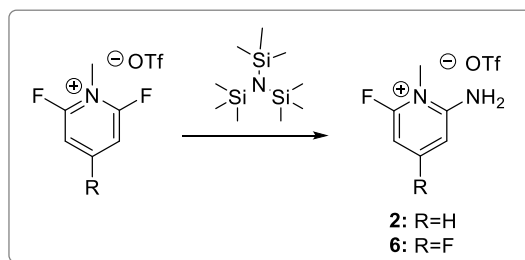
Scheme 54. Synthesis of **1**.

The purity of **1** was determined by ^1H NMR (

Appendix 1), which revealed three distinct resonances associated with the three protons on the thiophene ring (7.24 ppm, 7.11 ppm and 6.94 ppm). The resonances of the protons on the silyl groups were observed at 0.12 ppm, *i.e.*, close to the resonance of TMS. These results are in excellent agreement with literature data.⁷¹

9.1.2 2-Amino-6-fluoro-1-methylpyridin-1-ium trifluoromethanesulfonate **2** and 2-amino-4,6-difluoro-1-methylpyridin-1-ium trifluoromethanesulfonate **6**

Other important starting materials were 2-amino-6-fluoro-1-methylpyridin-1-ium trifluoromethanesulfonate (**2**) and 2-amino-4,6-difluoro-1-methylpyridin-1-ium trifluoromethanesulfonate (**6**) which were synthesized from structurally related precursors in which one of the fluorine atoms acts as a leaving group (Scheme 55). The reactions were catalyzed by tetrabutylammonium fluoride (deprotection of silyl groups).⁷² The solutions were stirred overnight at ambient temperature. Silyl groups were removed by addition of methanol and the resulting white solid was recrystallized from a mixture of dichloroethane and acetonitrile (6:1 ratio), giving **2** and **6** in good (*ca.* 70 – 80 %) yield.



Scheme 55. Synthesis of starting materials **2** and **6**.

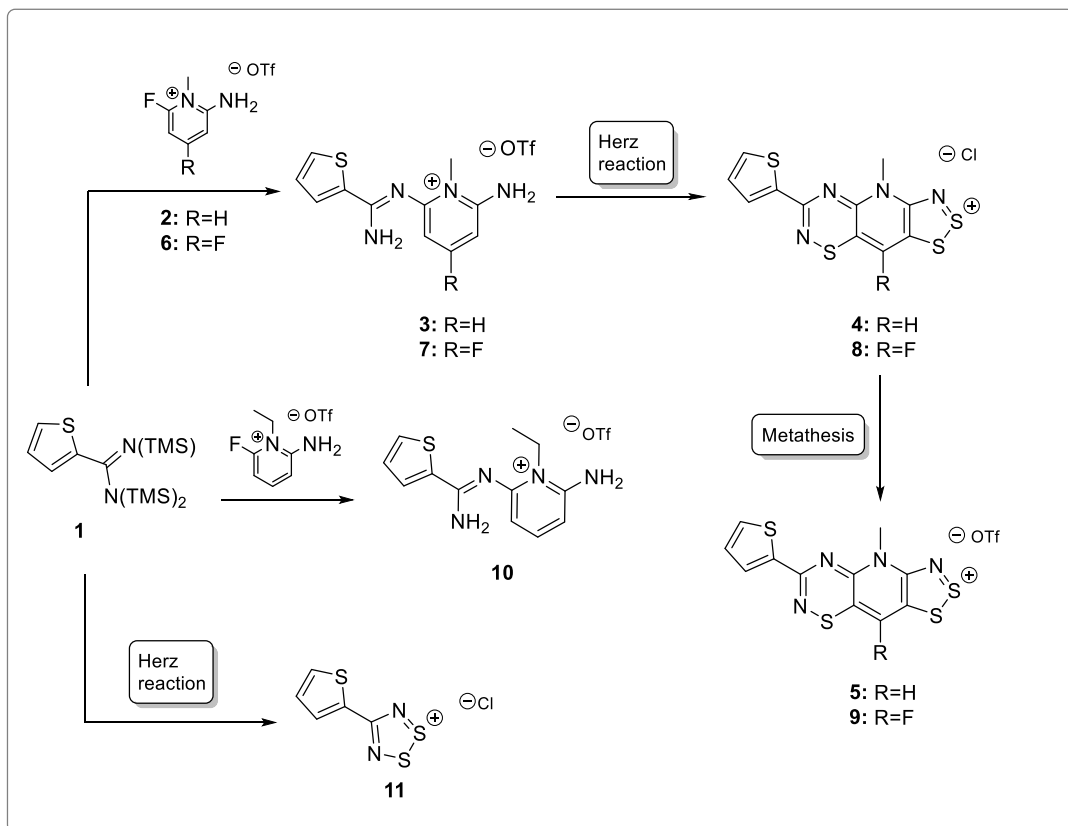
The purity of **6** was determined by ¹H NMR (

Appendix 5). The ^1H NMR spectrum of **6** shows a singlet at 7.22 ppm ($-\text{NH}_2$) and a multiplet at 6.69 ppm (aromatic protons). The resonance at 3.59 ppm is due to the proton of the methyl group.

9.2 PREPARATION OF CATIONS

9.2.1 Synthesis of thiophene-substituted cations

An overview of the synthesis of thiophene-substituted cations is shown in (Scheme 56). The first step in the synthetic route is the condensation reaction forming cations **3**, **7** and **10**. The reactions were catalysed by tetrabutylammonium fluoride (deprotection of silyl groups) and stirred overnight. Silyl groups were removed by addition of methanol and the products were purified by distillation. Products **3** and **7** were obtained as yellow solids in reasonable yield (40 – 50 %) whose purity was determined by ^1H NMR. However, the product **10** could not be obtained sufficiently pure by repeated recrystallizations for which reason it was not characterized in any detail nor was it used in any of the subsequent syntheses.

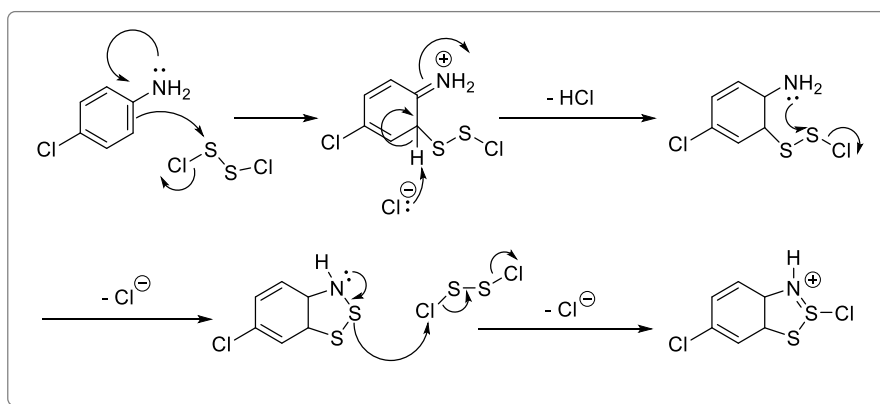


Scheme 56. Summary of syntheses of thiophene-substituted cations.

The ^1H NMR spectrum of **3** shows resonances of the thiophene protons at 7.81 – 7.67 ppm (Appendix 2). The proton at the para-position in the pyridinium gives a characteristic triplet at 7.16 ppm while the doublets of the adjacent protons are seen at 6.58 and 6.46 ppm. The singlet arising from the protons of the methyl group is seen at 3.59 ppm. The protons of the amino group could not be observed in the ^1H NMR spectrum, possibly due to the dilute sample used in the measurement. These results are in excellent agreement with literature data.¹

The ^1H NMR spectrum of **7** shows resonances of the thiophene protons at 7.72 – 7.19 ppm (Appendix 6). In addition, a singlet arising from the protons at meta-positions in the pyridinium ring is seen at 6.38 ppm. The resonance at 3.58 ppm is due to the methyl protons, while that at 6.61 ppm is due to the amino group. The similarity of the ^1H NMR data of **7** to that of **3** is understandable considering their similar structures.

The next synthetic step was ring closure that gives compounds **4** and **8**, and ultimately **5** and **9** via metathesis. This was achieved with the Herz reaction, also known as the Herz cyclization, where an aromatic amine is treated with an excess of disulfur dichloride (S_2Cl_2). The details of this reaction are not well-understood⁷³ but a mechanism to it has been proposed in which the nucleophilic double bond attracts the soft electrophilic sulfur atom (Scheme 57).^{74,72} The next step involves the attack of the amino nitrogen on sulfur to form the heterocycle.



Scheme 57. A general mechanism proposed for Herz cyclizations.⁷⁴

Because the Herz cyclization produces an excess of free chloride, it is possible that some anion exchange from trifluoromethanesulfonate to chloride takes place. To ensure that this exchange is complete, the compound **4** was treated with benzyltriethylammonium chloride, followed by treatment with trimethylsilyl trifluoromethanesulfonate to replace the trifluoromethanesulfonate anion and give compound **5**. The synthesis of the compound **9** was performed similarly but compound **8** was not treated with benzyltriethylammonium chloride as, after the addition of sulfur monochloride and refluxing, no precipitate stayed on the frit. This suggests that most of **8** existed as the trifluoromethanesulfonate salt **9** as they are more soluble than the respective chlorides.

Compounds **5** and **9** were obtained in low yield (10 – 20 %) and characterized by IR spectroscopy (Appendix 4 and Appendix 7). In addition, the solid-state structure of **9** was determined by single crystal X-ray crystallography (Figure 27) and its propensity to undergo one-electron reduction was analysed by cyclic voltammetry.

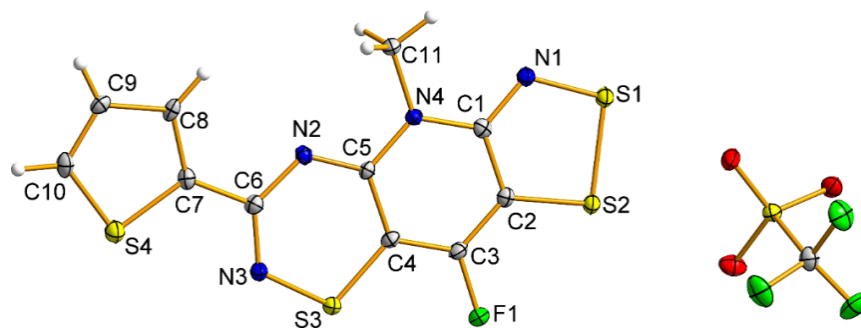


Figure 27. The solid-state structure of **9** with thermal ellipsoids at 30% probability. Solvent of crystallization (MeCN) is removed for clarity.

The cyclic voltammogram of **9** was measured in MeCN (Figure 28). The results were referenced internally to the ferrocene couple (Fc^+/Fc) vs. SCE. The cyclic voltammogram of **9** shows a reversible cation to neutral radical reduction with a half-cell potential $E_{1/2} = 0.194$ V. In contrast, the reduction of the neutral radical to the corresponding anion was found to be irreversible, most likely due to degradation of the sample during the experiment. Hence, E_{cell} was estimated as a difference between the two cathodic peaks, E_{pc} , and the result (0.760 V) was in excellent agreement with the literature value for cation **5** (0.760 V).¹

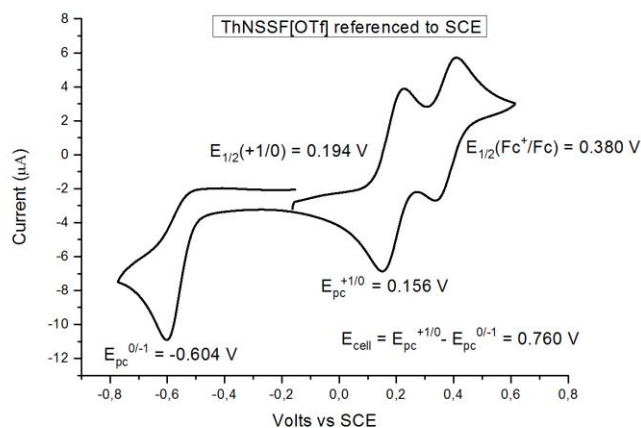


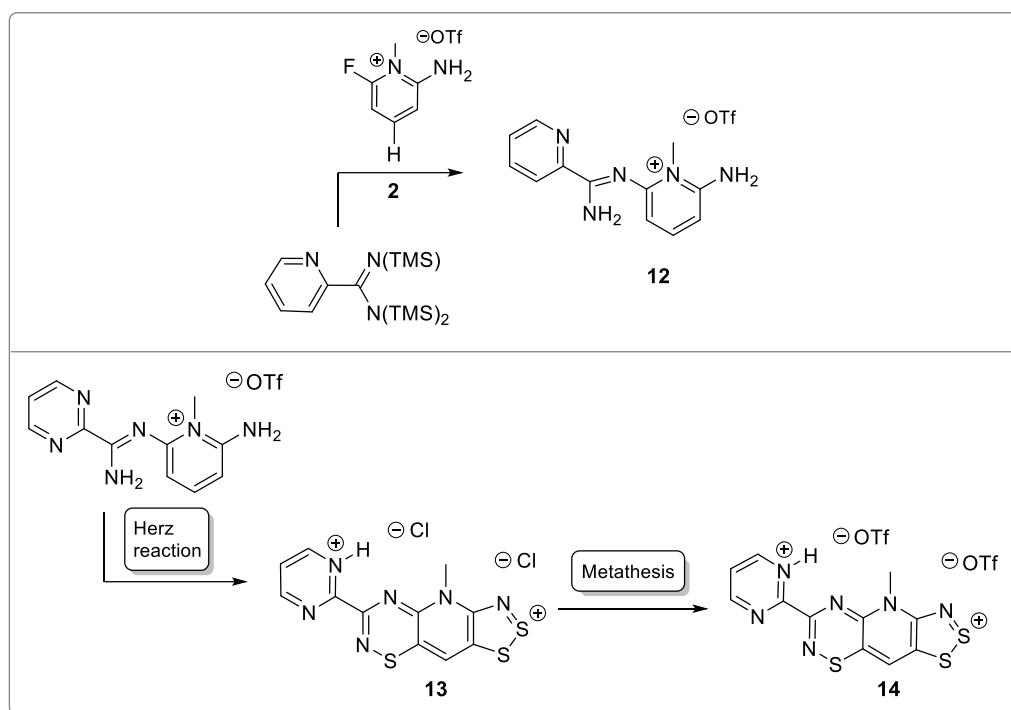
Figure 28. Cyclic voltammogram of **9** in MeCN.

Compound **1** was also reacted directly with S_2Cl_2 to give **11** as orange powder in reasonable yield (*ca.* 50 %). The product was characterized by IR spectroscopy (

Appendix 8) and no metathesis was performed to it prior to its reduction.

9.2.2 Synthesis of pyridine- and pyrimidine-substituted cations

Synthetic routes to pyridine- and pyrimidine-substituted cations (Scheme 58) followed the same procedure as for thiophene-substituted cations but pyridine- and pyrimidine-based starting materials were used. This gave, for example, compound **12** as a dark yellow solid in good yield (*ca.* 70 %). However, due to the lack of time, compound **12** was not used in any subsequent reactions.



Scheme 58. Summary of syntheses of pyridine- and pyrimidine-substituted cations.

The ^1H NMR spectrum of compound **12** shows two doublets (8.67 and 8.35 ppm) and two triplets (7.97 and 7.73 ppm) that can be assigned to the protons of the pyridine substituent (Appendix 9). The multiplet at 7.61 – 7.58 ppm can be assigned to the protons at the para-position of the 2-amino-1-methylpyridinium ring, while singlets at 6.66 ppm and 6.59 ppm are due to the protons at the meta-position. The resonance at 3.64 ppm is due to the methyl protons. The protons of the amino group could not be observed in the ^1H NMR spectrum, possibly due to the dilute sample used in the measurement. The spectrum of compound **12**

is in good overall agreement with literature data available for the related species **3** bearing a thiophene substituent.¹

Product **13** was prepared similarly as the thiophene-substituted products **4** and **8**. Disulfur dichloride was added to (2-amino-6-((amino(pyrimidin-2-yl)methylene)amino)-1-methylpyridin-1-ium trifluoromethanesulfonate) and the resulting product was treated with benzyltriethylammonium chloride, followed by metathesis with trimethylsilyl trifluoromethanesulfonate. This gave the trifluoromethanesulfonate salt **14** as a green powder in good (*ca.* 40 %) yield. The product was characterized by IR spectroscopy (Appendix 10).

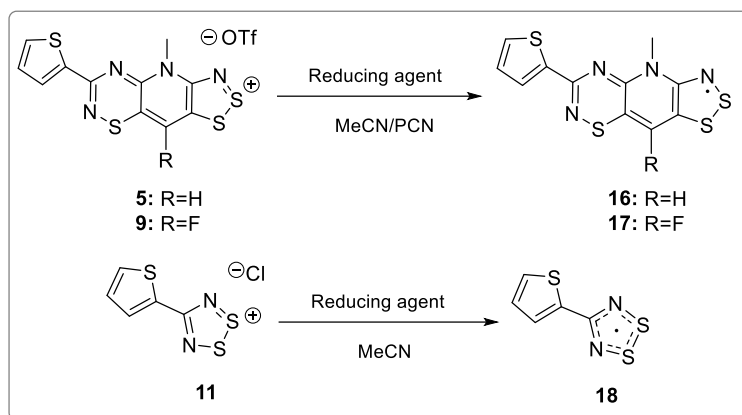
9.3 REDUCTION OF CATIONS

9.3.1 Reduction of thiophene-substituted cations

Radicals were generated by reducing cations **5**, **9** and **11** (Scheme 59). Suitable reducing agents were determined based on electrochemical results. For example, the reduction of **5** was done in MeCN and OMFc was used as the reducing agent. The reduction of **9** was repeated several times by varying the scale, solvent and reducing agent (Table 3). All small-scale reductions were done with the H-cell, whereas all large-scale reductions were performed using a filter stick and two flasks.

Table 3. All reductions of cation **9**.

Cation 9 (mg)	Reducing agent (mg)	Solvent (ml)	Method
55	OMFc (51)	MeCN (20+10)	H-cell
55	OMFc (51)	PCN (20+10)	H-cell
50	TMPDA (24)	MeCN (30+10)	H-cell
142	OMFc (103)	MeCN (35+25)	Minibulk
144	OMFc (131)	PCN (50+20)	Minibulk
50	DMFc (33)	MeCN (30+15)	H-cell



Scheme 59. Summary of reductions of thiophene-substituted cations.

Radical **17** was obtained as dark green needles in reasonable (*ca.* 40 %) yield and characterized by EPR and IR spectroscopy. In addition, the solid-state structure of **9** was determined by single crystal X-ray crystallography (Figure 29), allowing comparison with the metrical parameters of the cation in **9** (Table 4). It can be seen from the results, that the bonds involving sulfur atoms have elongated upon addition of an electron. For example, both S1–N1 and S1–S2 bonds elongate by 0.036 Å, while the lengthening of S2–C2 and S3–N4 bonds is slightly less, 0.028 and 0.017 Å, respectively. This indicates delocalization of spin density over the entire π -framework in **17**.

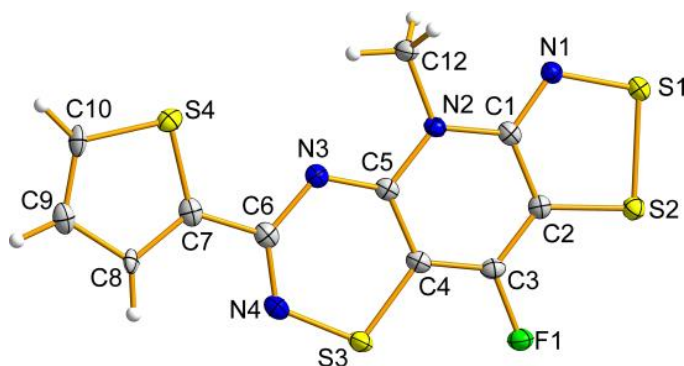


Figure 29. The solid-state structure of **17** with thermal ellipsoids at 30% probability.

Intermolecular interactions are important in mediating magnetic interactions as the demonstration of bulk magnetic properties depends on the propagation of magnetic interactions to all three dimensions.¹ In this respect, radical **17** packs into distinct planes in the solid-state with a mean plane separation (δ) of 3.446 Å (Figure 30) Within each plane,

the radicals **17** form close S \cdots N' and S \cdots S' intermolecular interactions of 3.159(3) and 3.303(1) Å, respectively. For comparison, the corresponding values for radical **16** are 3.165(6) Å and 3.487(3) Å,¹ which shows that the intermolecular sulfur \cdots sulfur contacts are significantly shorter in **17**, which can influence the magnetic interactions observed in the solid-state. The solid-state structure of **17** shows also a weak intramolecular N \cdots H'-C' hydrogen bond at 2.726 Å.

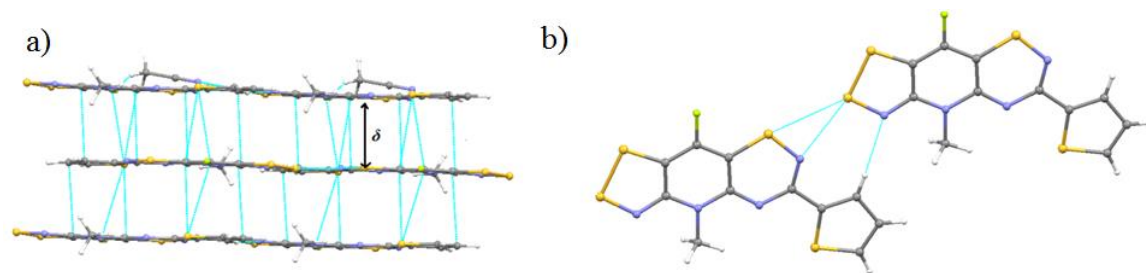


Figure 30. a) Planar packing of radicals **17** in the solid-state ($\delta = 3.446$ Å). b) Intermolecular S \cdots S', S \cdots N' and N \cdots H' interactions between adjacent radicals **17** in the solid-state.

Table 4. Bond lengths (in Ångström) of **9** and **17**.

Atom 1	Atom 2	Bond length (9)	Bond length (17)	Δ Bond length
C2	S2	1.703(3)	1.731(2)	0.028
S2	S1	2.073(1)	2.109(1)	0.036
S1	N1	1.621(3)	1.657(2)	0.036
N1	C1	1.307(4)	1.312(5)	0.005
C1	C2	1.430(4)	1.425(5)	-0.005
C1	N2	1.388(4)	1.379(4)	-0.009
N2	C5	1.372(4)	1.392(4)	0.020
C5	C4	1.442(4)	1.427(5)	-0.015
C4	C3	1.373(5)	1.373(4)	0.000
C3	C2	1.377(4)	1.372(5)	-0.005
N2	C11	1.466(4)	1.467(5)	0.001
C3	F1	1.361(4)	1.368(3)	0.007
C5	N3	1.313(4)	1.309(3)	-0.004
N3	C6	1.357(4)	1.372(5)	0.015
C6	N4	1.313(4)	1.303(5)	-0.010
N4	S3	1.645(3)	1.662(2)	0.017
S3	C4	1.707(3)	1.743(4)	0.036
C6	C7	1.458(4)	1.455(4)	-0.003

C7	S4	1.725(3)	1.683(4)	-0.042
S4	C10	1.694(3)	1.708(6)	0.014
C10	C9	1.356(4)	1.38(1)	0.024
C9	C8	1.422(4)	1.46(1)	0.038
C8	C7	1.407(4)	1.38(1)	-0.027

EPR spectroscopy is typically used to study molecules with unpaired electrons.⁷⁵ The EPR spectrum of radical **17** shows an eleven-line pattern (Figure 31), which can be simulated by taking into account the coupling of the unpaired electron to one ^{19}F ($a_{\text{F}} = 5.832$ G) and two non-equivalent ^{14}N nuclei ($a_{\text{N}1} = 3.831$ G and $a_{\text{N}2} = 2.042$ G). An excellent fit between the experimental and simulated spectrum is obtained by adding smaller hyperfine coupling constants to two additional non-equivalent ^{14}N nuclei ($a_{\text{N}3} = 1.194$ G and $a_{\text{N}4} = 0.407$ G) and using an appropriate line shape function.

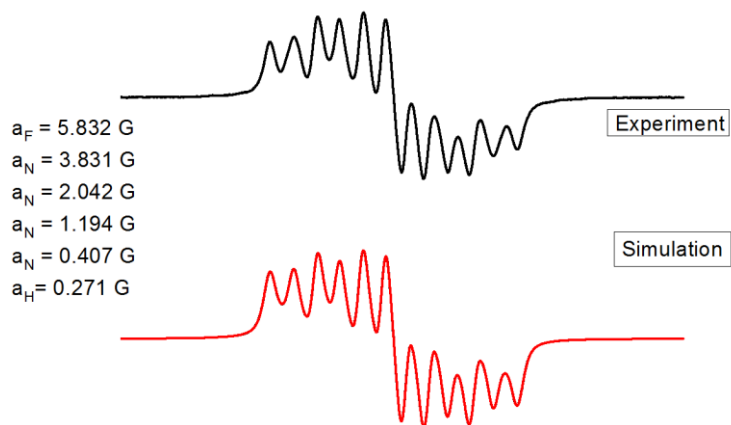


Figure 31. Experimental and simulated EPR spectrum of radical **17**.

The reduction of the cation **11** was done in MeCN and using triphenyl antimony as the reducing agent. The reduction was performed using a stoichiometric (or slightly sub-stoichiometric) amount of the reducing agent, which, however, gave an impure product and the radical **18** was purified by sublimation. The solid-state structure of radical **18** was determined using single crystal X-ray diffraction (Figure 32). The radical dimerizes in the solid-state and adopts a *cis*-cofacial arrangement typical for 1,2,3,5-dithiadizolyls (the average $\text{S}\cdots\text{S}'$ bond distance is 3.120 Å).⁵ The individual dimers adopt an edge-to-face packing pattern in the solid-state. The paramagnetic nature of radical **18** was confirmed

with EPR spectroscopy in DCM, which yielded a 1:2:3:2:1 pentet pattern that indicates coupling of the unpaired electron to two equivalent nitrogen ^{14}N nuclei. An excellent simulation of the experimental spectrum was obtained using $a_{\text{N}} = 5.01$ G, which is well in line with the couplings typically observed for 1,2,3,5-dithiadiazolyl radicals (Figure 33).¹⁶

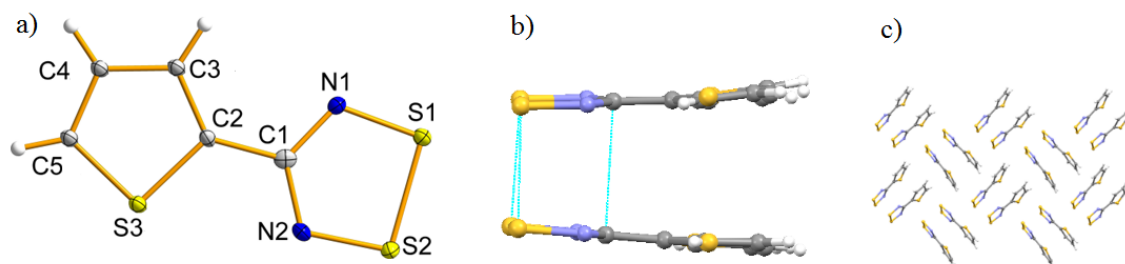


Figure 32. a) The solid-state structure of **18** with thermal ellipsoids at 30% probability. b) The *cis*-cofacial arrangement of two neighbouring radicals **18** in the solid-state. c) Packing of radical dimers creates edge-to-face π -stacks.

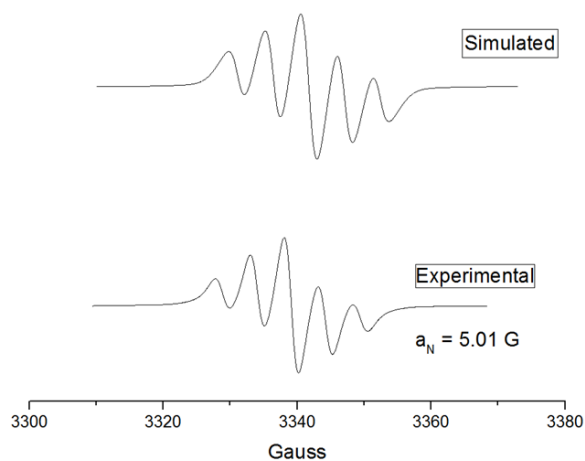
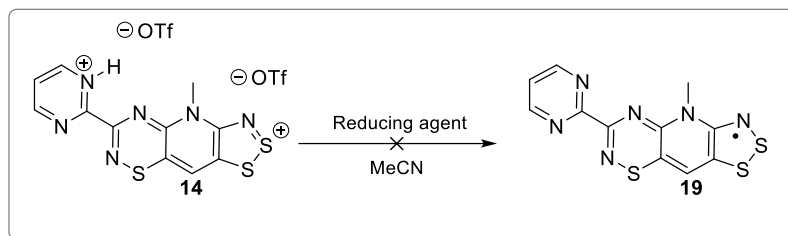


Figure 33. Experimental and simulated EPR spectrum of radical **18**.

9.3.2 Reduction of pyrimidine-substituted cations

The reduction of the cation **14** was attempted with TMPDA and OMF_e in MeCN using H-cell techniques (Scheme 60). However no crystalline product could be obtained, which is most likely due to the presence of a proton at one of the pyrimidine nitrogen centres.



Scheme 60. Summary of reductions of pyrimidine-substituted cations.

10 CONCLUSIONS

The main objective in this thesis was to examine syntheses and properties of organic thiazyl radicals. Thiazyls are radicals consisted of nitrogen and sulfur fragments which provide stability for unpaired electron allowing spin density to distribute to over the whole π -framework.⁵ To reach the goal of the thesis, six different types of precursor compounds, Herz salts, were synthesized. Reduction reactions were performed to generate radicals corresponding to cation of salt and as a result two novel main group radicals were synthesized and characterized. The other new radical belonged to the vast group of dithiadiazolyls but had an unseen structure with a thiophene substituent. Otherwise this new radical showed predictable behaviour for this class of thiazyls: it dimerized and hence it did not have interesting conductive or magnetic properties.

Another successfully synthesized radical was dithiazolothiadiazinyl. This group of radicals is a subgroup of 1,2,3-dithiazolyls but is more complex compound. Dithiazolothiadiazinyl is a combination of 1,2,3-dithiazolyl and thiazinyl and between these two groups there is a benzene ring and because of the construction of the π -framework the spin density is able to distribute over the whole molecule and the radicals are extremely stable. Dithiazolothiadiazinyls are relatively new group of thiazyl radicals and all the new characterized dithiazolothiadiazinyls give more important insight. In this work synthesized new radical was stable in the normal atmosphere and it had a crystal packing which differed from the earlier ones reported in the literature. The change in the crystal packing can lead to better exchange pathways and enhance the magnetism. However, interesting conductive properties could not be observed as radical to anion reduction was irreversible and sample degraded during the cyclic voltammetry experiment.

Also few trials of complexation reactions of dithiazolothiadiazinyl with metals centers were performed but unfortunately, no coordination complexes were obtained. By modification the substituents of radical **17** the complexation could be possibly obtained. The modification could be for example changing sulfur containing substituent thiophene to substituent containing nitrogen such as pyridine or pyrimidine. In other words, syntheses of 2-pyridine and pyrimidine radicals would deserve further examination as the syntheses could result a prospective metal coordinating radical.

Overall, the thiazyl radicals are still quite a novel research area as the first discoveries dating back to 1970. Coordination of paramagnetic metals and thiazyl radicals is a growing research field and the study can result developed molecules for future molecule-based devices. Organic thiazyls alone have also shown exceptional conductivity and magnetism. The future shows how far properties of these organic radicals can be developed.

11 REFERENCES

1. S. M. Winter, A. R. Balo, R. J. Roberts, K. Lakin, A. Assoud, P. a Dube and R. T. Oakley, Hybrid dithiazolothiadiazinyl radicals; versatile building blocks for magnetic and conductive materials., *Chem. Commun. (Camb)*., **2013**, *49*, 1603–5.
2. A. Mailman, S. M. Winter, X. Yu, C. M. Robertson, W. Yong, J. S. Tse, R. A. Secco, Z. Liu, P. A. Dube, J. A. K. Howard and R. T. Oakley, Crossing the insulator-to-metal barrier with a thiazyl radical conductor, *J. Am. Chem. Soc.*, **2012**, *134*, 9886–9889.
3. D. Tian, S. M. Winter, A. Mailman, J. W. L. Wong, W. Yong, H. Yamaguchi, Y. Jia, J. S. Tse, S. Desgreniers, R. A. Secco, S. R. Julian, C. Jin, M. Mito, Y. Ohishi and R. T. Oakley, The Metallic State in Neutral Radical Conductors: Dimensionality, Pressure and Multiple Orbital Effects, *J. Am. Chem. Soc.*, **2015**, *137*, 14136–14148.
4. I. Ratera and J. Veciana, Molecule-based magnets themed issue Playing with organic radicals as building blocks for functional molecular materials, *Chem. Soc. Rev. Chem. Soc. Rev*, **2012**, *41*, 303–349.
5. R. G. Hicks, *Stable Radicals: Fundamentals and Applied Aspects of Odd-Electron Compounds*, Wiley-Blackwell, Chichester, UK, **2010**.
6. S. A. Wolf, Spintronics: A Spin-Based Electronics Vision for the Future, *Science (80-.)*., **2001**, *294*, 1488–1495.
7. C. Chappert, A. Fert and F. N. Van Dau, The emergence of spin electronics in data storage, *Nat. Mater.*, **2007**, *6*, 813–823.
8. O. Fujita, C. J. Awaga, W. E. Hatfield and D. J. Hodgson, Room-Temperature Magnetic Bistability in Organic Radical Crystals., *Science*, **1999**, *286*, 261–263.
9. J. M. Rawson, A. Alberola and A. Whalley, Thiazyl radicals: old materials for new molecular devices, *J. Mater. Chem.*, **2006**, *16*, 2560.
10. R. L. Carroll and C. B. Gorman, The Genesis of Molecular Electronics.pdf, *Angew. Chemie Int. Ed.*, **2002**, *41*, 4378–4400.
11. Z. H. Xiong, D. Wu, Z. V. Vardeny and J. Shi, Giant magnetoresistance in organic spin-valves, *Nature*, **2004**, *427*, 821–824.
12. K. Lakin, J. W. L. Wong, S. M. Winter, A. Mailman, P. A. Dube and R. T. Oakley, Bisdithiazolyl radical spin ladders, *Inorg. Chem.*, **2013**, *52*, 2188–2198.
13. K. E. Preuss, Metal complexes of thiazyl radicals, *Dalt. Trans.*, **2007**, *21*, 2357.
14. R. T. Oakley, in *Prog. Inorg. Chem*, **1988**, 299–391.
15. M. Gomberg, AN INSTANCE OF TRIVALENT CARBON: TRIPHENYLMETHYL., *J. Am. Chem. Soc.*, **1900**, *22*, 757–771.
16. R. G. Hicks, What's new in stable radical chemistry?, *Org. Biomol. Chem.*, **2007**, *5*,

- 1321–1338.
17. G. Herzberg, Gerhard Herzberg - Nobel Lecture: Spectroscopic Studies of Molecular Structure, *Nobel Lect.*, **1971**.
 18. D. Griller and K. U. Ingold, Persistent carbon-centered radicals, *Acc. Chem. Res.*, **1976**, *9*, 13–19.
 19. M. Ballester, Inert free radicals (IFR): a unique trivalent carbon species, *Acc. Chem. Res.*, **1985**, *18*, 380–387.
 20. H. G. Viehe, Z. Janousek, R. Merenyi and L. Stella, The captodative effect, *Acc. Chem. Res.*, **1985**, *18*, 148–154.
 21. E. V. Anslyn and D. A. Doughert, Modern Physical Organic Chemistry, University Science, **2006**.
 22. P. P. Power, Persistent and stable radicals of the heavier main group elements and related species, *Chem. Rev.*, **2003**, *103*, 789–809.
 23. R. L. Greene, G. B. Street and L. J. Suter, Superconductivity in Polysulfur Nitride (SN)_x, *Phys. Rev. Lett.*, **1975**, *34*, 577–579.
 24. M. M. Labes, P. Love and L. F. Nichols, Polysulfur nitride - a metallic, superconducting polymer, *Chem. Rev.*, **1979**, *79*, 1–15.
 25. N. J. Tro, Chemistry : a molecular approach, Pearson Prentice Hall, **2011**.
 26. A. W. Cordes, R. C. Haddon and R. T. Oakley, A MOLECULE LIKE SODIUM, *Phosphorus. Sulfur. Silicon Relat. Elem.*, **2004**, *179*, 673–684.
 27. M. Imada, A. Fujimori and Y. Tokura, Metal-insulator transitions, *Rev. Mod. Phys.*, **1998**, *70*, 1039–1263.
 28. G. Saito and Y. Yoshida, Development of Conductive Organic Molecular Assemblies: Organic Metals, Superconductors, and Exotic Functional Materials, *Bull. Chem. Soc. Jpn.*, **2007**, *80*, 1–137.
 29. R. T. Boere and K. H. Moock, Solution Disproportionation Energies of 1,2,3,5-Dithia- and Diselenadiazoles. Direct Comparison of Solution Oxidation Potentials with Ionization Energies in the Gas Phase, *J. Am. Chem. Soc.*, **1995**, *117*, 4755–4760.
 30. R. a. Serway and L. D. Kirkpatrick, Physics for Scientists and Engineers with Modern Physics, *Phys. Teach.*, **1988**, *26*, 254–255.
 31. N. A. Spaldin, Magnetic materials: Fundamentals and applications, Cambridge University Press, 2nd edn., **2011**.
 32. O. Kahn, Chemistry and Physics of Supramolecular Magnetic Materials, *Acc. Chem. Res.*, **2000**, *33*, 647–657.

33. J. S. Miller, Magnetically ordered molecule-based materials, *Chem. Soc. Rev.*, **2011**, *40*, 3266.
34. D. MacDonald, 1, 2, 3-Dithiazolyl and 1, 2, 3, 5-Dithiadiazolyl Radicals as Spin-Bearing Ligands Towards the Design of New Molecular Materials, **2012**.
35. A. Vegas, A. Pérez-Salazar, A. J. Banister and R. G. Hey, Crystal structure of 4-phenyl-1,2-dithia-3,5-diazole dimer, *J. Chem. Soc., Dalt. Trans.*, **1980**, 1812–1815.
36. K. E. Preuss, Pancake bonds: π -Stacked dimers of organic and light-atom radicals, *Polyhedron*, **2014**, *79*, 1–15.
37. L. Beer, A. Wallace Cordes, R. C. Haddon, M. E. Itkis, R. T. Oakley, R. W. Reed and C. M. Robertson, A π -stacked 1,2,3-dithiazolyl radical. Preparation and solid state characterization of (Cl₂C₃NS)(C₁C₂NS₂), *Chem. Commun.*, **2002**, *4*, 1872–1873.
38. A. W. Cordes, C. D. Bryan, W. M. Davis, R. H. de Laat, S. H. Glarum, J. D. Goddard, R. C. Haddon, R. G. Hicks and D. K. Kennepohl, Prototypal 1,2,3,5-dithia- and -diselenadiazolyl [HCN₂E₂].bul. (E = sulfur, selenium): molecular and electronic structures of the radicals and their dimers, by theory and experiment, *J. Am. Chem. Soc.*, **1993**, *115*, 7232–7239.
39. A. D. Bond, D. A. Haynes, C. M. Pask and J. M. Rawson, Concomitant polymorphs: structural studies on the trimorphic dithiadiazolyl radical, ClCNSSN, *J. Chem. Soc. Dalt. Trans.*, **2002**, *6*, 2522.
40. C. Knapp, E. Lork, K. Gupta and R. Mews, Structure investigations on 4-halo-1,2,3,5-dithiadiazolyl radicals XC₂NSSN* (X = F, Cl, Br): The shortest intradimer S--S distance in dithiadiazolyl dimers, *Zeitschrift für Anorg. und Allg. Chemie*, **2005**, *631*, 1640–1644.
41. A. J. Banister, A. S. Batsanov, O. G. Dawe, P. L. Herbertson, J. A. K. Howard, S. Lynn, I. May, J. N. B. Smith, J. M. Rawson, T. E. Rogers, B. K. Tanner, G. Antorrena and F. Palacio, Modification of molecular packing: crystal structures and magnetic properties of monomeric and dimeric difluorophenyl-1,2,3,5-dithiadiazolyl radicals, *J. Chem. Soc. Dalt. Trans.*, **1997**, *62*, 2539–2542.
42. A. W. Cordes, C. M. Chamchoumis, R. G. Hicks, R. T. Oakley, K. M. Young and R. C. Haddon, Mono- and difunctional furan-based 1,2,3,5-dithiadiazolyl radicals; preparation and solid state structures of 2,5-[(S₂N₂C)OC₄H₂(CN₂S₂)] and 2,5-[(S₂N₂C)OC₄H₂(CN)], *Can. J. Chem.*, **1992**, *70*, 919–925.
43. A. W. Cordes, R. C. Haddon, R. G. Hicks, R. T. Oakley and T. T. M. Palstra, Preparation and solid-state structures of (cyanophenyl)dithia- and (cyanophenyl)diselenadiazolyl radicals, *Inorg. Chem.*, **1992**, *31*, 1802–1808.
44. N. Bricklebank, S. Hargreaves and S. E. Spey, Modification of the solid state structures of dithiadiazolyl radicals: crystal structure of p-iodophenyl-1,2,3,5-dithiadiazolyl, *Polyhedron*, **2000**, *19*, 1163–1166.

45. A. J. Banister, N. Bricklebank, I. Lavender, J. M. Rawson, C. I. Gregory, B. K. Tanner, W. Clegg, M. R. J. Elsegood and F. Palacio, Spontaneous Magnetization in a Sulfur–Nitrogen Radical at 36 K, *Angew. Chemie Int. Ed.*, **1996**, *35*, 2533–2535.
46. J. S. Miller, Polymorphic Molecular Materials—The Importance of Tertiary Structures, *Adv. Mater.*, **1998**, *10*, 1553–1557.
47. A. Alberola, R. J. Less, C. M. Pask, J. M. Rawson, F. Palacio, P. Oliete, C. Paulsen, A. Yamaguchi, R. D. Farley and D. M. Murphy, A Thiazyl-Based Organic Ferromagnet, *Angew. Chemie Int. Ed.*, **2003**, *42*, 4782–4785.
48. A. J. Banister, I. Lavender, J. M. Rawson and R. J. Whitehead, Dalton communications. Convenient preparations of the mixed 1,3,2,4-/1,2,3,5-dithiadiazolylium salt [SNSNC–C₆H₄–CNSSN][AsF₆][–] and the first mixed free radical, p-[SNSNC–C₆H₄–CNSSN][•], *J. Chem. Soc., Dalt. Trans.*, **1992**, *113*, 1449–1450.
49. J. L. Brusso, O. P. Clements, R. C. Haddon, M. E. Itkis, A. A. Leitch, R. T. Oakley, R. W. Reed and J. F. Richardson, Bistabilities in 1,3,2-dithiazolyl radicals, *J. Am. Chem. Soc.*, **2004**, *126*, 8256–8265.
50. L. Beer, J. F. Britten, O. P. Clements, R. C. Haddon, M. E. Itkis, K. M. Matkovich, R. T. Oakley and M. E. Itkis, Dithiazolodithiazolyl radicals: Substituent effects on solid state structures and properties, *Chem. Mater.*, **2004**, *16*, 1564–1572.
51. D. Tian, S. M. Winter, A. Mailman, J. W. L. Wong, W. Yong, H. Yamaguchi, Y. Jia, J. S. Tse, S. Desgreniers, R. A. Secco, S. R. Julian, C. Jin, M. Mito, Y. Ohishi and R. T. Oakley, The Metallic State in Neutral Radical Conductors: Dimensionality, Pressure and Multiple Orbital Effects, *J. Am. Chem. Soc.*, **2015**, *137*, 14136–14148.
52. R. Hoffmann, Building Bridges Between Inorganic and Organic Chemistry (Nobel Lecture), *Angew. Chemie Int. Ed.*, **1982**, *21*, 711–724.
53. A. A. Leitch, R. T. Oakley, R. W. Reed and L. K. Thompson, Electronic and Magnetic Interactions in π -Stacked Bisthiadiazinyl Radicals, *Inorg. Chem.*, **2007**, *46*, 6261–6270.
54. L. A. Berben, B. de Bruin and A. F. Heyduk, Non-innocent ligands, *Chem. Commun.*, **2015**, *51*, 1553–1554.
55. T. M. Barclay, R. G. Hicks, M. T. Lemaire and L. K. Thompson, Weak Magnetic Coupling of Coordinated Verdazyl Radicals through Diamagnetic Metal Ions. Synthesis, Structure, and Magnetism of a Homoleptic Copper(I) Complex, *Inorg. Chem.*, **2001**, *40*, 6521–6524.
56. A. J. Banister, I. B. Gorrell, W. Clegg and K. A. Jørgensen, The 4-phenyl-1,2,3,5-dithiadiazole complex [Fe₂(CO)₆(PhCN₂S₂)]: its preparation, crystal structure, and an extended-Hückel molecular-orbital study of the bonding, *J. Chem. Soc., Dalt. Trans.*, **1989**, 2229–2233.

57. A. J. Banister, I. B. Gorrell, S. E. Lawrence, C. W. Lehmann, I. May, G. Tate, A. J. Blake and J. M. Rawson, Novel bonding modes in metallo–dithiadiazolyl complexes: preparation and crystal structures of [Pt(SNCPhNS-S,S)(PPh₃)₂].MeCN and [Pt₃(μ-SNCPhNS-S,S)₂(PPh₃)₄].2PhMe, *J. Chem. Soc., Chem. Commun.*, **1994**, 41, 1779–1780.
58. H. F. Lau, V. W. L. Ng, L. L. Koh, G. K. Tan, L. Y. Goh, T. L. Roemmele, S. D. Seagrave and R. T. Boéré, Cyclopentadienylchromium Complexes of 1,2,3,5-Dithiadiazolyls: η² π Complexes of Cyclic Sulfur–Nitrogen Compounds, *Angew. Chemie Int. Ed.*, **2006**, 45, 4498–4501.
59. N. G. R. Hearn, K. E. Preuss, J. F. Richardson and S. Bin-Salamon, Design and Synthesis of a 4-(2'-Pyridyl)-1,2,3,5-Dithiadiazolyl Cobalt Complex, *J. Am. Chem. Soc.*, **2004**, 126, 9942–9943.
60. J. Britten, N. G. R. Hearn, K. E. Preuss, J. F. Richardson and S. Bin-Salamon, Mn(II) and Cu(II) Complexes of a Dithiadiazolyl Radical Ligand: Monomer/Dimer Equilibria in Solution, *Inorg. Chem.*, **2007**, 46, 3934–3945.
61. M. Jennings, K. E. Preuss and J. Wu, Synthesis and magnetic properties of a 4-(2'-pyrimidyl)-1,2,3,5-dithiadiazolyl dimanganese complex, *Chem. Commun.*, **2006**, 22, 341–343.
62. M. B. Mills, A. G. Hollingshead, A. C. Maahs, D. V. Soldatov and K. E. Preuss, Isomerization of a lanthanide complex using a humming top guest template: a solid-to-solid reaction, *CrystEngComm*, **2015**, 17, 7816–7819.
63. S. S. Batsanov, No Title, *Inorg. Mater.*, **2001**, 37, 871–885.
64. N. G. R. Hearn, K. D. Hesp, M. Jennings, J. L. Korčok, K. E. Preuss and C. S. Smithson, Monodentate N-coordination of a 1,2,3,5-dithiadiazolyl to Mn(II), Co(II) and Ni(II): A new coordination mode, *Polyhedron*, **2007**, 26, 2047–2053.
65. Y. Umezono, W. Fujita and K. Awaga, Coordination Bond Formation at Charge-Transfer Phase Transition in (BDTA)₂ [Co(mnt)₂], *J. Am. Chem. Soc.*, **2006**, 128, 1084–1085.
66. K. Awaga, T. Tanaka, T. Shirai, M. Fujimori, Y. Suzuki, H. Yoshikawa and W. Fujita, Multi-Dimensional Crystal Structures and Unique Solid-State Properties of Heterocyclic Thiazyl Radicals and Related Materials, *Bull. Chem. Soc. Jpn.*, **2006**, 79, 25–34.
67. V. I. Minkin, Bistable organic, organometallic, and coordination compounds for molecular electronics and spintronics, *Russ. Chem. Bull.*, **2008**, 57, 687–717.
68. G. M. Sheldrick, A short history of SHELX, *Acta Crystallogr. Sect. A Found. Crystallogr.*, **2008**, 64, 112–122.
69. C. F. Macrae, P. R. Edgington, P. McCabe, E. Pidcock, G. P. Shields, R. Taylor, M. Towler, J. van de Streek, C. R. I., H. S. E. and O. A. G., Mercury : visualization and

analysis of crystal structures, *J. Appl. Crystallogr.*, **2006**, *39*, 453–457.

70. J. A. Bertrand and R. I. Kaplan, A Study of Bis(hexafluoroacetylacetonato)copper(II), *Inorg. Chem.*, **1966**, *5*, 489–491.
71. S. S. Afjeh, A. A. Leitch, I. Korobkov, J. L. Brusso, R. W. Reed, P. A. Dube, R. T. Oakley, G. Durocher, Y. Tao and M. Leclerc, Optoelectronic and structural properties of a family of thiophene functionalized 1,5-dithia-2,4,6,8-tetrazocines, *RSC Adv.*, **2013**, *3*, 23438.
72. T. Jeffries, *Organic Chemistry*, Oxford University Press, **1970**, *i*.
73. J. M. Rawson and G. D. McManus, Benzo-fused dithiazolyl radicals: from chemical curiosities to materials chemistry., *Coord. Chem. Rev.*, **1999**, *189*, 135–168.
74. J. J. Li, *Name Reactions A Collection of Detailed Mechanisms And synthetic Applications*, Springer, **2009**.
75. J. A. and J. R. B. Weil, *Electron paramagnetic resonance Elementary Theory and Practical Applications*, Wiley, **2007**.
76. IUPAC Gold Book online , IUPAC, 2.3.3., **2011**, *33*.
77. Y. Pei, Y. Journaux and O. Kahn, Irregular spin state structure in trinuclear species: magnetic and EPR properties of manganese(II)-copper(II)-manganese(II) and nickel(II)-copper(II)-nickel(II) compounds, *Inorg. Chem.*, **1988**, *27*, 399–404.

12 APPENDICES

Appendix 1. ^1H NMR- spectrum of compound **1**.

Appendix 2. ^1H NMR- spectrum of compound **3**.

Appendix 3. IR-spectrum of compound **4**.

Appendix 4. IR- spectrum of compound **5**.

Appendix 5. ^1H NMR- spectrum of compound **6**.

Appendix 6. ^1H NMR- spectrum of compound **7**.

Appendix 7. IR- spectrum of compound **9**.

Appendix 8. IR- spectrum of compound **11**.

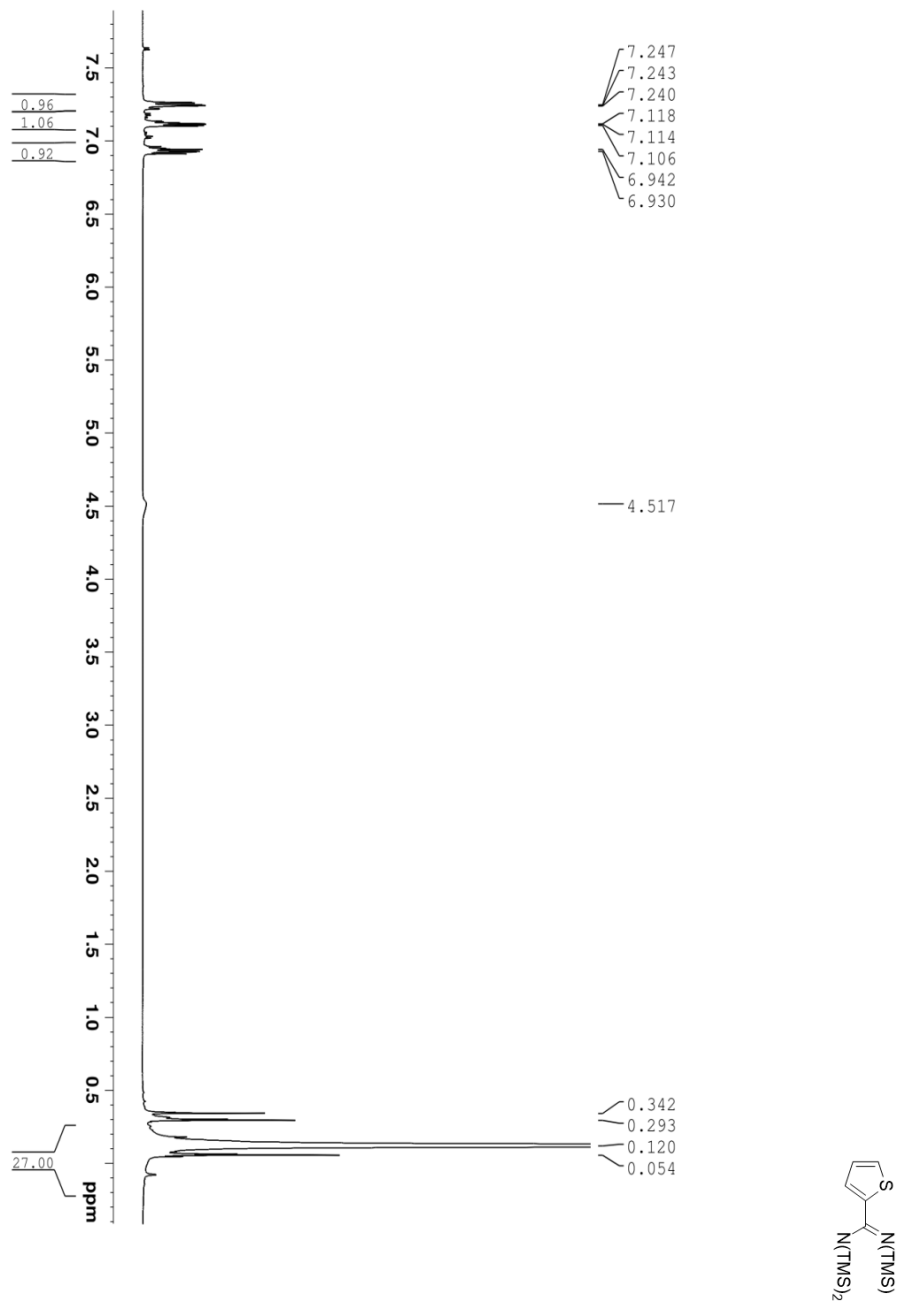
Appendix 9. ^1H NMR- spectrum of compound **12**.

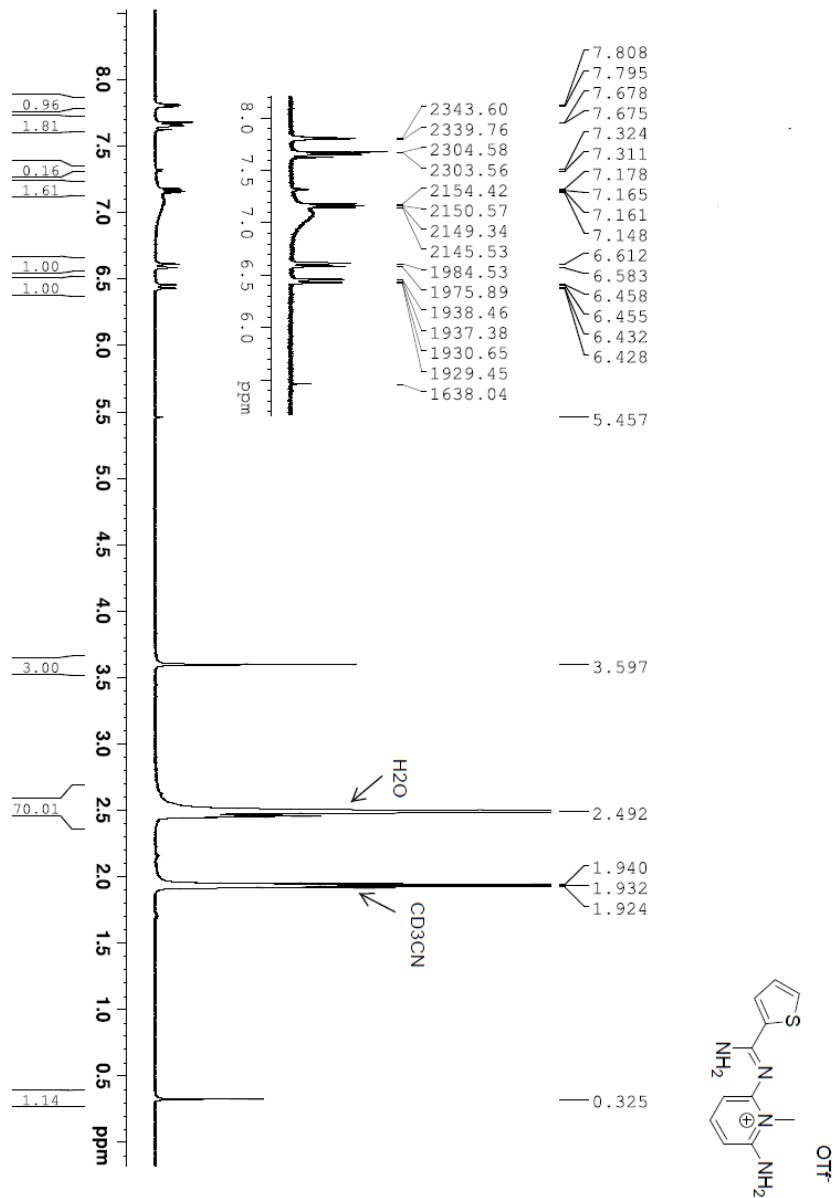
Appendix 10. IR- spectrum of compound **14**.

Appendix 11. IR- spectrum of compound **15**.

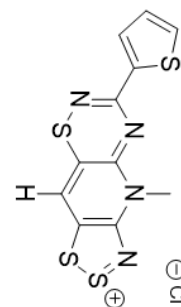
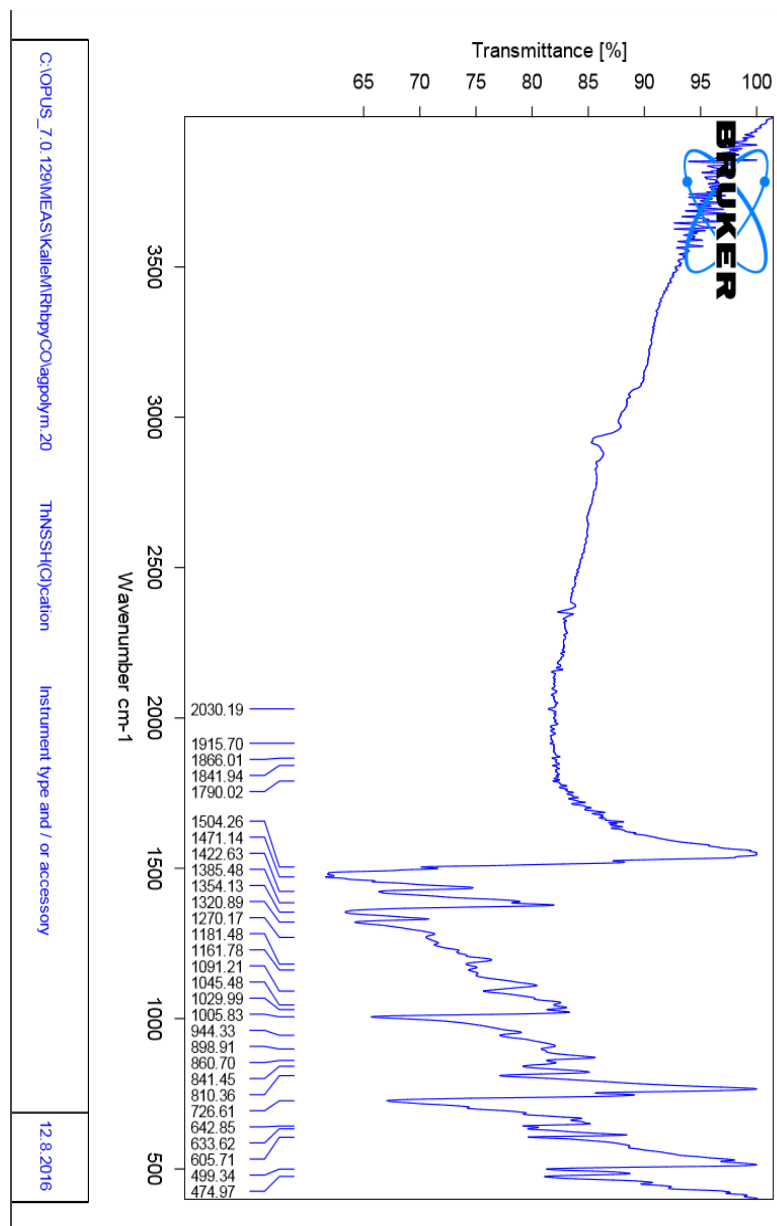
Appendix 12. IR- spectrum of compound **17**.

Appendix 13. IR- spectrum of compound **19**.

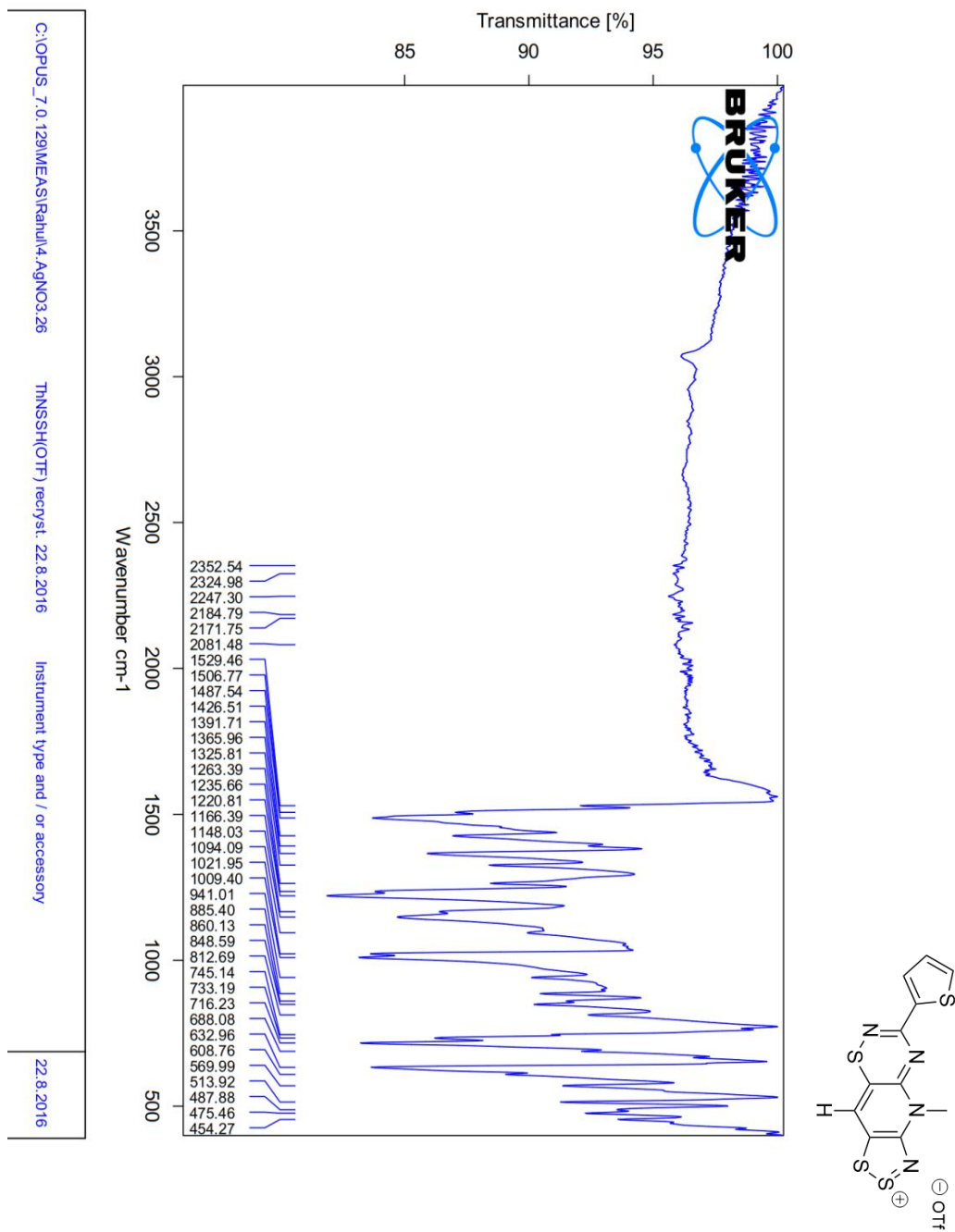
Appendix 1. ^1H NMR- spectrum of compound **1**.

Appendix 2. ^1H NMR- spectrum of compound **3**.

Appendix 3. IR-spectrum of compound 4.



Appendix 4. IR- spectrum of compound 5.

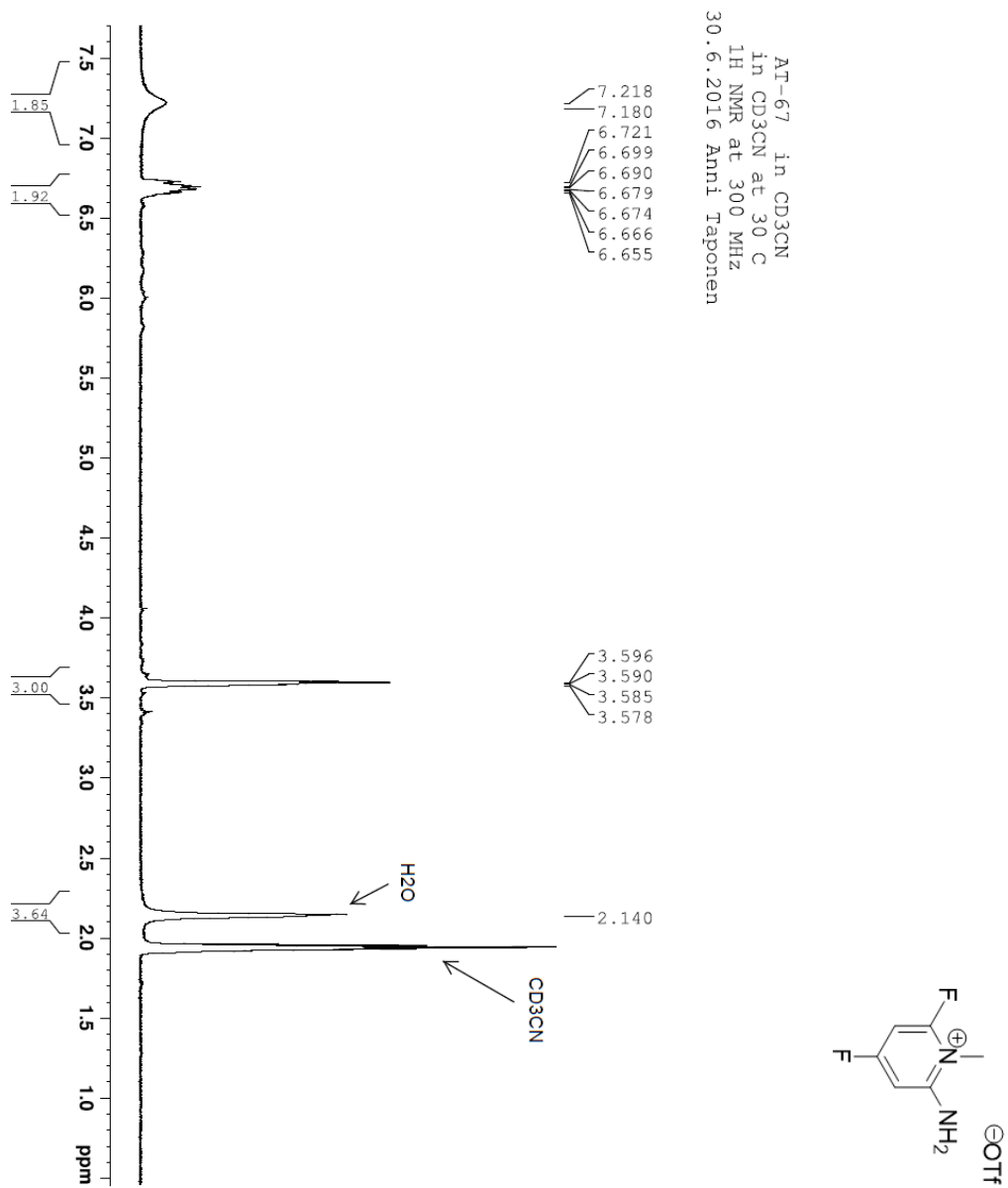


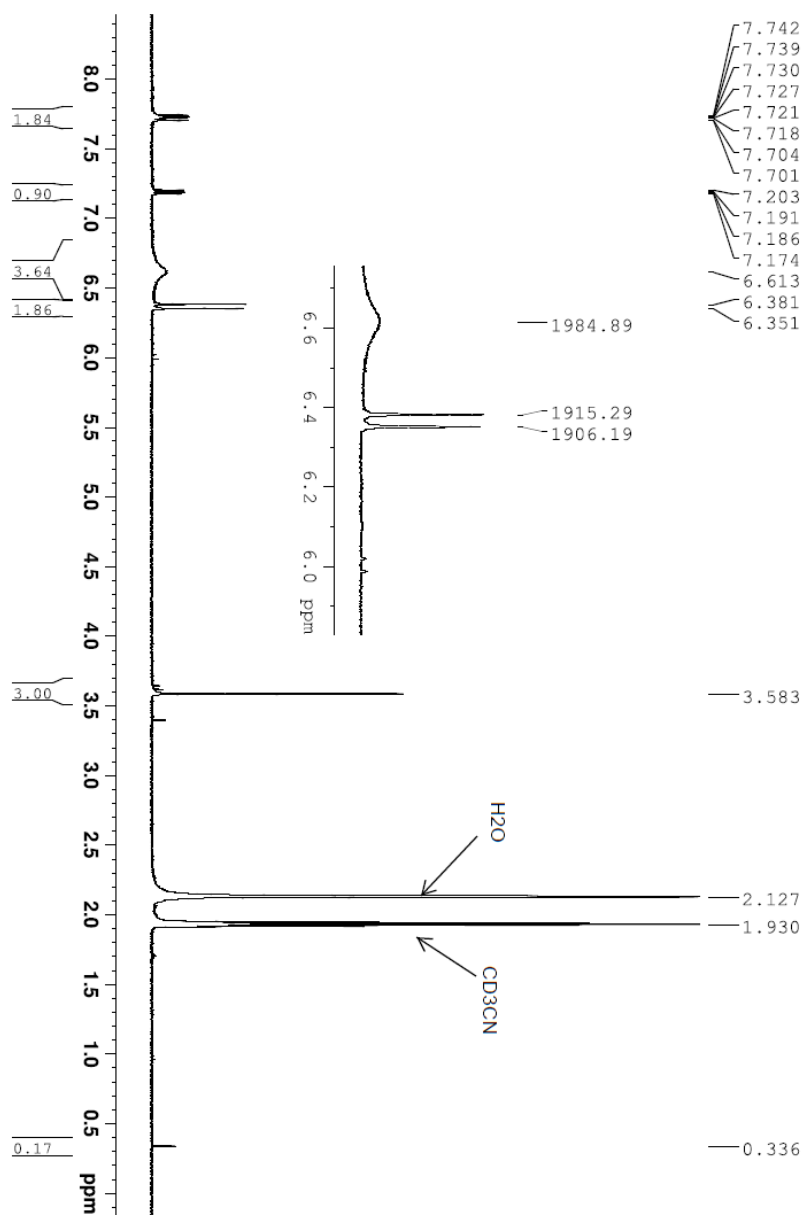
C:\OPUS_7.0.129\MEAS\ Rahul4_AgNO3.26

THNSH(OTF) recryst. 22.8.2016

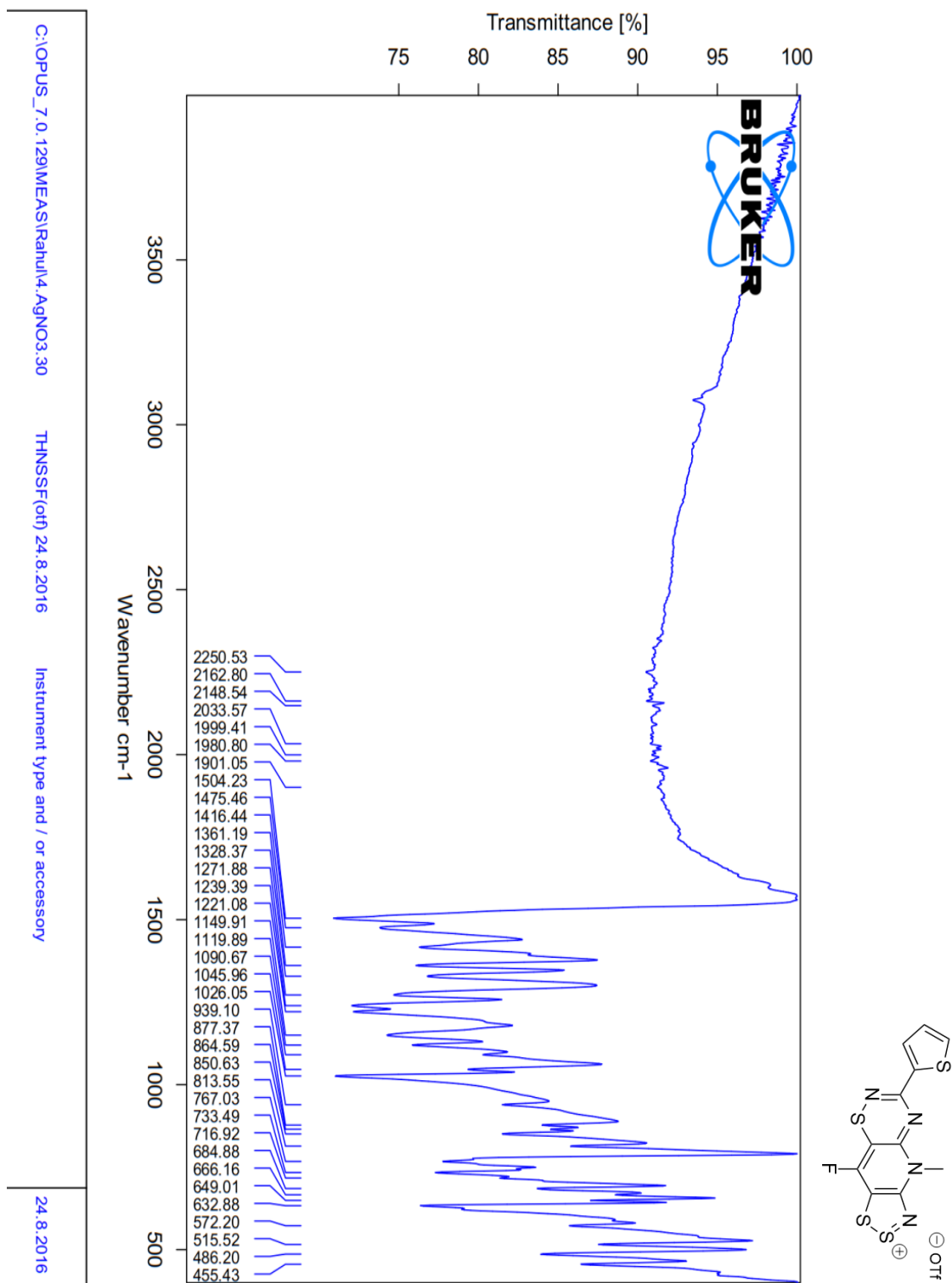
Instrument type and / or accessory

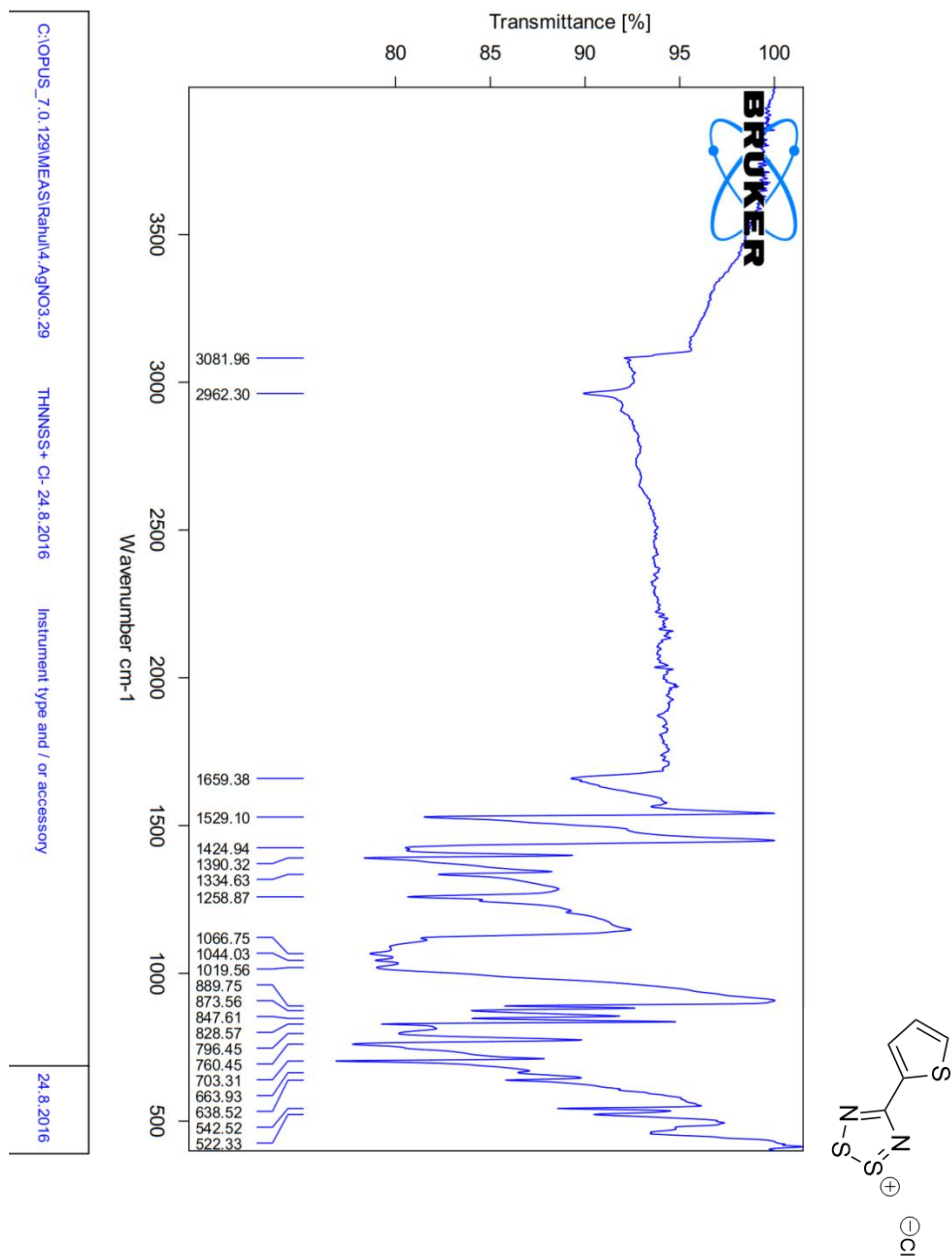
22.8.2016

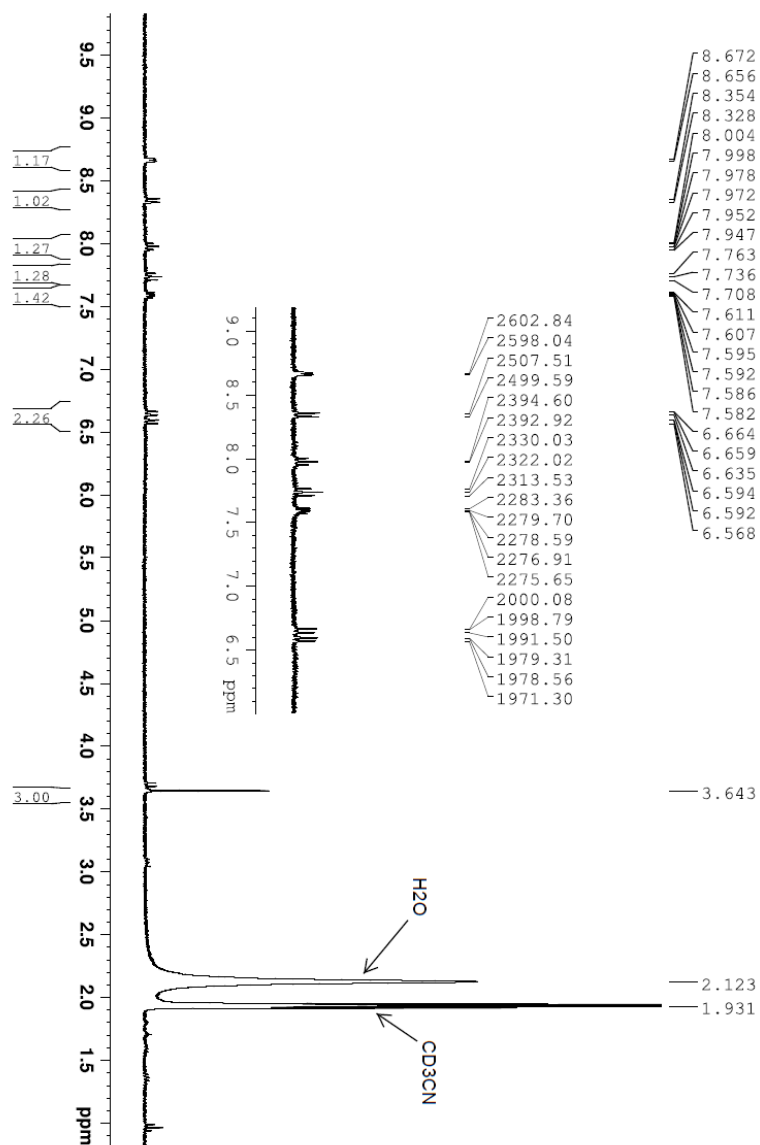
Appendix 5. ¹H NMR- spectrum of compound **6**.

Appendix 6. ^1H NMR- spectrum of compound 7.

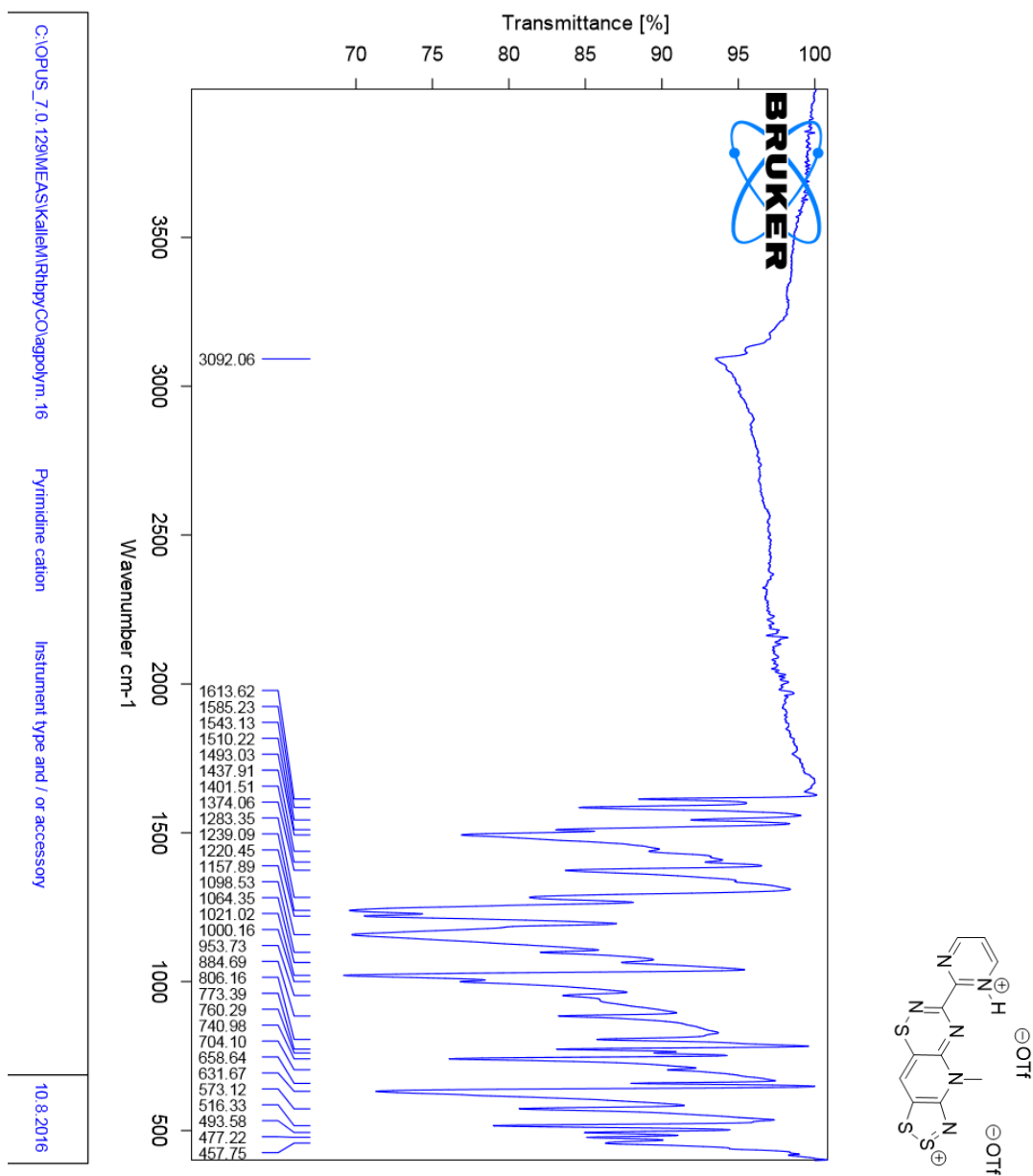
Appendix 7. IR- spectrum of compound 9.



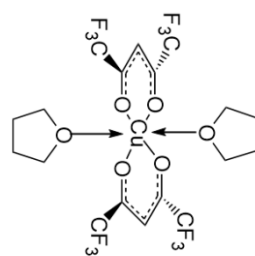
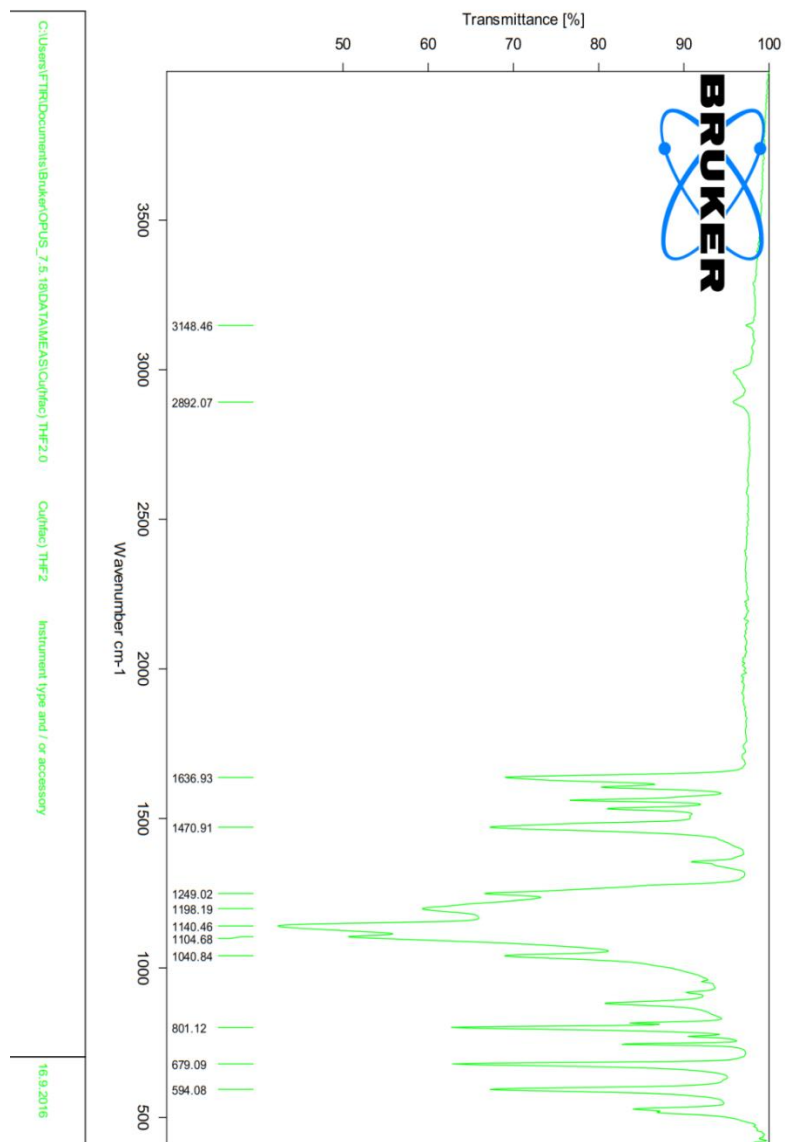
Appendix 8. IR- spectrum of compound **11**.

Appendix 9. ¹H NMR- spectrum of compound **12**.

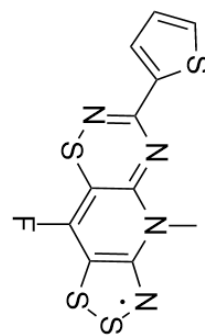
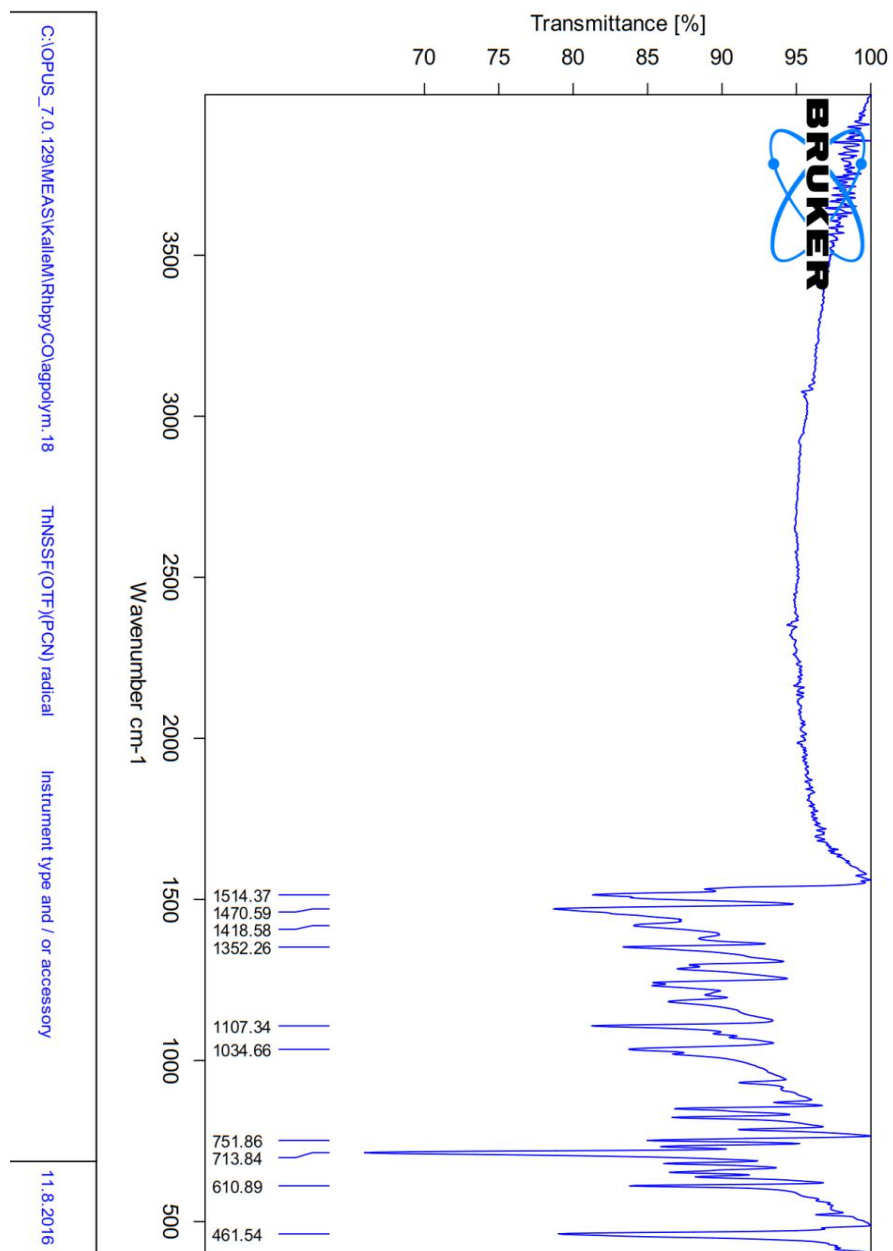
Appendix 10. IR- spectrum of compound 14.



Appendix 11. IR- spectrum of compound 15.



Appendix 12. IR- spectrum of compound 17.



Appendix 13. IR- spectrum of compound **19**.